SUPPLEMENTARY APPENDIX

Clonal evolution in chronic lymphocytic leukemia is scant in relapsed but accelerated in refractory cases after chemo(immune) therapy

Marc Zapatka,[1*] Eugen Tausch,[2*] Selcen Öztürk,[1] Deyan Yordanov Yosifov,[2,3] Martina Seiffert,[1] Thorsten Zenz,[4] Christof Schneider,[2] Johannes Bloehdorn,[2] Hartmut Döhner,[2] Daniel Mertens,[2,3] Peter Lichter[1] and Stephan Stilgenbauer[2]

[1]Division of Molecular Genetics, German Cancer Research Center, Heidelberg, Germany; [2]Department of Internal Medicine III, Ulm University Hospital, Ulm, Germany; [3]Mechanisms of Leukemogenesis, German Cancer Research Center (DKFZ), Heidelberg, Germany and [4]University Hospital, University of Zürich, Zürich, Switzerland

**MZ and ET contributed equally as co-first authors.*

 doi:10.3324/haematol.2020.265777

Received: July 7, 2020.

Accepted: February 26, 2021.

Pre-published: March 11, 2021.

Correspondence: *PETER LICHTER* - Peter.Lichter@dkfz-heidelberg.de

STEPHAN STILGENBAUER - Stephan.Stilgenbauer@uniklinik-ulm.de

Supplementary Methods

Alignment and variant calling

Alignment and variant calling were performed as described in [1]. In summary, paired-end DNA sequencing reads were mapped to the hg19 assembly (NCBI build 37.1, downloaded from the UCSC genome browser at http://genome.ucsc.edu/) of the human reference genome using BWA version 0.5.10 [2] and processed with samtools (version 0.1.17) and Picard tools (version 1.61, http://broadinstitute.github.io/picard). Single nucleotide variants (SNVs) and small insertions or deletions (indels) were identified based on our in-house analysis pipeline using samtools mpileup and bcftools. For patients without germline sample we called variants using samtools mpileup and bcftools. SNVs with a genotype quality lower than 80 and with no genotype change between consecutive samples were filtered.

CNV calling and calculation of absolute copy numbers

Estimation of the copy number state based on the exome sequencing data was achieved using Varscan 2 on the target regions [3]. Counting the uniquely mapped reads, log2 ratios were calculated for all segments against the respective germline control. Absolute copy numbers were calculated following[4]. In summary, first the ploidy was identified manually based on the FISH results available (see supplementary figures 3, for depiction of the exome sequencing based log2 ratios in regions analyzed by FISH). Incorporating the clinically assessed sample purity measured using FACS, the log2 ratio derived from the read counts of the exome sequencing were transformed into absolute copy numbers for the respective segments of the individual genomes.

Estimation of clonal composition by TrAP

Changes in clonal tumor composition were calculated integrating the CCF at the respective time points using TrAP [5]. In summary, the individual cancer cell fractions across samples per

patient were hierarchically clustered (R: hclust, complete linkage). The CCF profiles were grouped into six clusters (R: cutree k=6). The resulting mean centroids for the six clusters across timepoints were used as input data for TrAP (datatype GAUSSIAN, the error is estimated based on a normal approximation, see [5] for details). For the cluster the median error was calculated for the TrAP based estimation of the subclonal tumor composition. From the possible solutions the solution with the best fit was selected for each patient.

Quantification of DNA methylation and estimation of correlation between time points

DNA from the first and second time point of 10 patient phases (3 long-term untreated, 2 relapsed and 5 refractory) was bisulfite-converted using the EZ DNA Methylation Kit (Zymo Research) and then whole-genome amplified, fragmented and hybridized to Illumina Infinium HumanMethylation450 BeadChips according to the manufacturer's protocol. After single-base extension and staining, the BeadChips were scanned using an Illumina iScan reader. Quality control of the raw data, preprocessing and basic analysis were performed using R/Bioconductor with the RnBeads package [6]. Illumina probes known to be cross-reactive or overlapping known SNPs [7] were excluded from analysis. This was also done for probes giving unreliable measurements as determined by the Greedycut algorithm implemented in RnBeads. The data from the remaining probes were subjected to background subtraction using the Noob method [8] and beta-mixture quantile normalization (BMIQ [9]). In a subsequent step, probes of non-CpG context, probes binding to sequences on sex chromosomes and probes with low standard deviation were filtered out. The data obtained by the remaining probes were used in downstream analyses. Methylation levels of CpG sites were calculated as β-values (β = intensity of the methylated allele (M)/[intensity of the unmethylated allele (U) + intensity of the methylated allele (M) + 100]. For each patient, the shift in overall methylation was estimated by calculating the square of the Pearson correlation coefficient (R^2) between time points using the 40,000 most variable probes in all available samples. Differential methylation analysis between time points for each of the patient groups was performed using the limma

method as implemented in the RnBeads package. For downstream enrichment analyses, we used only differentially methylated CpGs with absolute difference in mean β-values of at least 0.1 at FDR 0.05. Possible enrichment of hypomethylated and hypermethylated CpGs within particular chromatin states was assessed using the R/Bioconductor package LOLA (Locus Overlap Analysis)[10] and published reference CLL epigenomes1[11]. Before the analysis, the genomic coordinates of the reference chromatin state regions were lifted over from hg38 to hg19 using liftOver. Enrichment analyses at the individual patient level were performed using CpGs with absolute difference in β-values between the two time points of at least 0.3.

1. Jones DT, Hutter B, Jager N, et al. Recurrent somatic alterations of FGFR1 and NTRK2 in pilocytic astrocytoma. Nat Genet. 2013;45(8):927-932.
2. Li H, Durbin R. Fast and accurate short read alignment with Burrows-Wheeler transform. Bioinformatics. 2009;25(14):1754-1760.
3. Koboldt DC, Zhang Q, Larson DE, et al. VarScan 2: somatic mutation and copy number alteration discovery in cancer by exome sequencing. Genome Res. 2012;22(3):568-576.
4. Carter SL, Cibulskis K, Helman E, et al. Absolute quantification of somatic DNA alterations in human cancer. Nat Biotechnol. 2012;30(5):413-421.
5. Strino F, Parisi F, Micsinai M, Kluger Y. TrAp: a tree approach for fingerprinting subclonal tumor composition. Nucleic Acids Res. 2013;41(17):e165.
6. Assenov Y, Muller F, Lutsik P, Walter J, Lengauer T, Bock C. Comprehensive analysis of DNA methylation data with RnBeads. Nat Methods. 2014;11(11):1138-1140.
7. Price ME, Cotton AM, Lam LL, et al. Additional annotation enhances potential for biologically-relevant analysis of the Illumina Infinium HumanMethylation450 BeadChip array. Epigenetics Chromatin. 2013;6(1):4.
8. Triche TJ, Jr., Weisenberger DJ, Van Den Berg D, Laird PW, Siegmund KD. Low-level processing of Illumina Infinium DNA Methylation BeadArrays. Nucleic Acids Res. 2013;41(7):e90.
9. Teschendorff AE, Marabita F, Lechner M, et al. A beta-mixture quantile normalization method for correcting probe design bias in Illumina Infinium 450 k DNA methylation data. Bioinformatics. 2013;29(2):189-196.
10. Sheffield NC, Bock C. LOLA: enrichment analysis for genomic region sets and regulatory elements in R and Bioconductor. Bioinformatics. 2016;32(4):587-589.
11. Beekman R, Chapaprieta V, Russinol N, et al. The reference epigenome and regulatory chromatin landscape of chronic lymphocytic leukemia. Nat Med. 2018;24(6):868-880.

Supplementary Information

Supplementary tables

Suppl. table 1:

Clinical information for the patient samples

Suppl. table 2:

Treatment and sampling information

Suppl. table 3:

Table of driver events

Suppl. table 4:

Evolution types across clinical phases

Suppl. table 5:

Table of SNVs identified

Suppl. table 6:

Representation of samples and figures explaining which samples were used in the different analyses

Supplementary figures

Suppl. figure 1: Graphical representation of clinical course of analyzed patients. Three patients are lost to follow-up (HU-1-09, -13, -15). (Black box: sample collection for WES; Grey box: under treatment; Red box: Death, Green box: last follow up;

Transparent boxes: therapy response (CR = complete response; PR: partial response; SD: stable disease; PD: progressive disease) and Richter syndrome (= Richter); Therapy information: R = Rituximab; O = Ofatumumab; F = Fludarabin; C = Cyclophoshamid; CBL=Chlorambucil; B=Bendamustin; A=Alemtuzumab; M=Mitoxantron; CHOP = Cyclophosphamid + Doxorubicin + Vincristin + Prednisolon; MCP = Melphalan + Cyclophosphamid + Prednisolon; PCR = Rituximab + Pentostatin + Cyclophosphamid; RLB = Rituximab + Lenalidomide + Bendamustin; RBM= Rituximab + Bendamustin + Mitoxantron; DBEAM = Dexamethason + Carmustin + Etoposid + AraC + Melphalan; Ibr = Ibrutinib; allo = allogeneic transplant, auto = autologous transplant, DLI = Donor lymphocyte infusion)

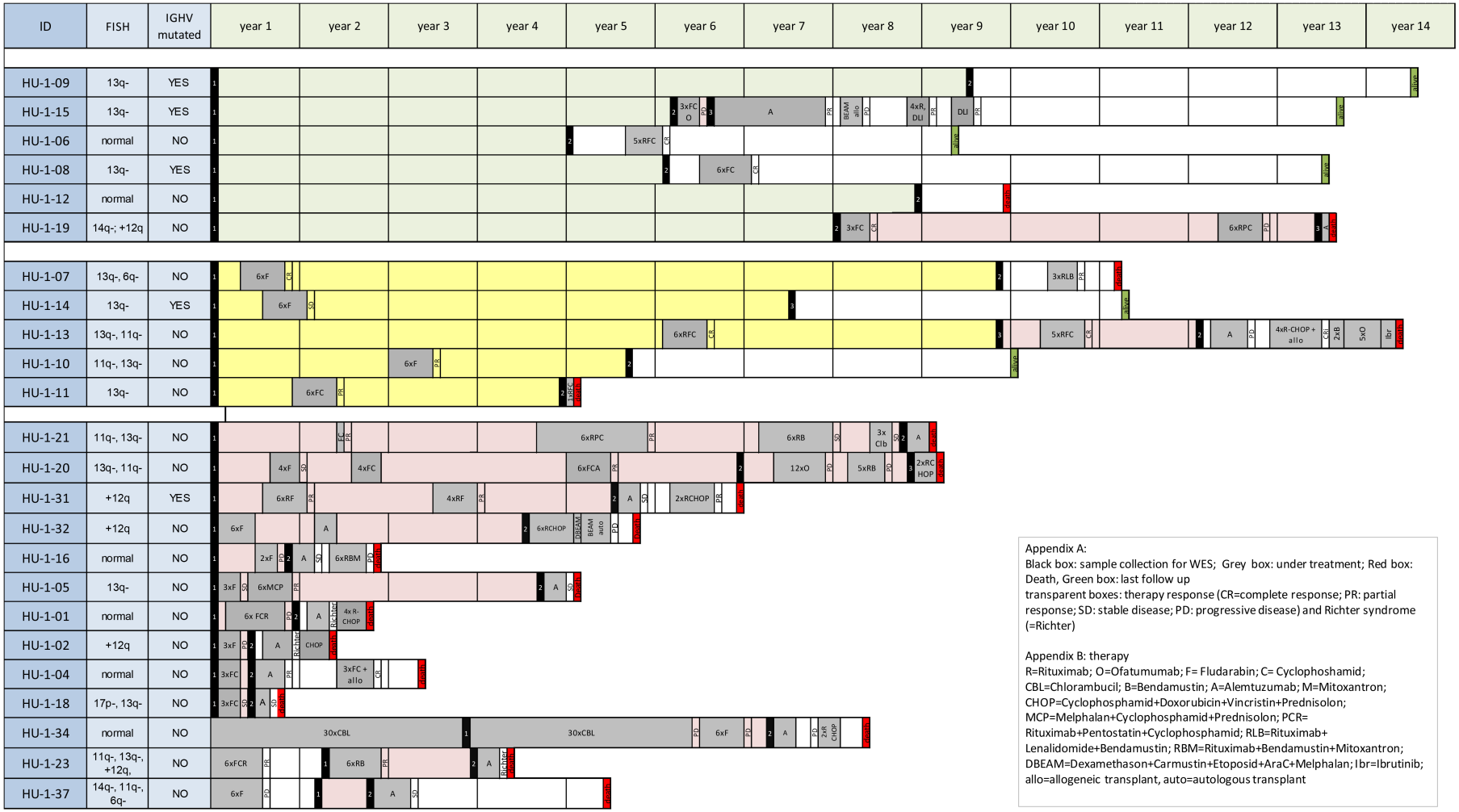
ID
FISH
IGHV mutated
year 1
year 2
year 3
year 4
year 5
year 6
year 7
year 8
year 9
year 10
year 11
year 12
year 13
year 14
HU-1-09 13q- YES
HU-1-15 13q- YES
HU-1-06 normal NO
HU-1-08 13q- YES
HU-1-12 normal NO
HU-1-19 14q-; +12q NO
HU-1-07 13q-, 6q- NO
HU-1-14 13q- YES
HU-1-13 13q-, 11q- NO
HU-1-10 11q-, 13q- NO
HU-1-11 13q- NO
HU-1-21 11q-, 13q- NO
HU-1-20 13q-, 11q- NO
HU-1-31 +12q YES
HU-1-32 +12q NO
HU-1-16 normal NO
HU-1-05 13q- NO
HU-1-01 normal NO
HU-1-02 +12q NO
HU-1-04 normal NO
HU-1-18 17p-, 13q- NO
HU-1-34 normal NO
HU-1-23 11q-, 13q-, +12q, NO
HU-1-37 14q-, 11q-, 6q- NO
6xF
3xFC O
A
4xR, DLI
DLI
5xRFC
6xFC
3xFC
6xRPC
3xRLB
6xF
6xRFC
5xRFC
4xR-CHOP + allo
2xB
5xO
Ibr
6xF
6xFC
6xRPC
6xRB
3x Clb
4xF
4xFC
6xFCA
12xO
5xRB
2xRCHOP
6xRF
4xRF
2xRCHOP
6xF
6xRCHOP
DBEAM
BEAM
allo
2xF
6xRBM
3xF
6xMCP
6x FCR
4x R-CHOP
3xF
CHOP
3xFC + allo
3xFC
30xCBL
30xCBL
6xF
2xR CHOP
6xFCR
6xRB
6xF
alive
death
Appendix A:
Black box: sample collection for WES; Grey box: under treatment; Red box: Death, Green box: last follow up
transparent boxes: therapy response (CR=complete response; PR: partial response; SD: stable disease; PD: progressive disease) and Richter syndrome (=Richter)
Appendix B: therapy
R=Rituximab; O=Ofatumumab; F= Fludarabin; C= Cyclophoshamid; CBL=Chlorambucil; B=Bendamustin; A=Alemtuzumab; M=Mitoxantron; CHOP=Cyclophosphamid+Doxorubicin+Vincristin+Prednisolon; MCP=Melphalan+Cyclophosphamid+Prednisolon; PCR= Rituximab+Pentostatin+Cyclophosphamid; RLB=Rituximab+ Lenalidomide+Bendamustin; RBM=Rituximab+Bendamustin+Mitoxantron; DBEAM=Dexamethason+Carmustin+Etoposid+AraC+Melphalan; Ibr=Ibrutinib; allo=allogeneic transplant, auto=autologous transplant

Suppl. figure 2: Scatter plot of variant allele frequency changes between consecutive time points. Known cancer and CLL driver genes (Landau et al. 2015, Bailey et al. 2018) are highlighted in lightred if their change in allele frequency is significant based on Fisher's test on the reference and alternative allele counts other SNVs presented in blue. Excluded are SNVs which are in dbSNP, have a coverage below 20 or a higher frequency than 5 % in 1000 genomes. Gray lines represent error bars for the allele frequency calculation estimated from the read counts.

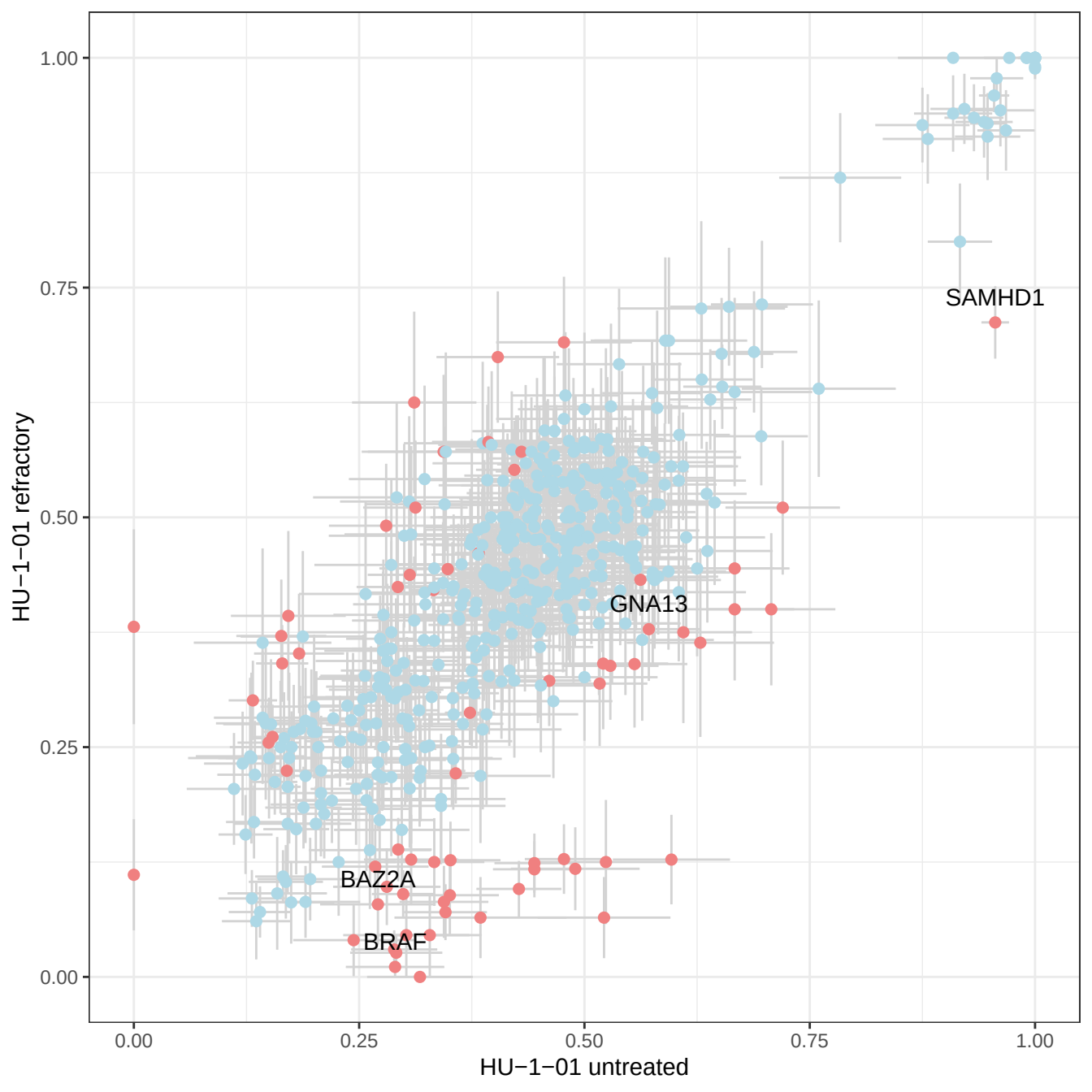
1.00
0.75
0.50
0.25
0.00
HU−1−01 refractory
0.00
0.25
0.50
0.75
1.00
HU−1−01 untreated
SAMHD1
GNA13
BAZ2A
BRAF

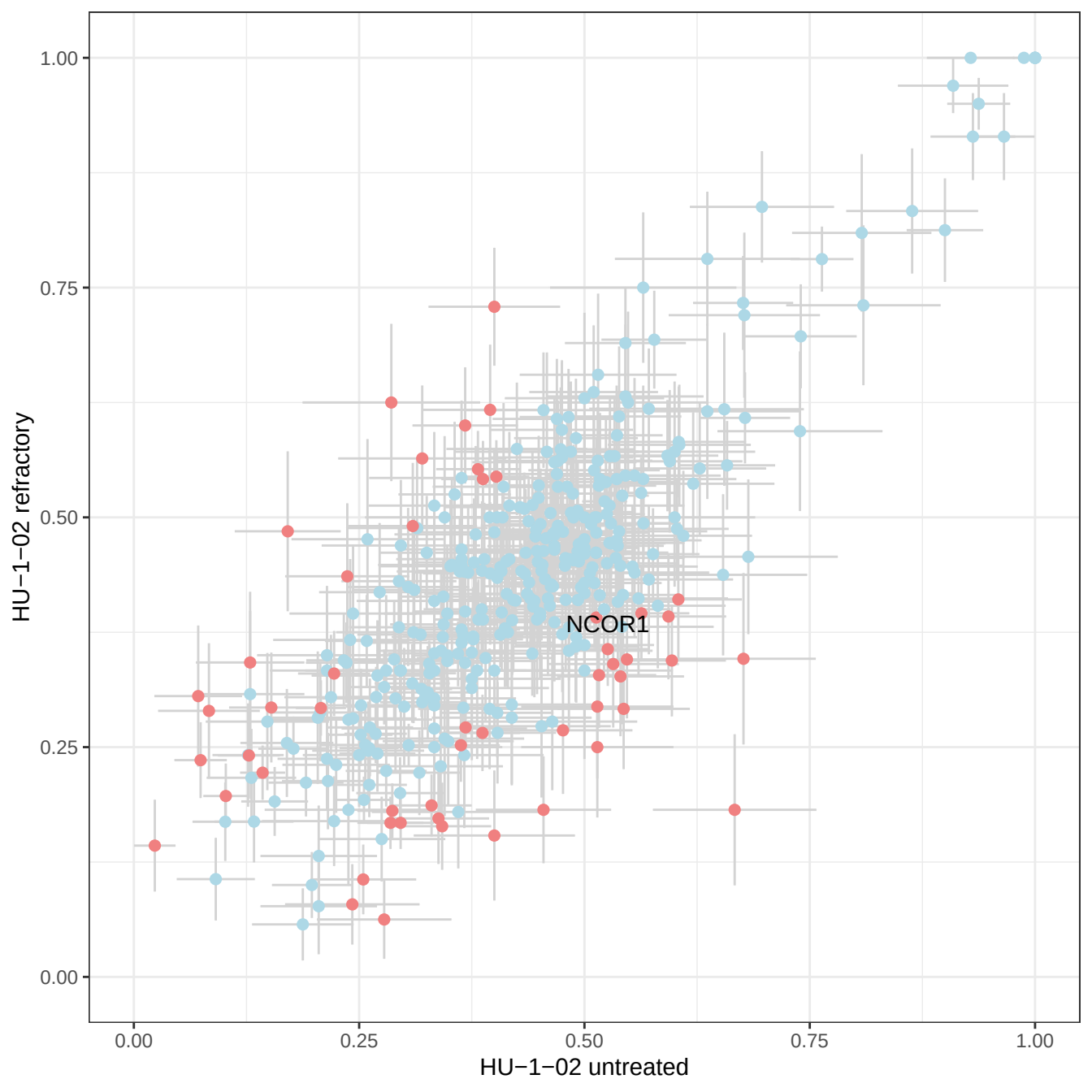
1.00
0.75
0.50
0.25
0.00
HU−1−02 refractory
0.00
0.25
0.50
0.75
1.00
HU−1−02 untreated
NCOR1

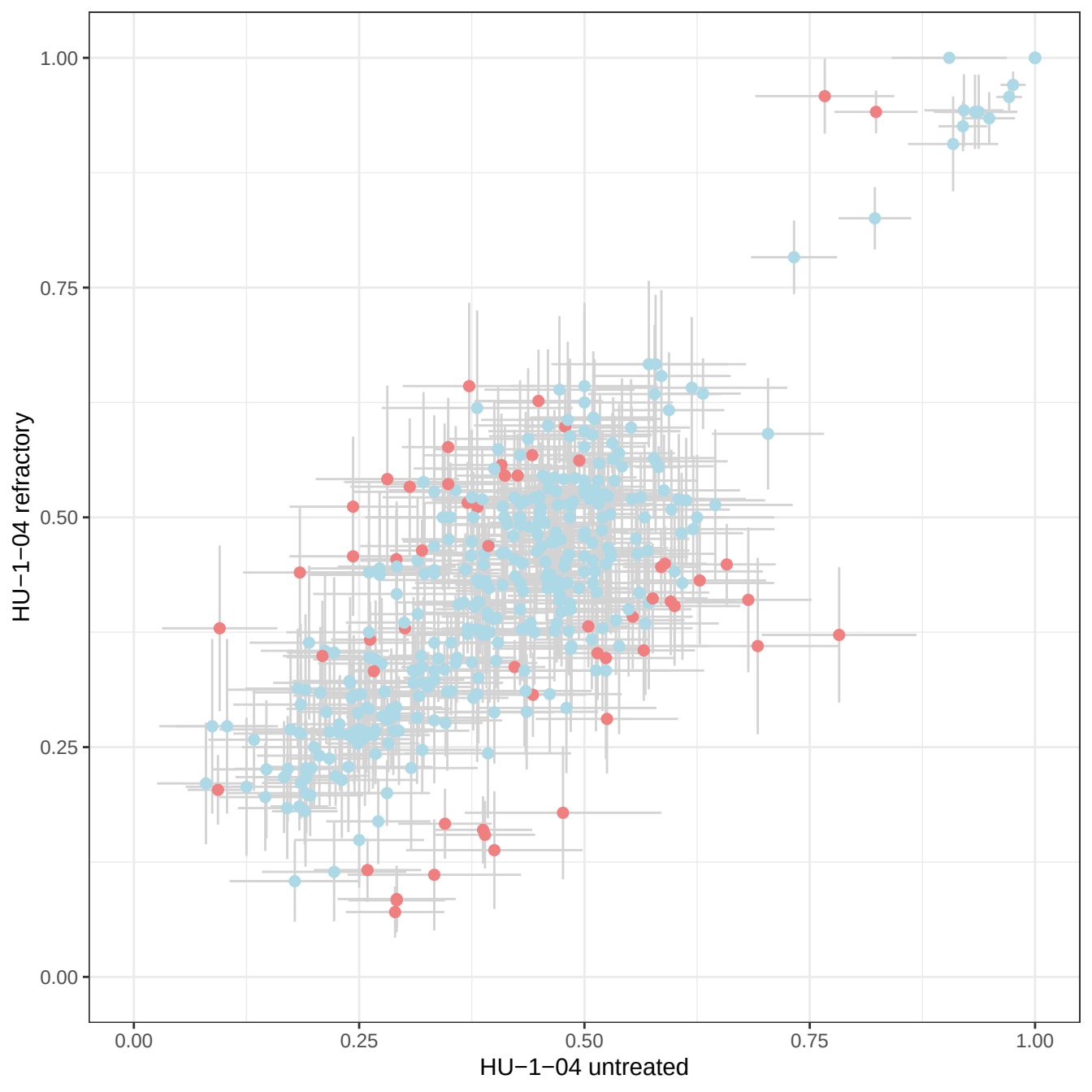
1.00
0.75
0.50
0.25
0.00
HU−1−04 refractory
0.00
0.25
0.50
0.75
1.00
HU−1−04 untreated

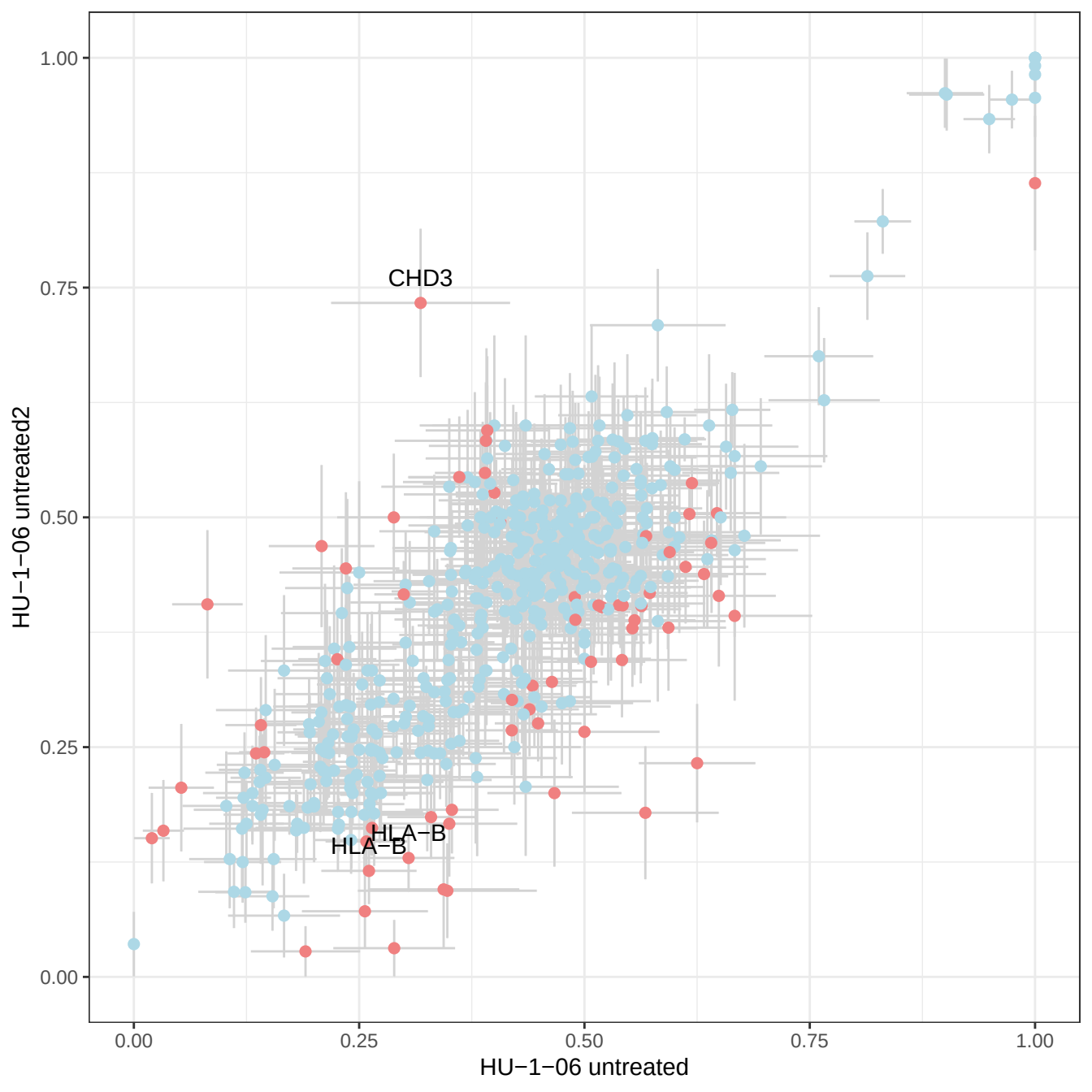
CHD3
HLA−B
HLA−B
1.00
0.75
0.50
0.25
0.00
0.00
0.25
0.50
0.75
1.00
HU−1−06 untreated2
HU−1−06 untreated

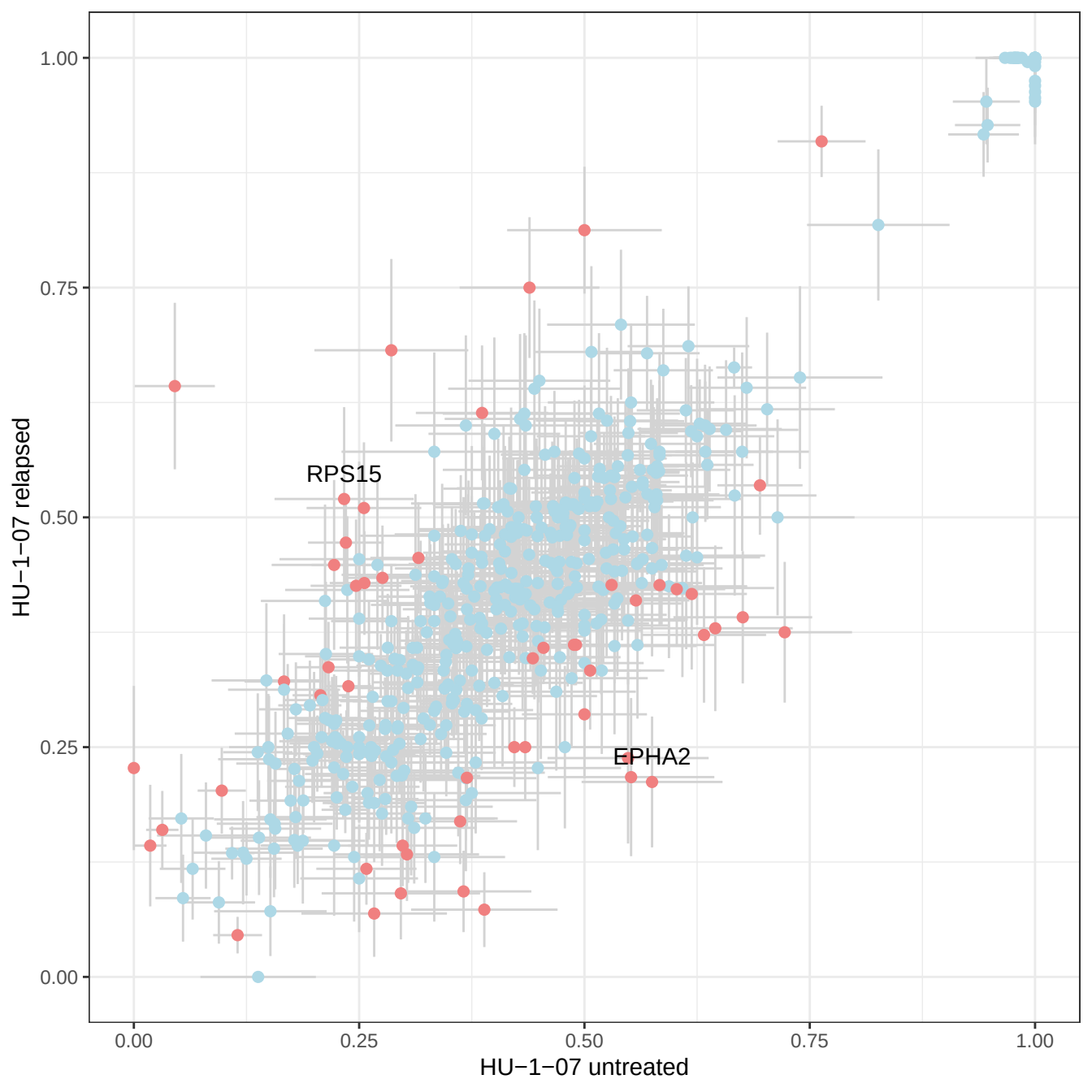
1.00
0.75
0.50
0.25
0.00
HU−1−07 relapsed
RPS15
EPHA2
0.00
0.25
0.50
0.75
1.00
HU−1−07 untreated

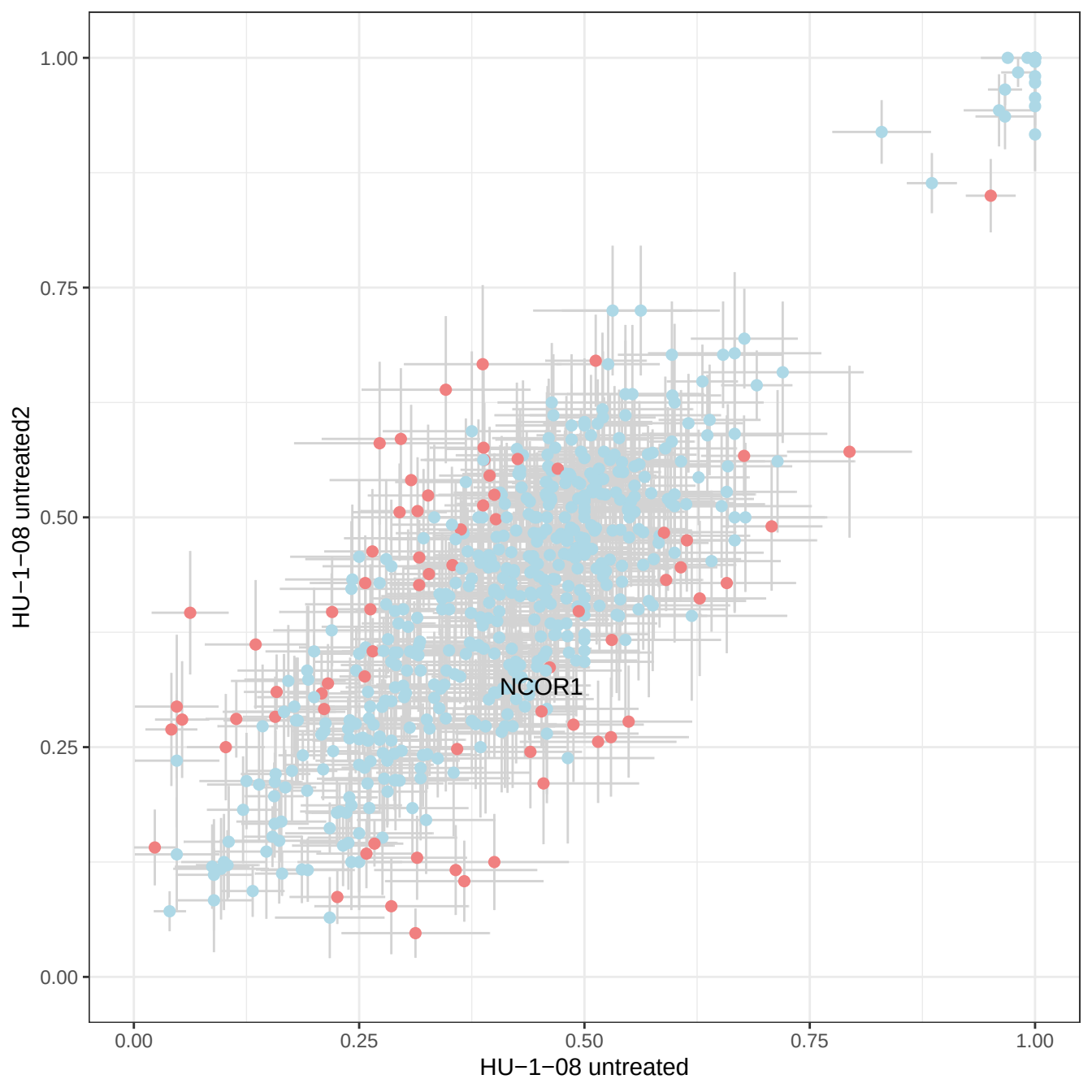
1.00
0.75
0.50
0.25
0.00
HU−1−08 untreated2
0.00
0.25
0.50
0.75
1.00
HU−1−08 untreated
NCOR1

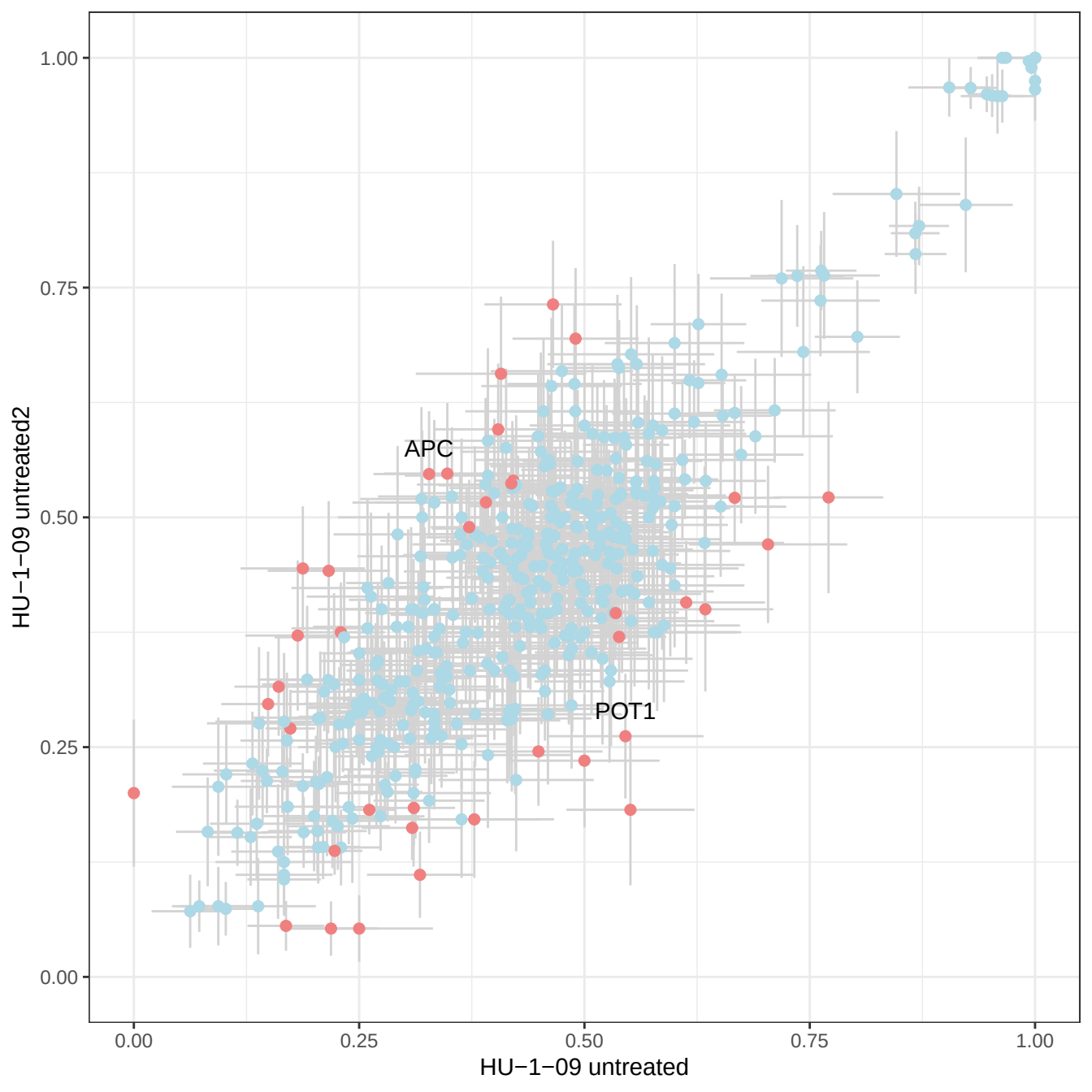
1.00
0.75
0.50
0.25
0.00
HU−1−09 untreated2
APC
POT1
0.00
0.25
0.50
0.75
1.00
HU−1−09 untreated

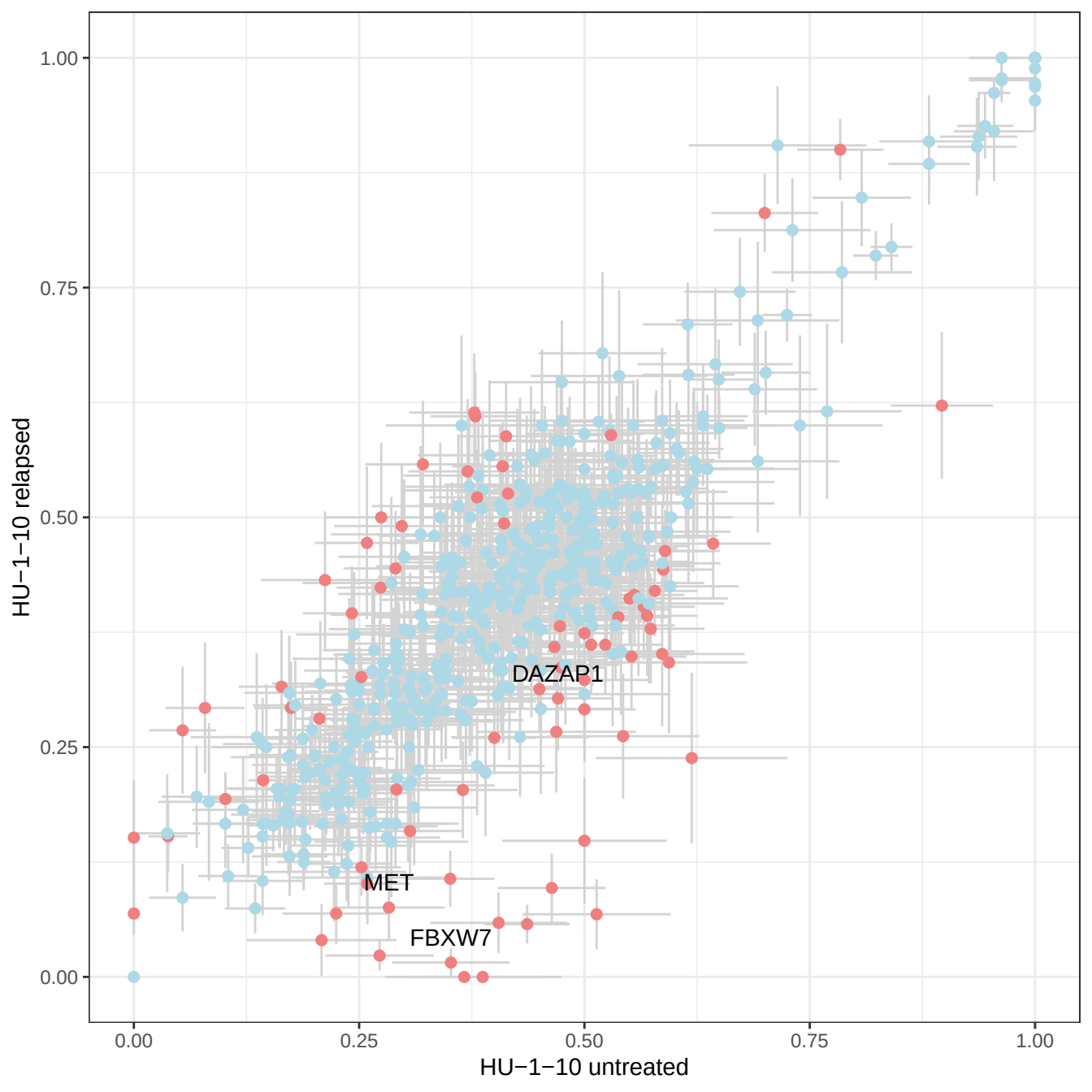
1.00
0.75
0.50
0.25
0.00
HU−1−10 relapsed
0.00
0.25
0.50
0.75
1.00
HU−1−10 untreated
DAZAP1
MET
FBXW7

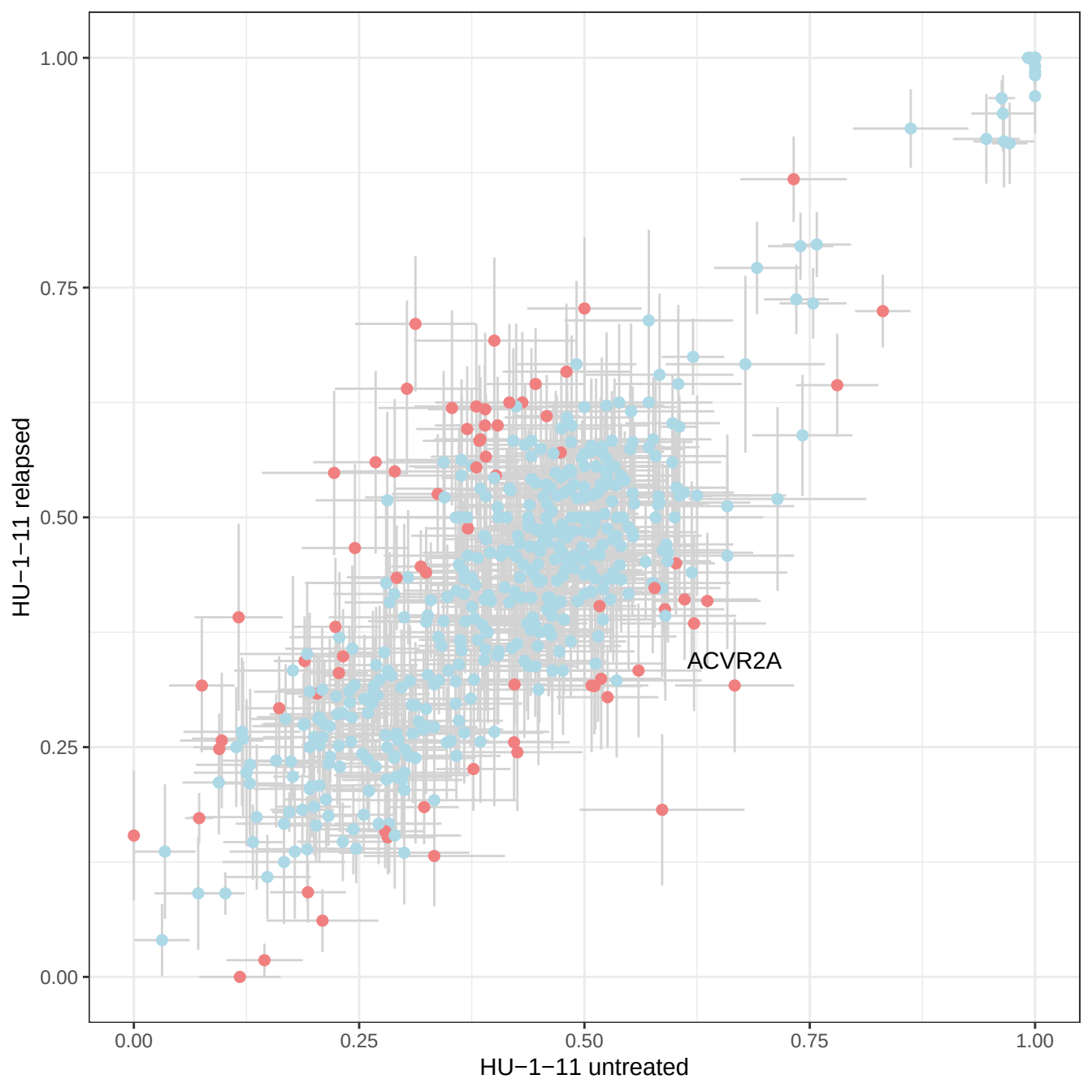
1.00
0.75
0.50
0.25
0.00
HU−1−11 relapsed
0.00
0.25
0.50
0.75
1.00
HU−1−11 untreated
ACVR2A

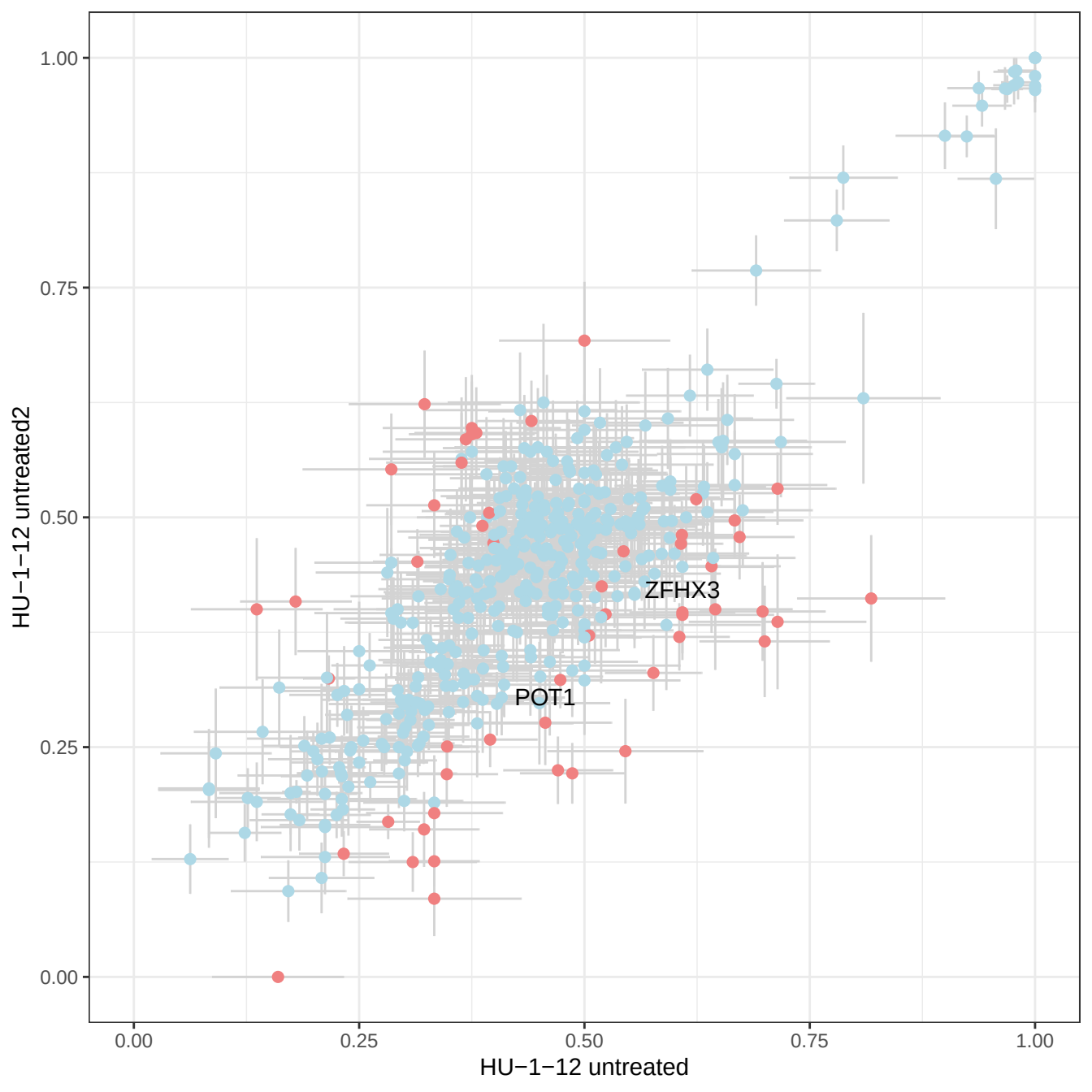
1.00
0.75
0.50
0.25
0.00
HU−1−12 untreated2
0.00
0.25
0.50
0.75
1.00
HU−1−12 untreated
ZFHX3
POT1

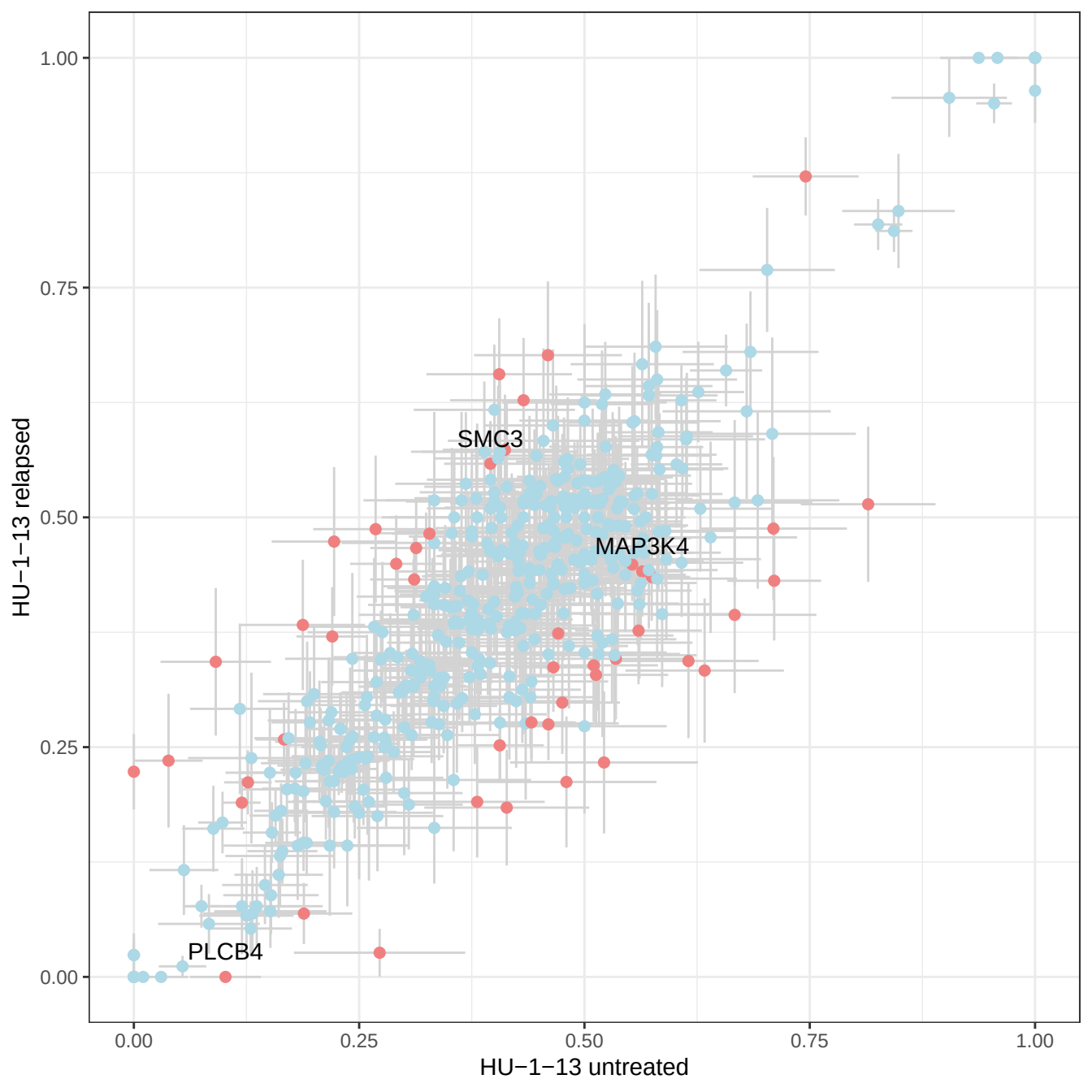
1.00
0.75
0.50
0.25
0.00
HU−1−13 relapsed
SMC3
MAP3K4
PLCB4
0.00
0.25
0.50
0.75
1.00
HU−1−13 untreated

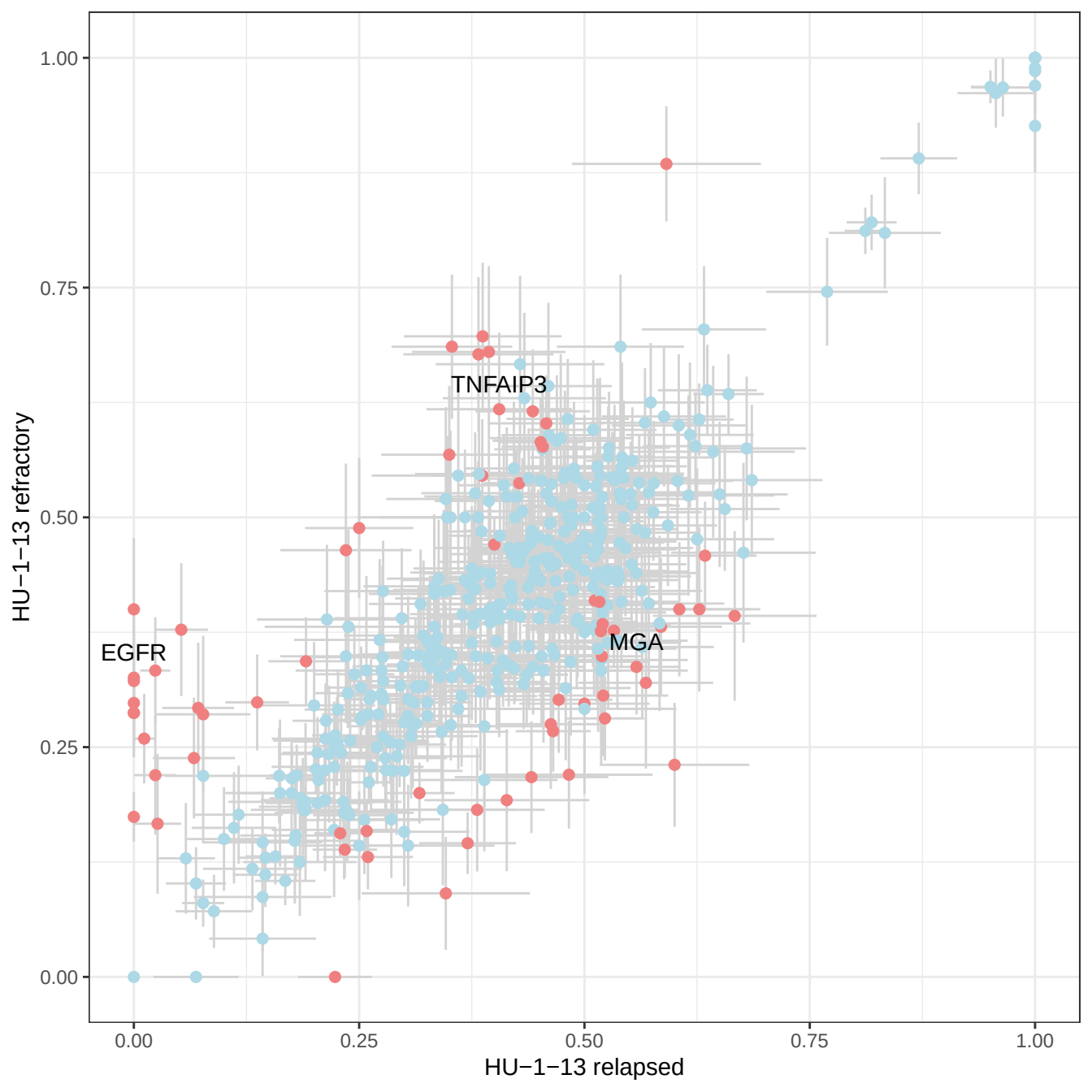
1.00
0.75
0.50
0.25
0.00
HU−1−13 refractory
0.00
0.25
0.50
0.75
1.00
HU−1−13 relapsed
TNFAIP3
MGA
EGFR

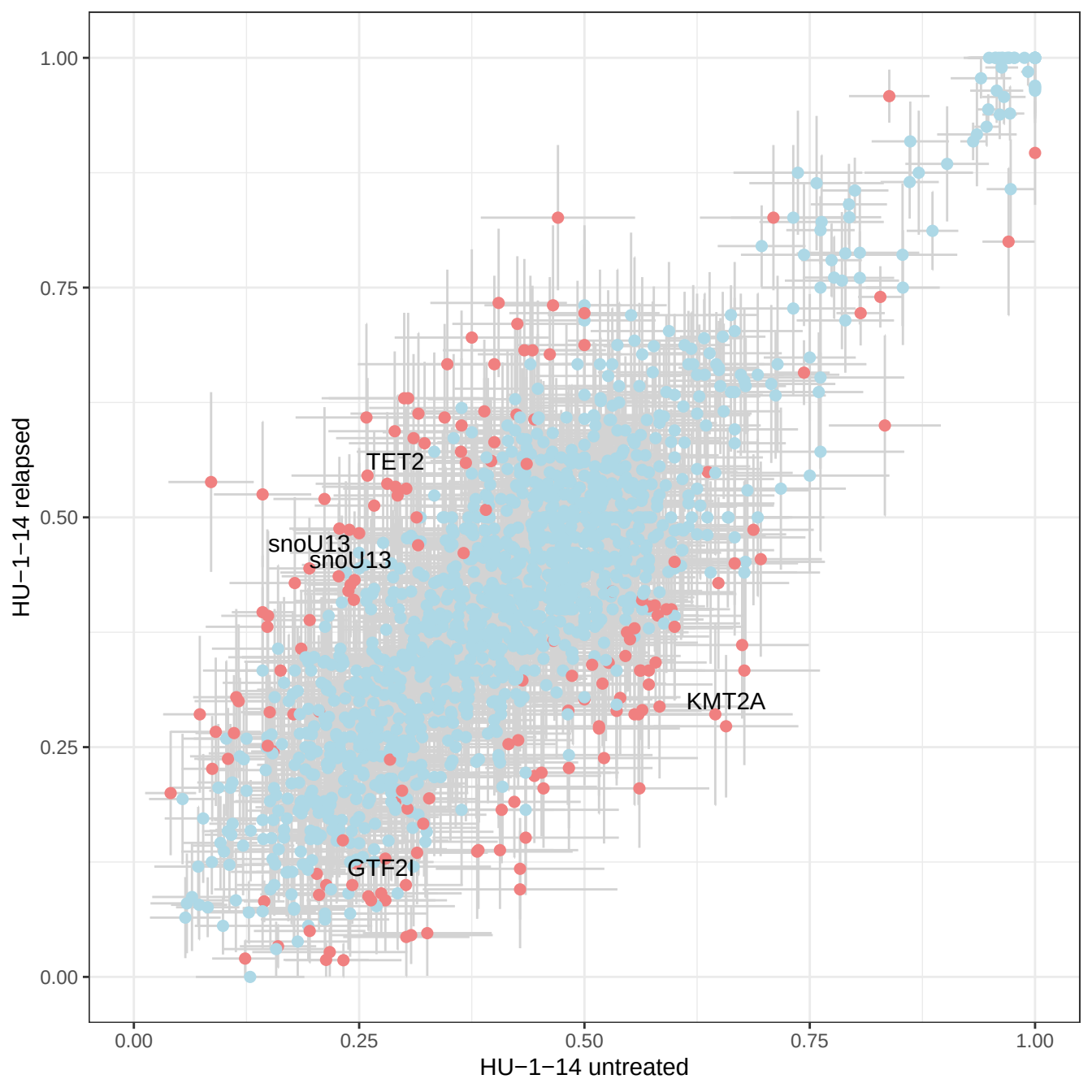
1.00
0.75
0.50
0.25
0.00
HU−1−14 relapsed
0.00
0.25
0.50
0.75
1.00
HU−1−14 untreated
TET2
snoU13
snoU13
KMT2A
GTF2I

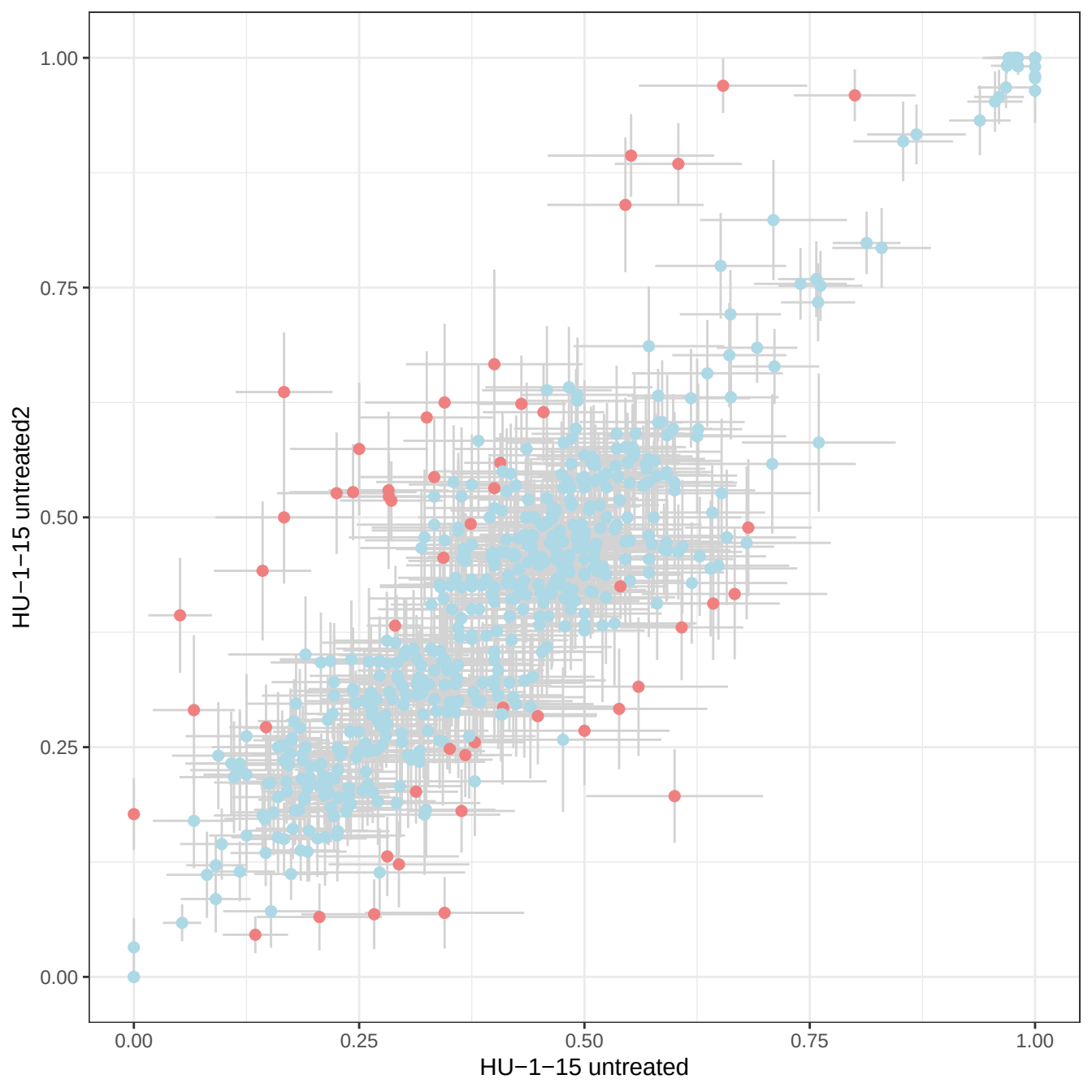
1.00
0.75
0.50
0.25
0.00
HU−1−15 untreated2
0.00
0.25
0.50
0.75
1.00
HU−1−15 untreated

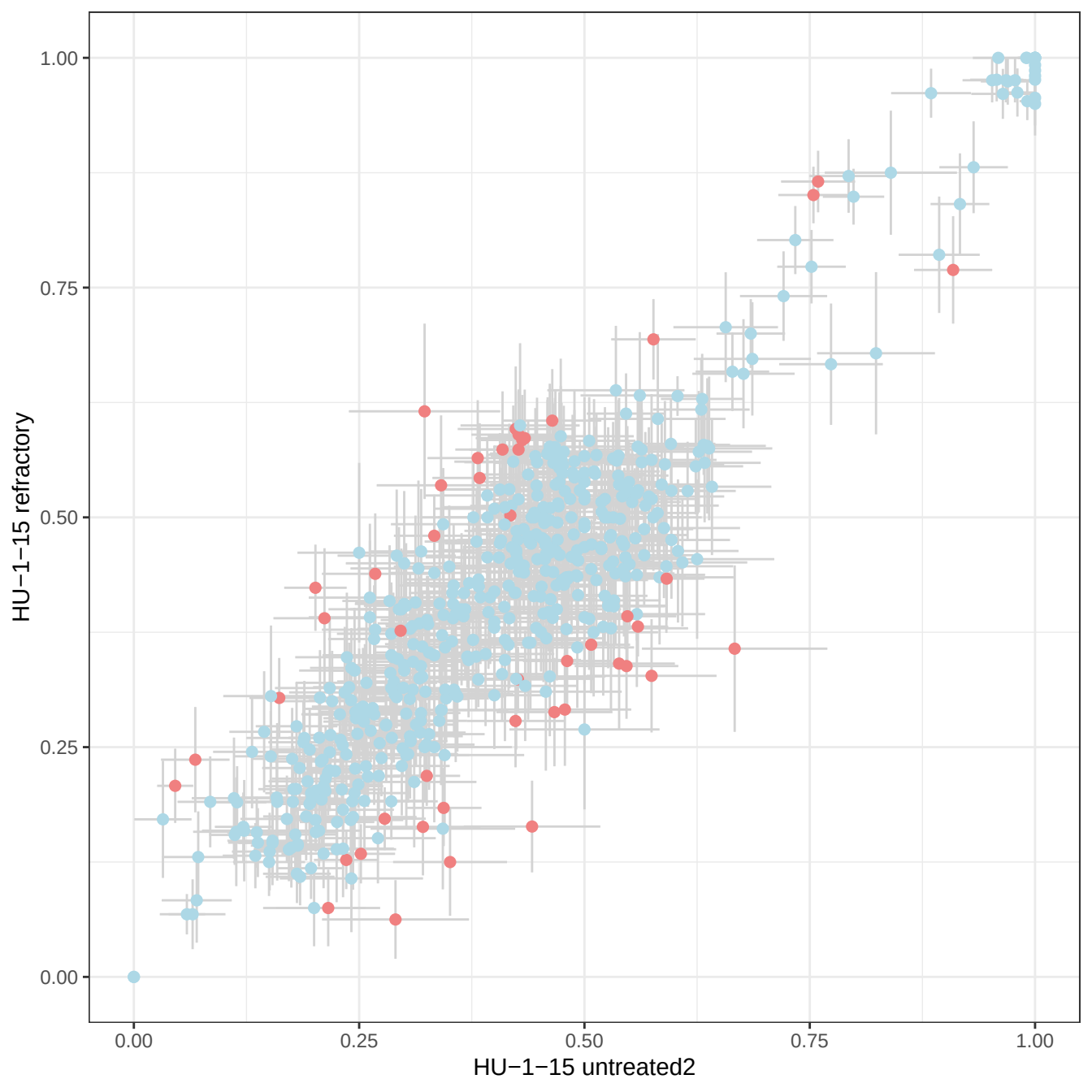
1.00
0.75
0.50
0.25
0.00
HU−1−15 refractory
0.00
0.25
0.50
0.75
1.00
HU−1−15 untreated2

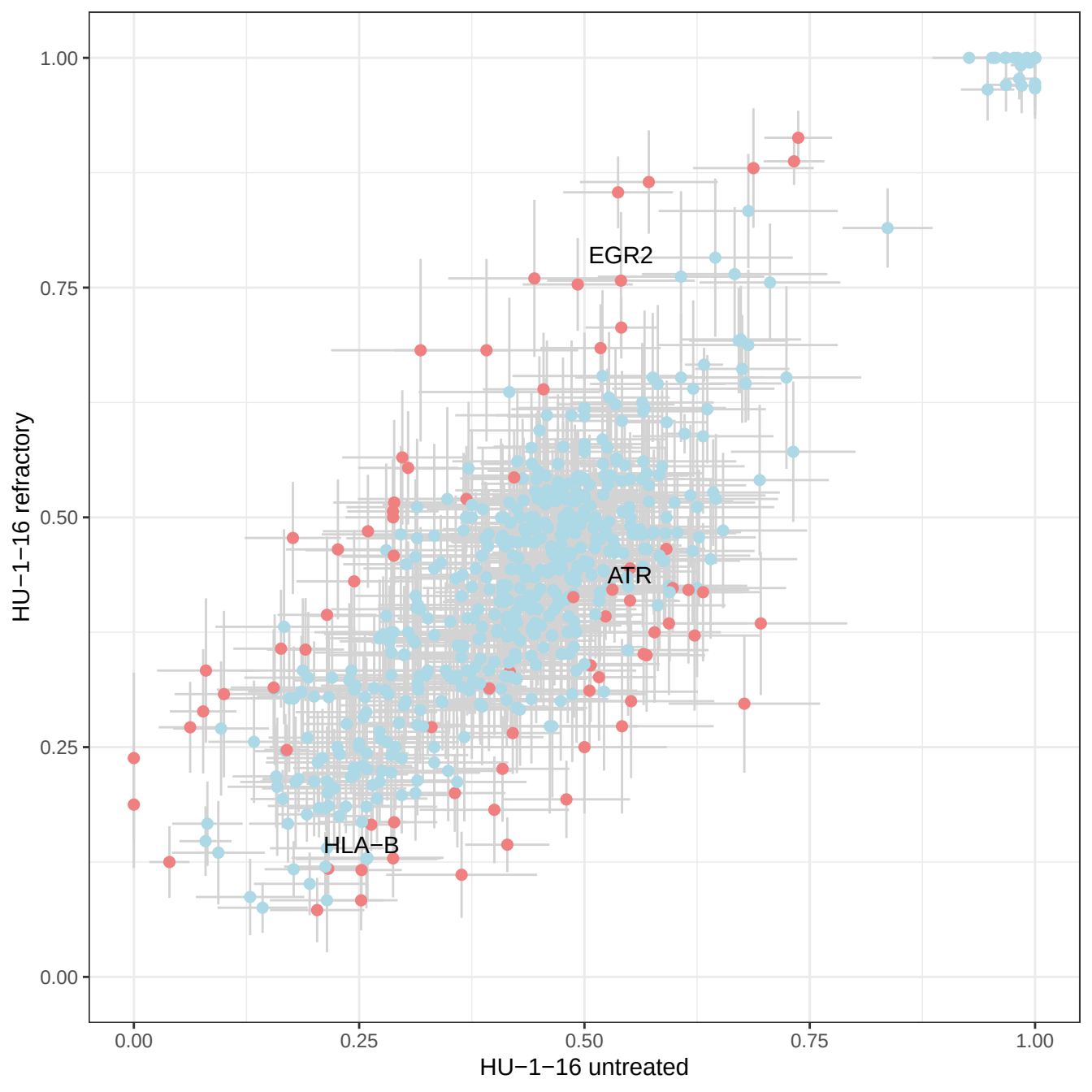
EGR2
ATR
HLA−B
1.00
0.75
0.50
0.25
0.00
HU−1−16 refractory
0.00
0.25
0.50
0.75
1.00
HU−1−16 untreated

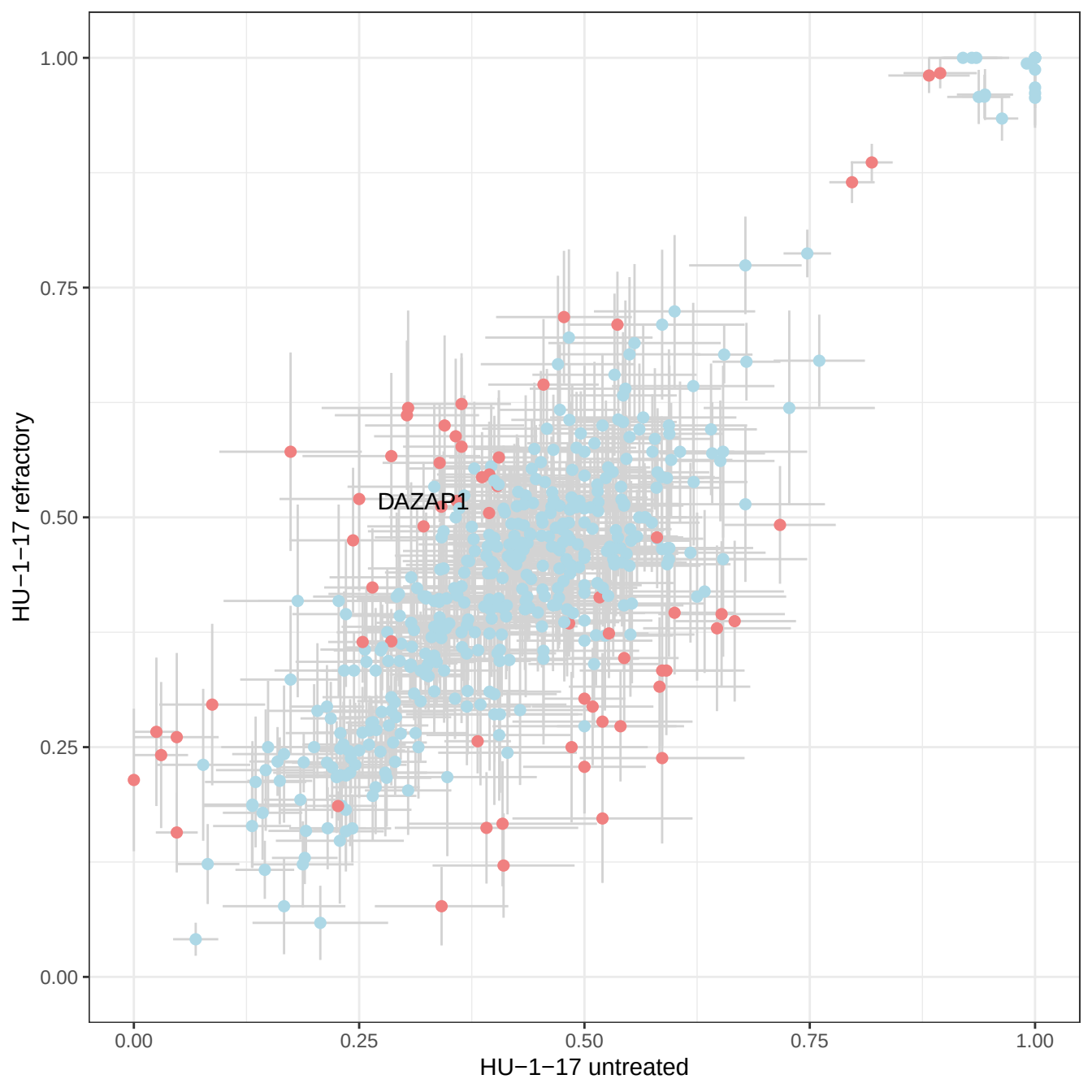
DAZAP1
HU−1−17 refractory
HU−1−17 untreated
0.00
0.25
0.50
0.75
1.00

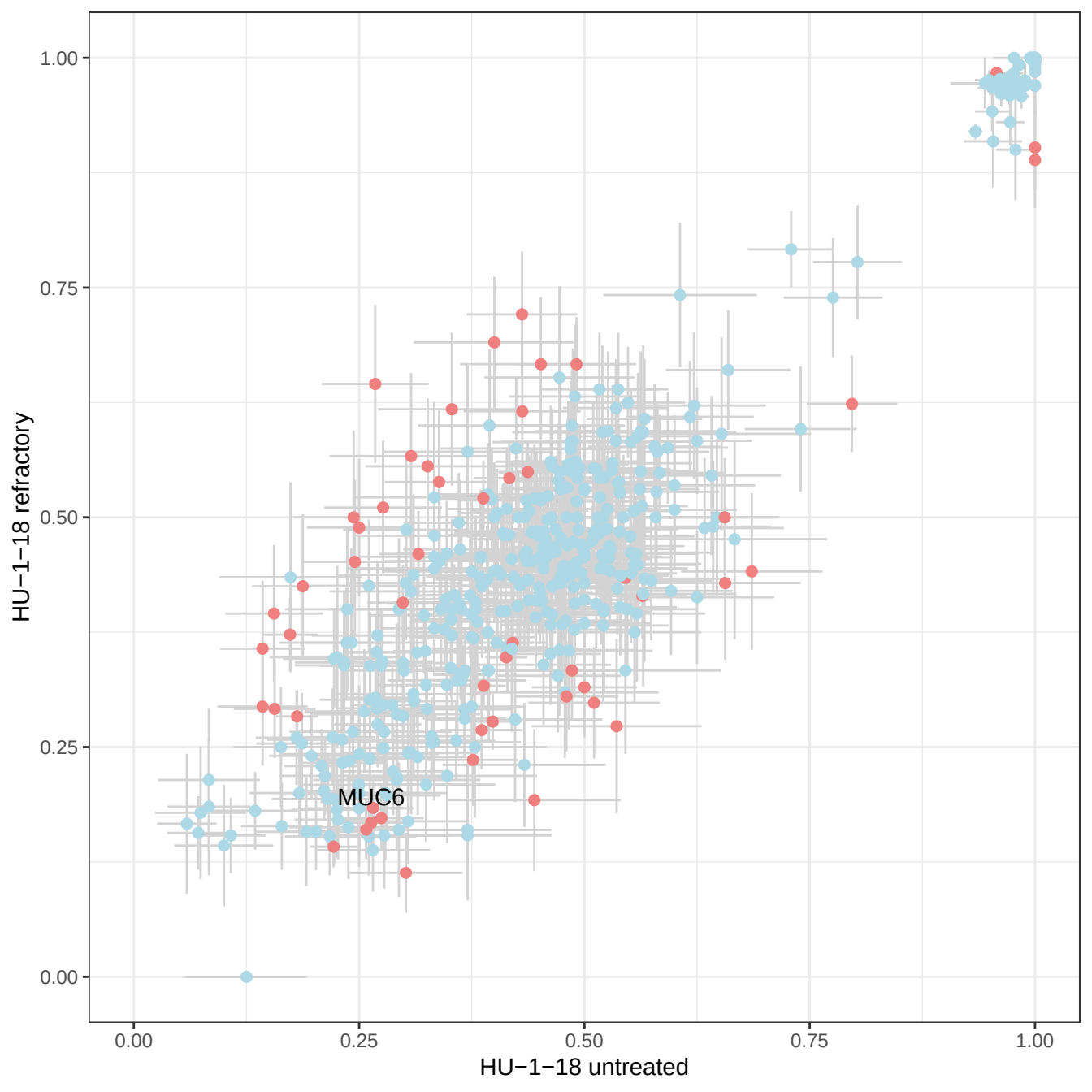
1.00
0.75
0.50
0.25
0.00
HU−1−18 refractory
MUC6
0.00
0.25
0.50
0.75
1.00
HU−1−18 untreated

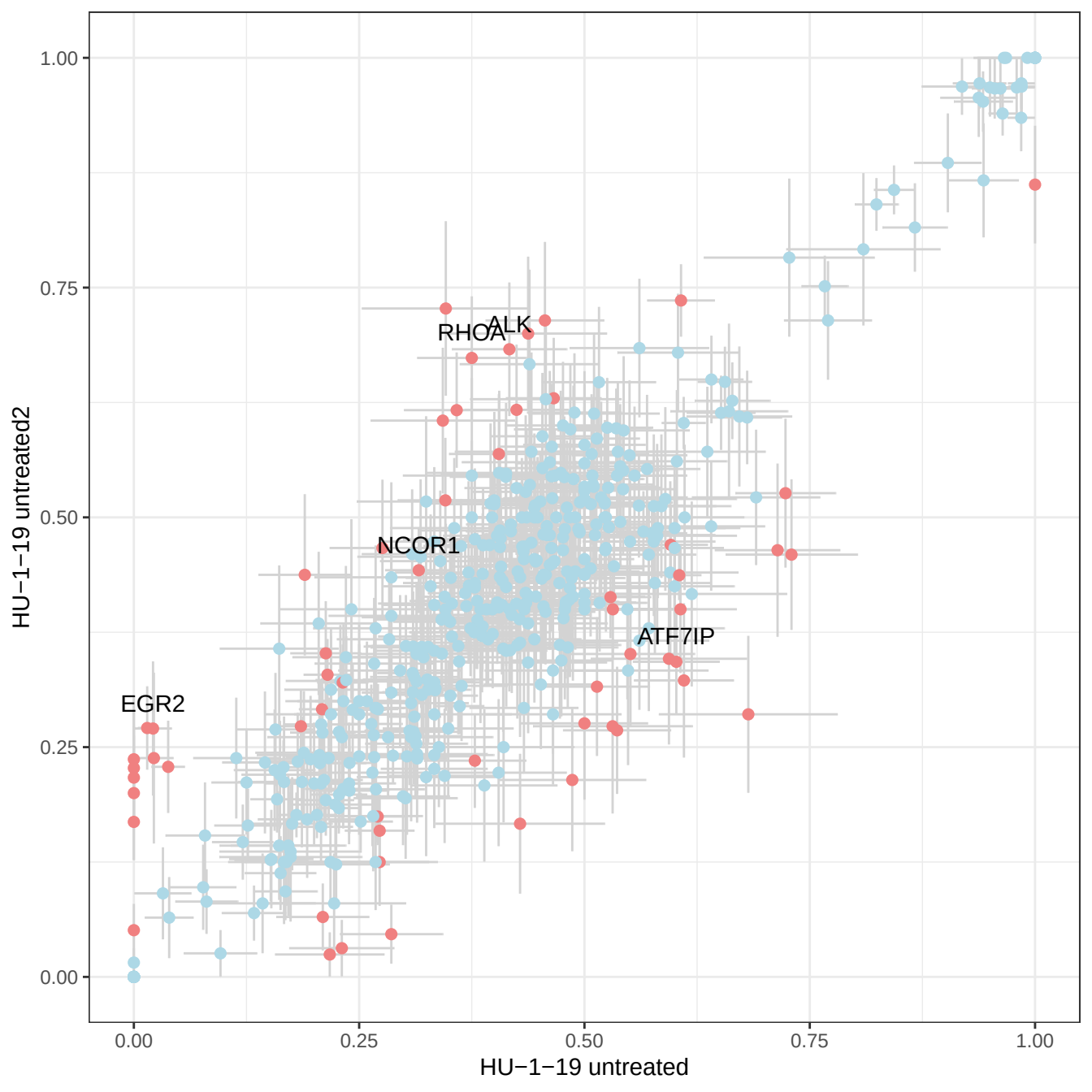
RHOA
ALK
NCOR1
ATF7IP
EGR2
1.00
0.75
0.50
0.25
0.00
HU−1−19 untreated2
0.00
0.25
0.50
0.75
1.00
HU−1−19 untreated

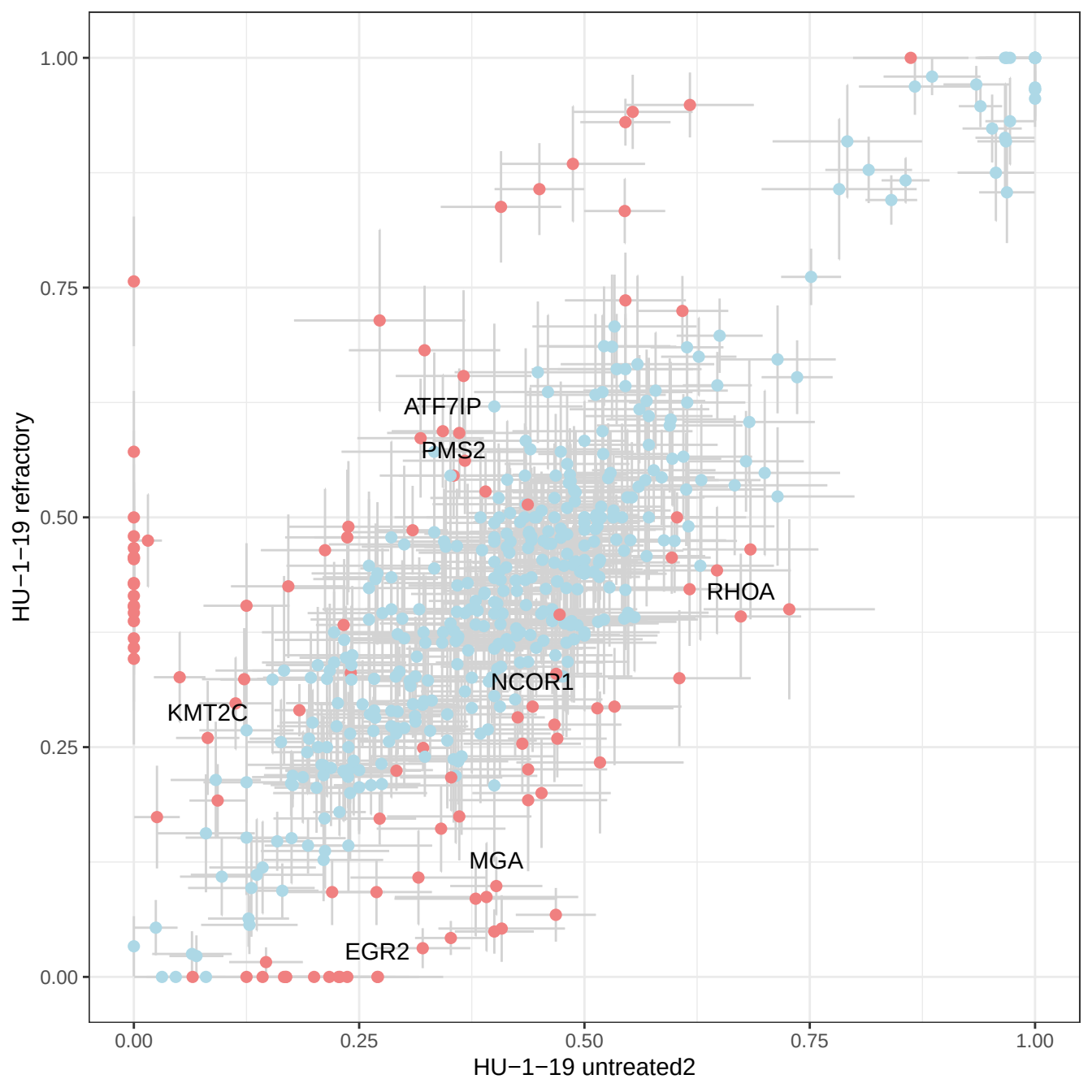
1.00
0.75
0.50
0.25
0.00
HU−1−19 refractory
0.00
0.25
0.50
0.75
1.00
HU−1−19 untreated2
ATF7IP
PMS2
RHOA
NCOR1
KMT2C
MGA
EGR2

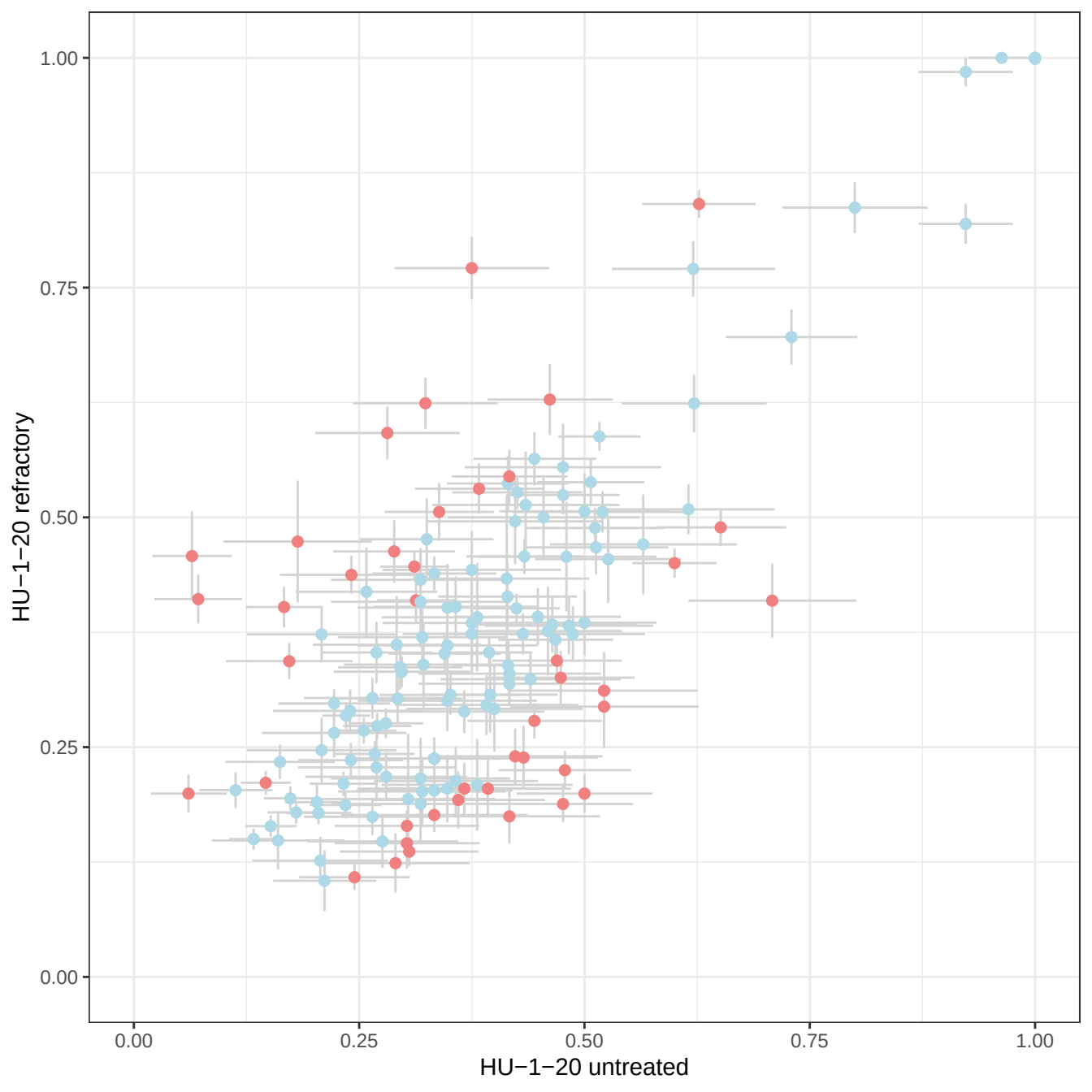
1.00
0.75
0.50
0.25
0.00
HU−1−20 refractory
0.00
0.25
0.50
0.75
1.00
HU−1−20 untreated

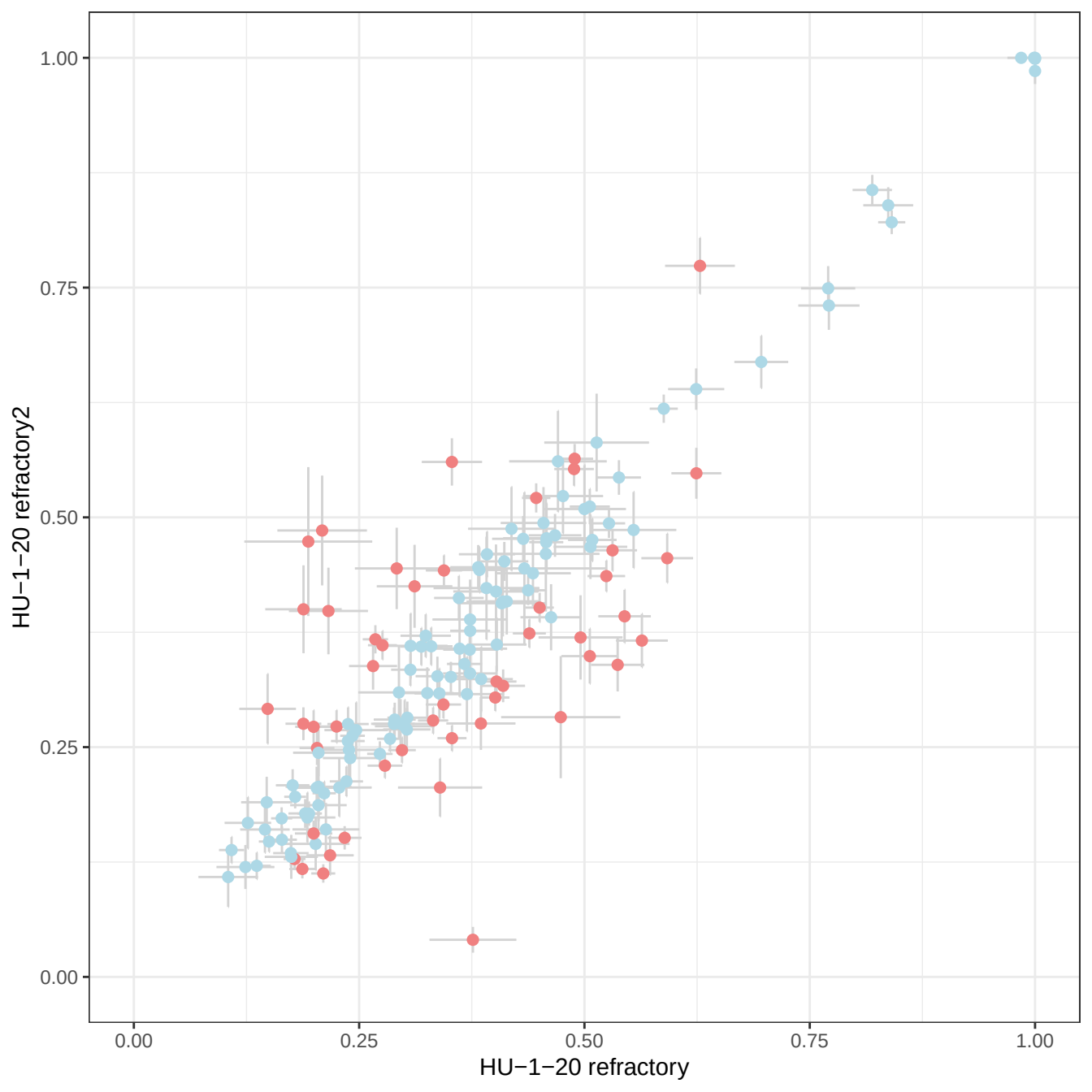
1.00
0.75
0.50
0.25
0.00
HU−1−20 refractory2
0.00
0.25
0.50
0.75
1.00
HU−1−20 refractory

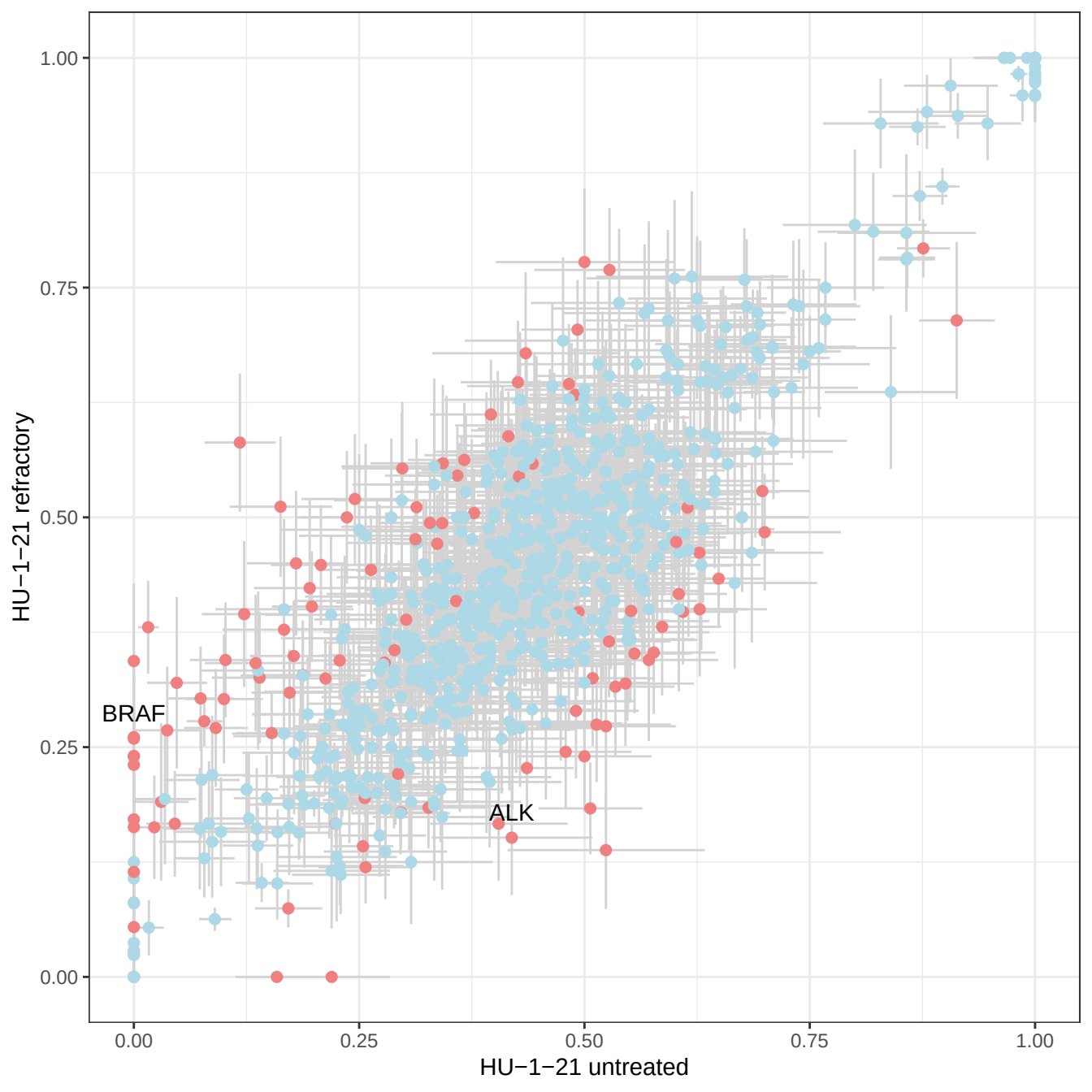
1.00
0.75
0.50
0.25
0.00
HU−1−21 refractory
BRAF
ALK
0.00
0.25
0.50
0.75
1.00
HU−1−21 untreated

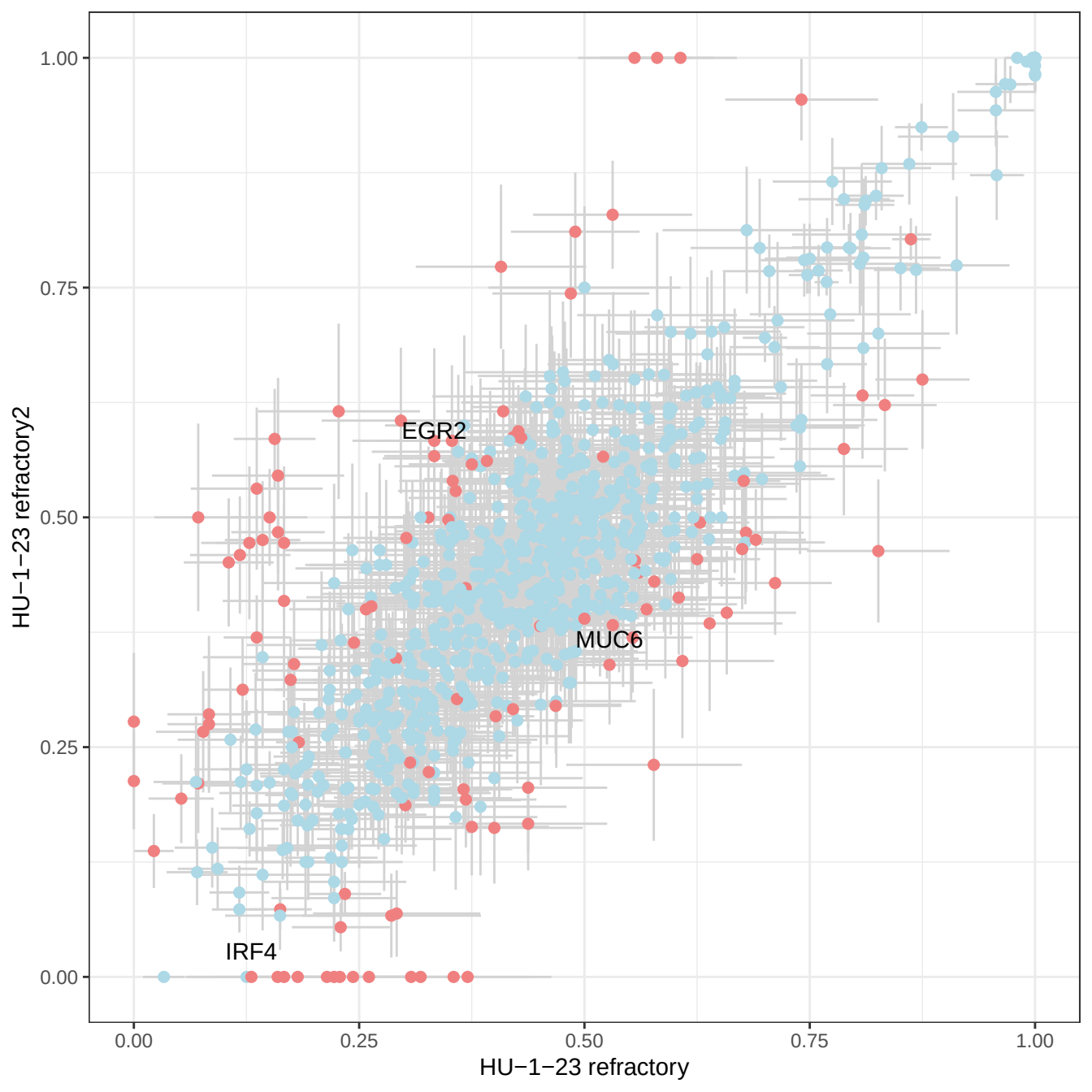
EGR2
MUC6
IRF4
1.00
0.75
0.50
0.25
0.00
HU−1−23 refractory2
0.00
0.25
0.50
0.75
1.00
HU−1−23 refractory

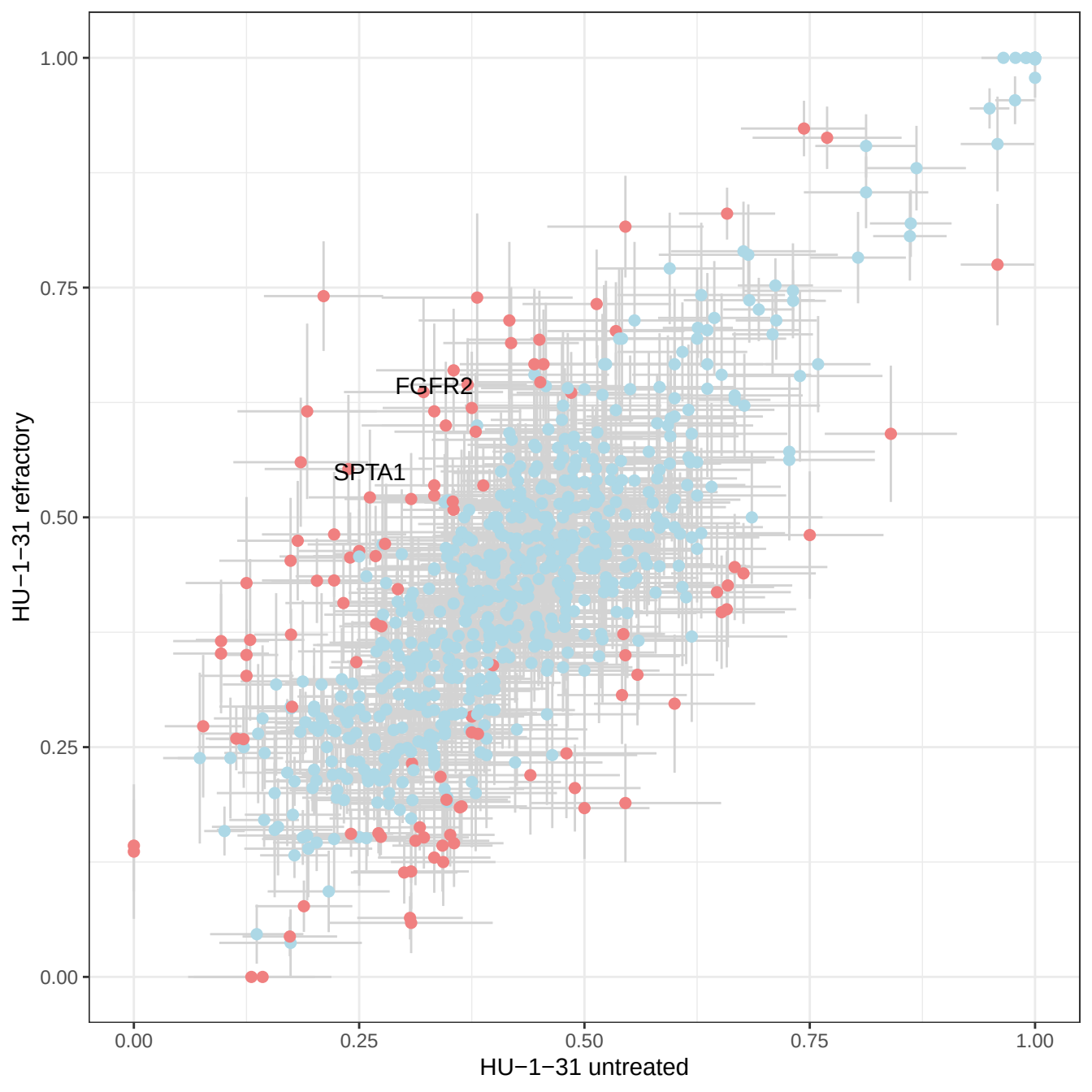
FGFR2
SPTA1
1.00
0.75
0.50
0.25
0.00
HU−1−31 refractory
0.00
0.25
0.50
0.75
1.00
HU−1−31 untreated

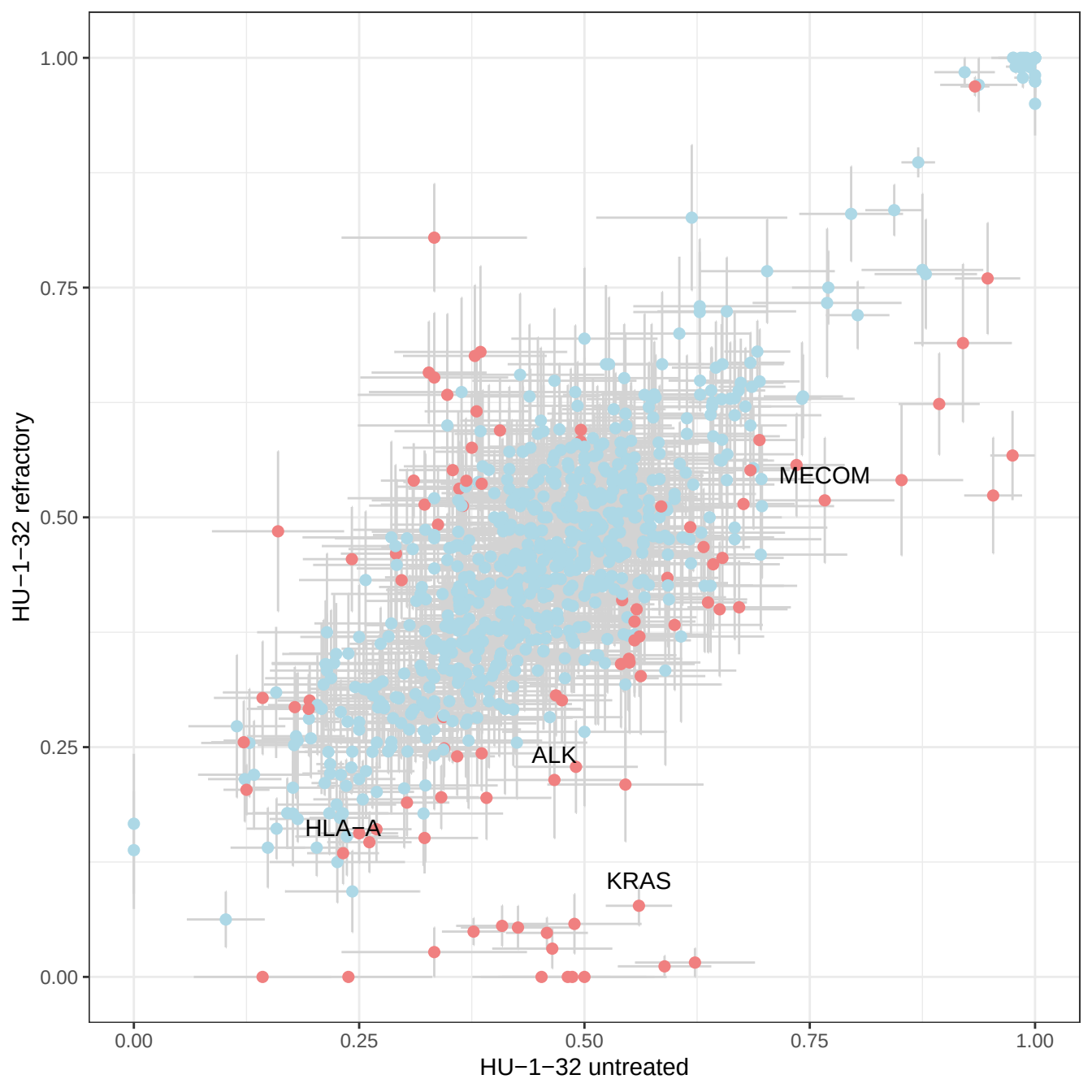
1.00
0.75
0.50
0.25
0.00
HU−1−32 refractory
0.00
0.25
0.50
0.75
1.00
HU−1−32 untreated
MECOM
ALK
HLA−A
KRAS

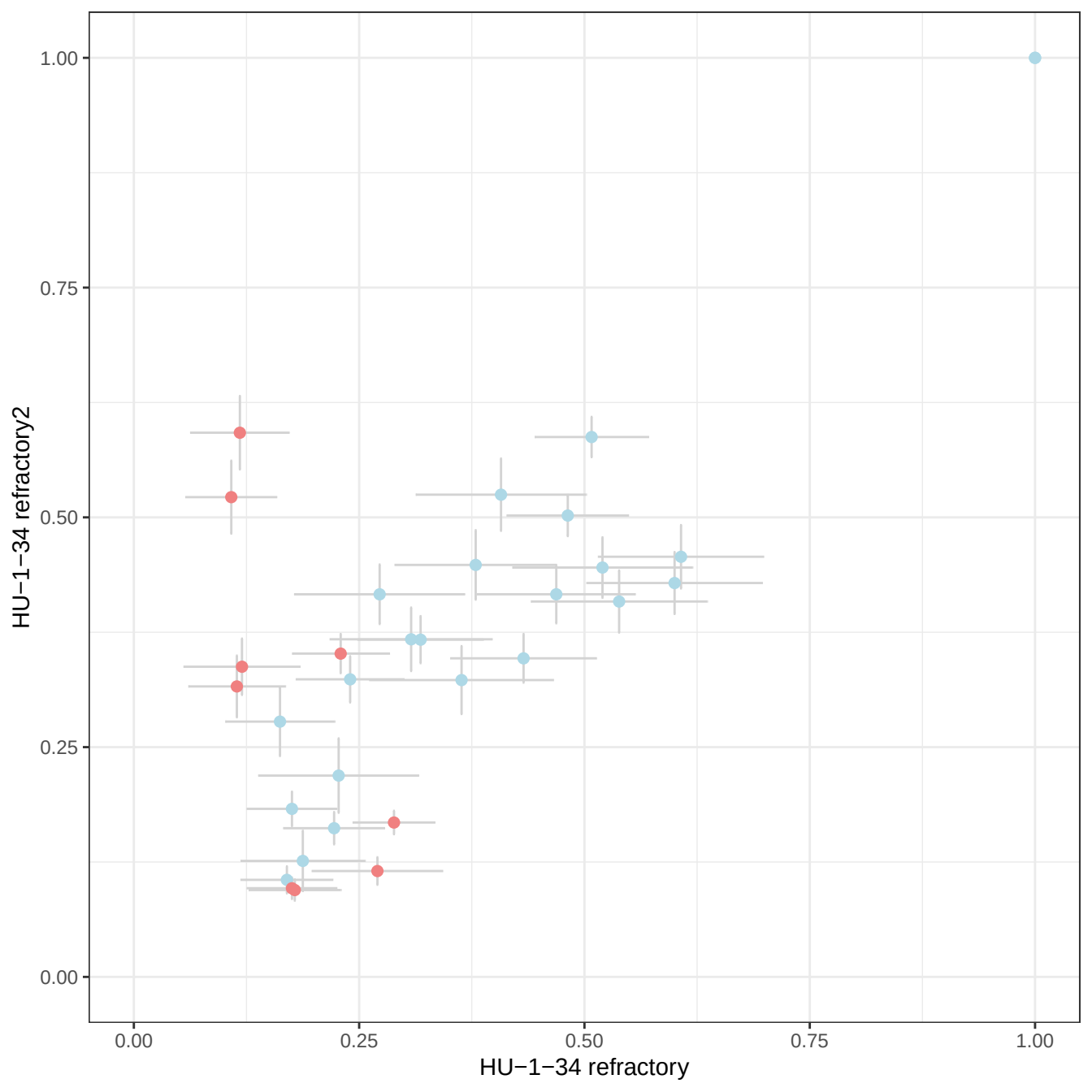
1.00
0.75
0.50
0.25
0.00
HU−1−34 refractory2
0.00
0.25
0.50
0.75
1.00
HU−1−34 refractory

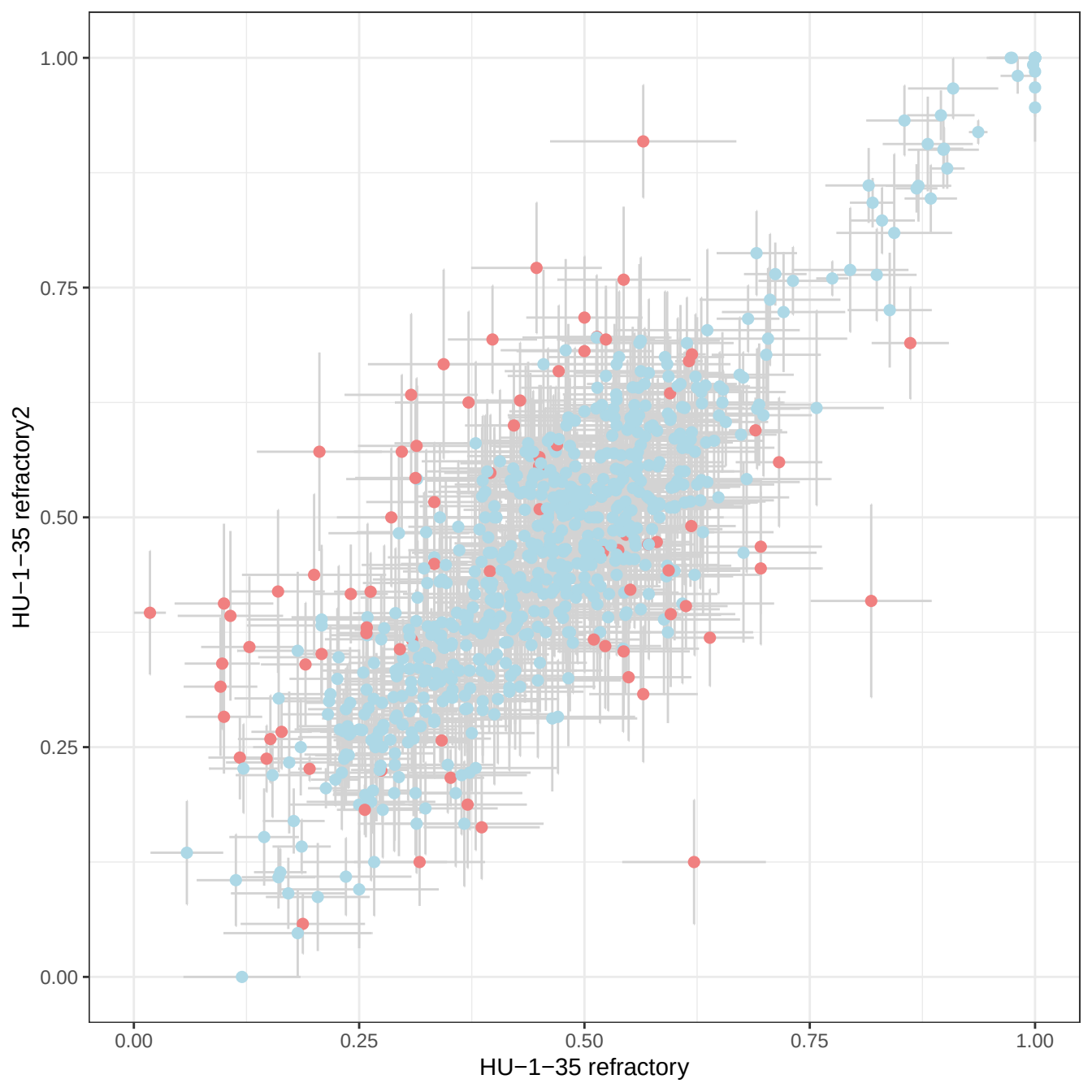
1.00
0.75
0.50
0.25
0.00
HU−1−35 refractory2
0.00
0.25
0.50
0.75
1.00
HU−1−35 refractory

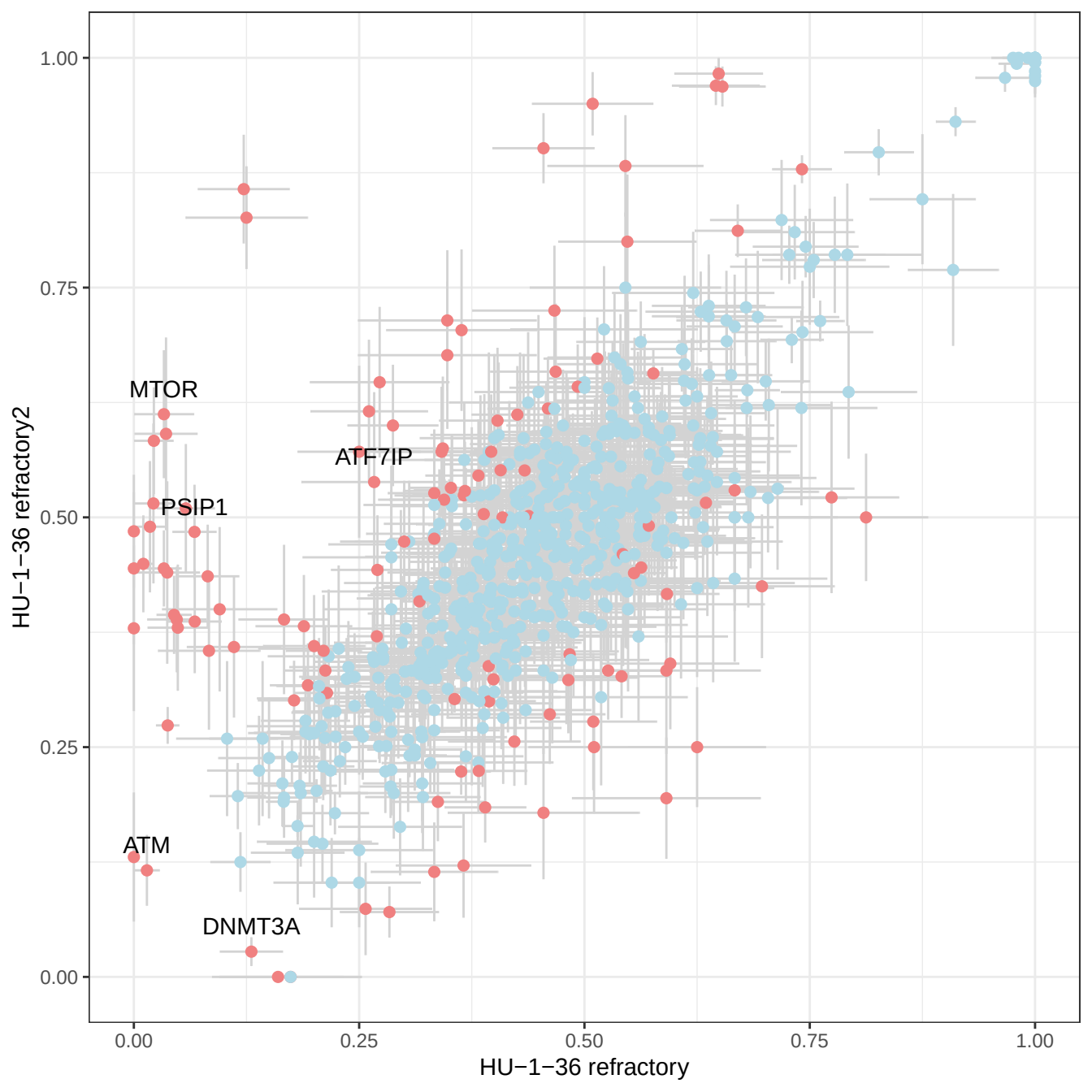
MTOR
ATF7IP
PSIP1
ATM
DNMT3A
1.00
0.75
0.50
0.25
0.00
HU−1−36 refractory2
0.00
0.25
0.50
0.75
1.00
HU−1−36 refractory

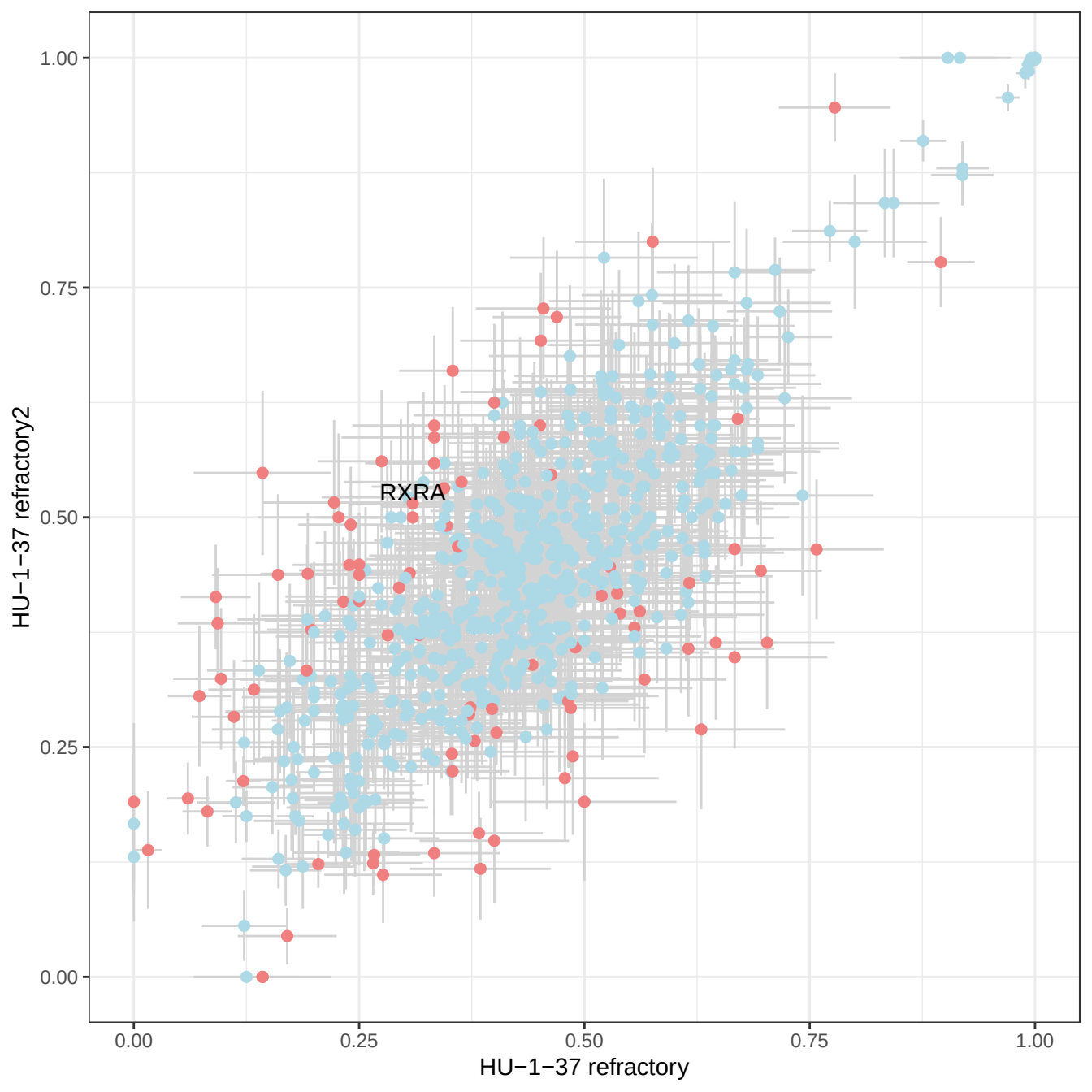
RXRA
1.00
0.75
0.50
0.25
0.00
HU−1−37 refractory2
0.00
0.25
0.50
0.75
1.00
HU−1−37 refractory

Suppl. figure 3: Copy number estimation based on read counts from exome sequencing. First panel genome wide log2 ratio of tumor vs. control counts. Second panel copy number log2 ratio plot for regions analyzed by FISH. Third panel presenting density of log2 ratio regions. Fourth panel presenting genome wide log2 copy number.

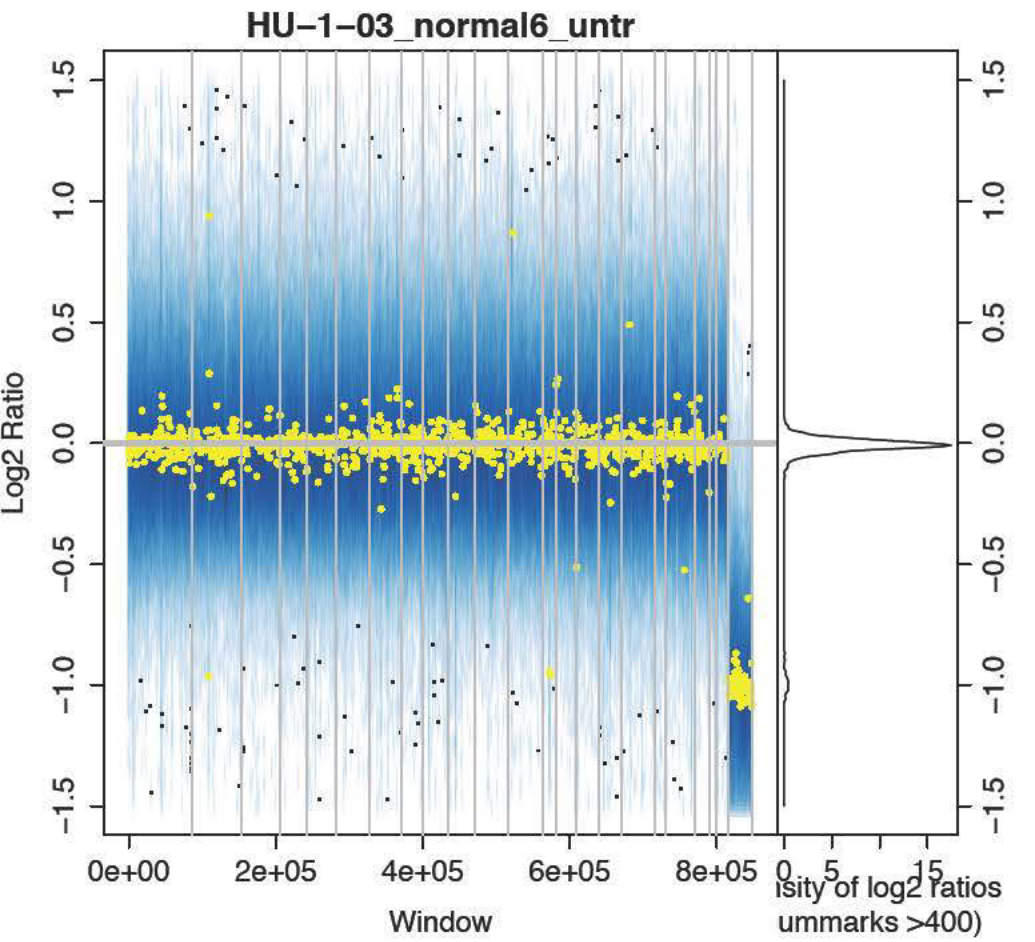
HU−1−03_normal6_untr
Log2 Ratio
1.5
1.0
0.5
0.0
−0.5
−1.0
−1.5
0e+00
2e+05
4e+05
6e+05
8e+05
Window
0
5
15
sity of log2 ratios
ummarks >400)

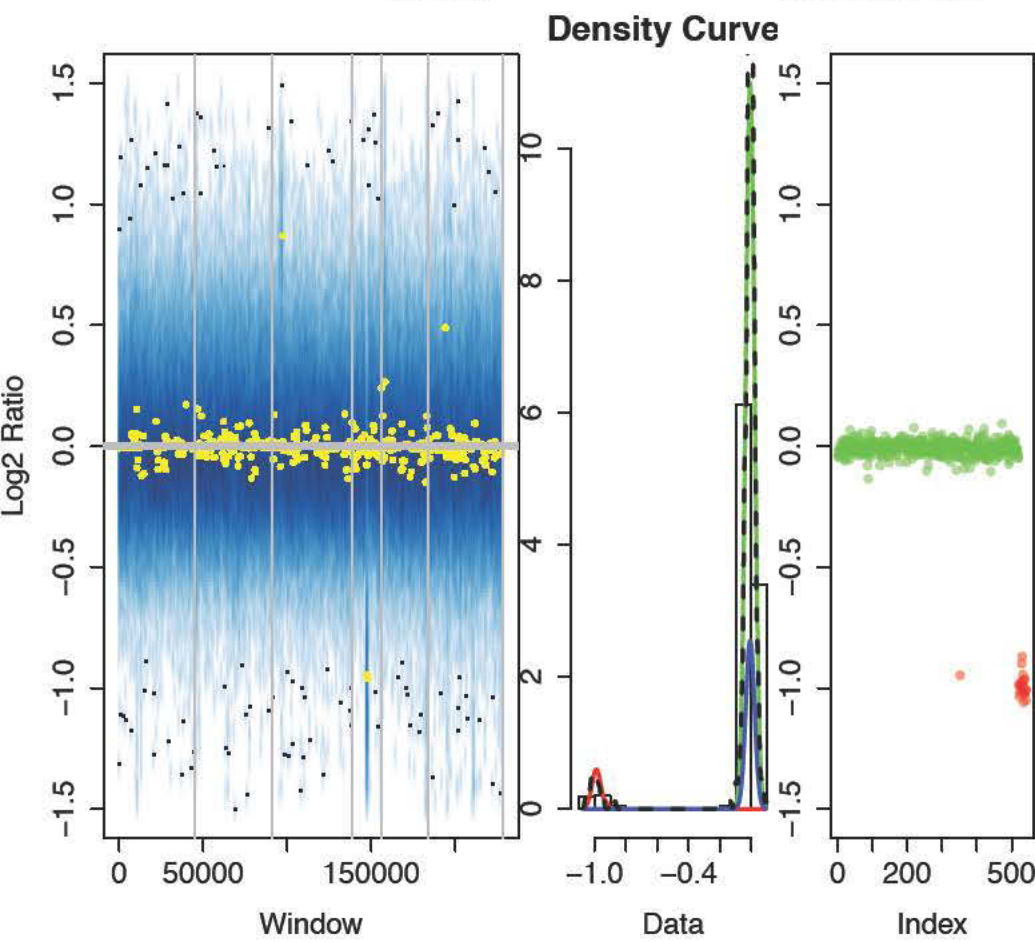
Density Curve
Log2 Ratio
1.5
1.0
0.5
0.0
−0.5
−1.0
−1.5
0
50000
150000
Window
0
2
4
6
8
10
−1.0
−0.4
Data
0
200
500
Index

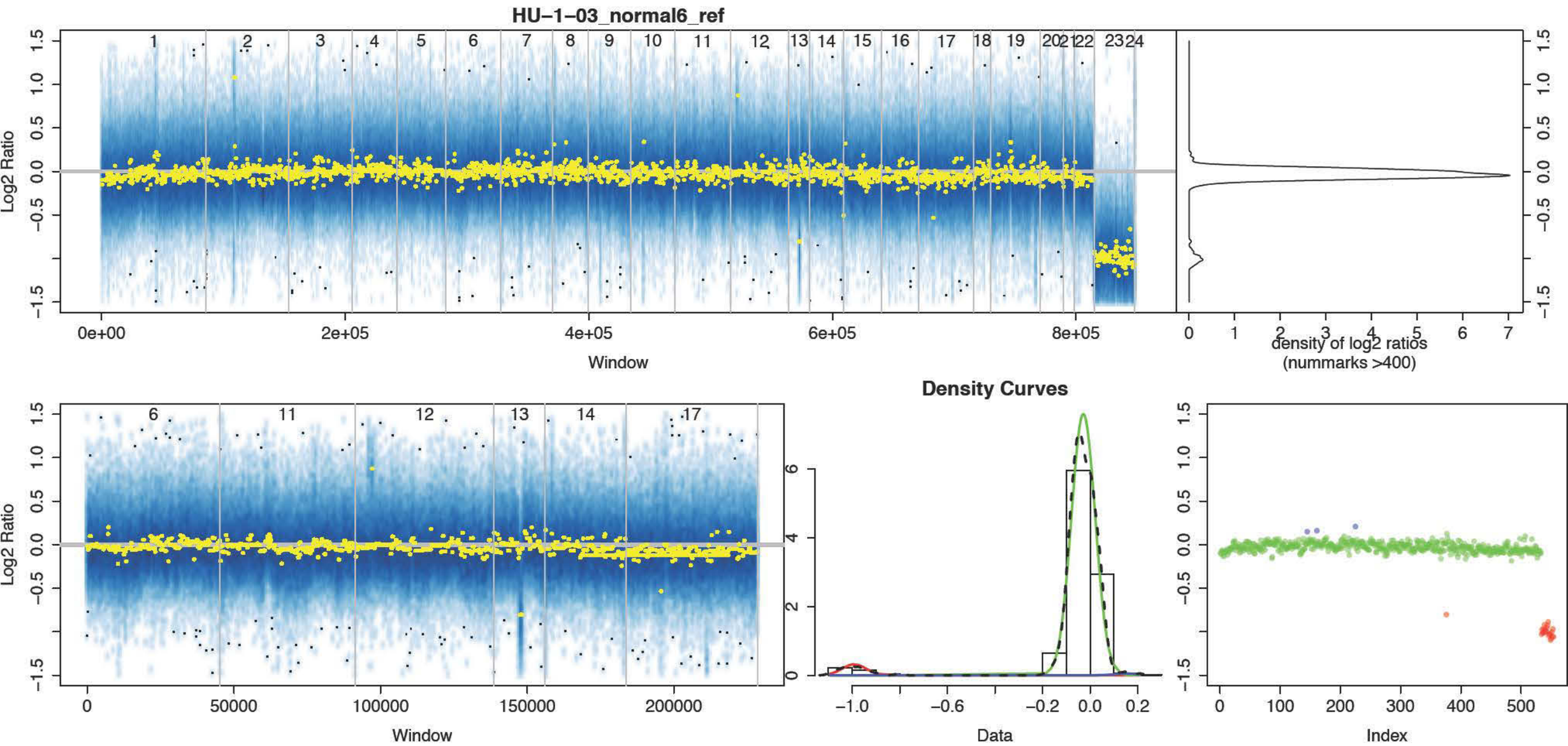
HU−1−03_normal6_ref
Log2 Ratio
Window
density of log2 ratios
(nummarks >400)
Density Curves
Data
Index

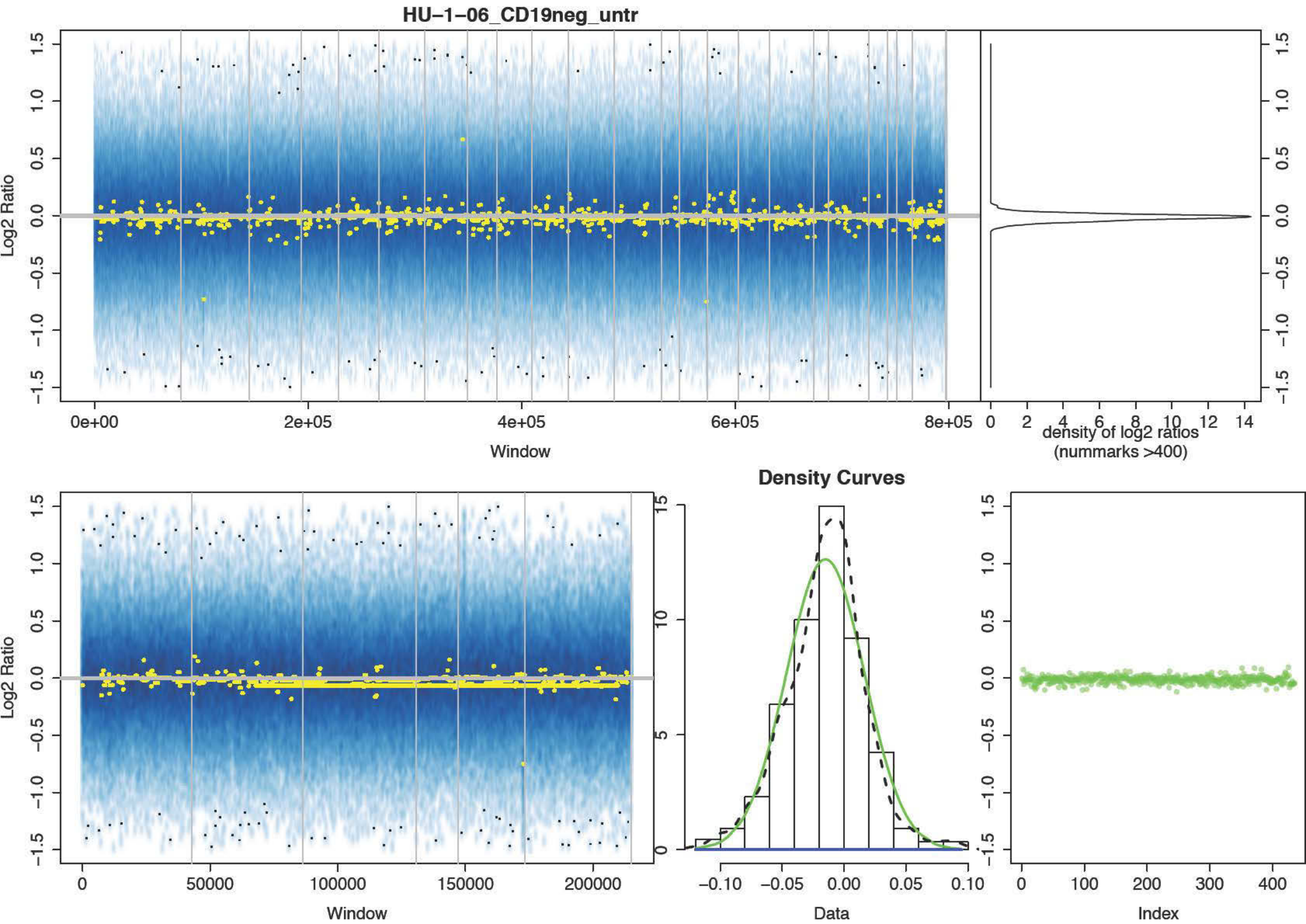
HU−1−06_CD19neg_untr
Log2 Ratio
Window
density of log2 ratios
(nummarks >400)
Density Curves
Log2 Ratio
Window
Data
Index

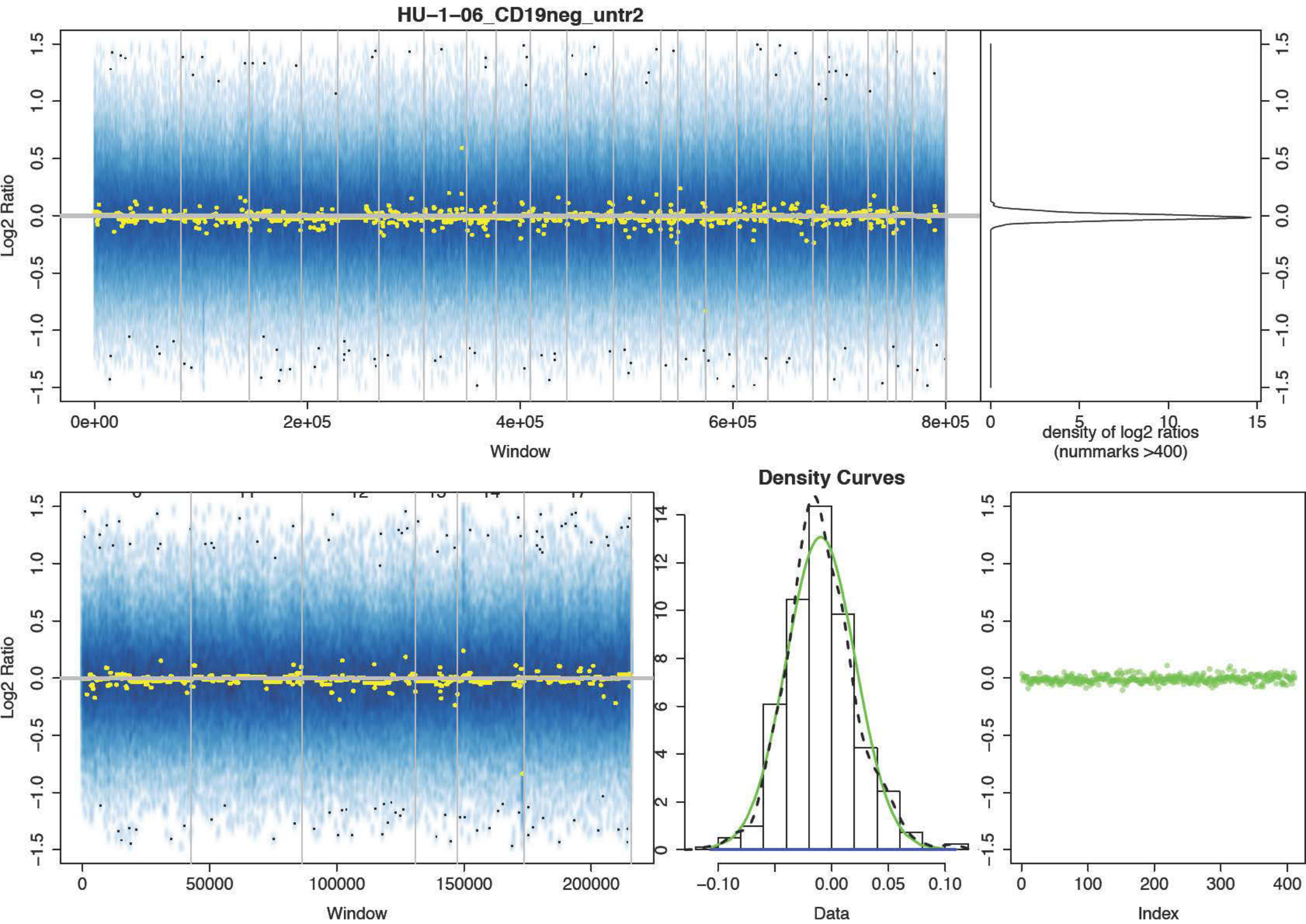
HU−1−06_CD19neg_untr2
Log2 Ratio
Window
density of log2 ratios
(nummarks >400)
Density Curves
Log2 Ratio
Window
Data
Index

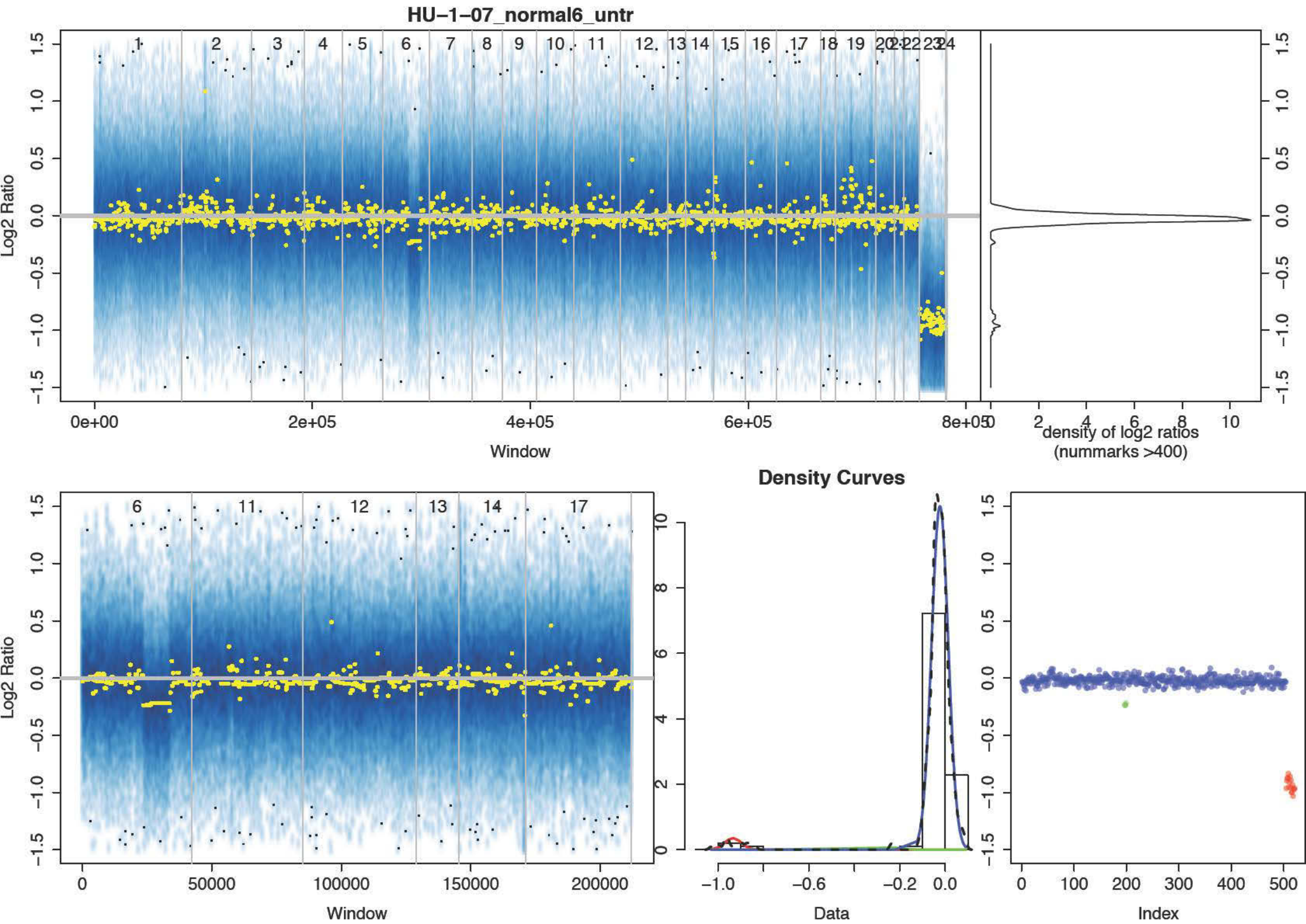
HU−1−07_normal6_untr
Log2 Ratio
Window
density of log2 ratios
(nummarks >400)
Density Curves
Data
Index

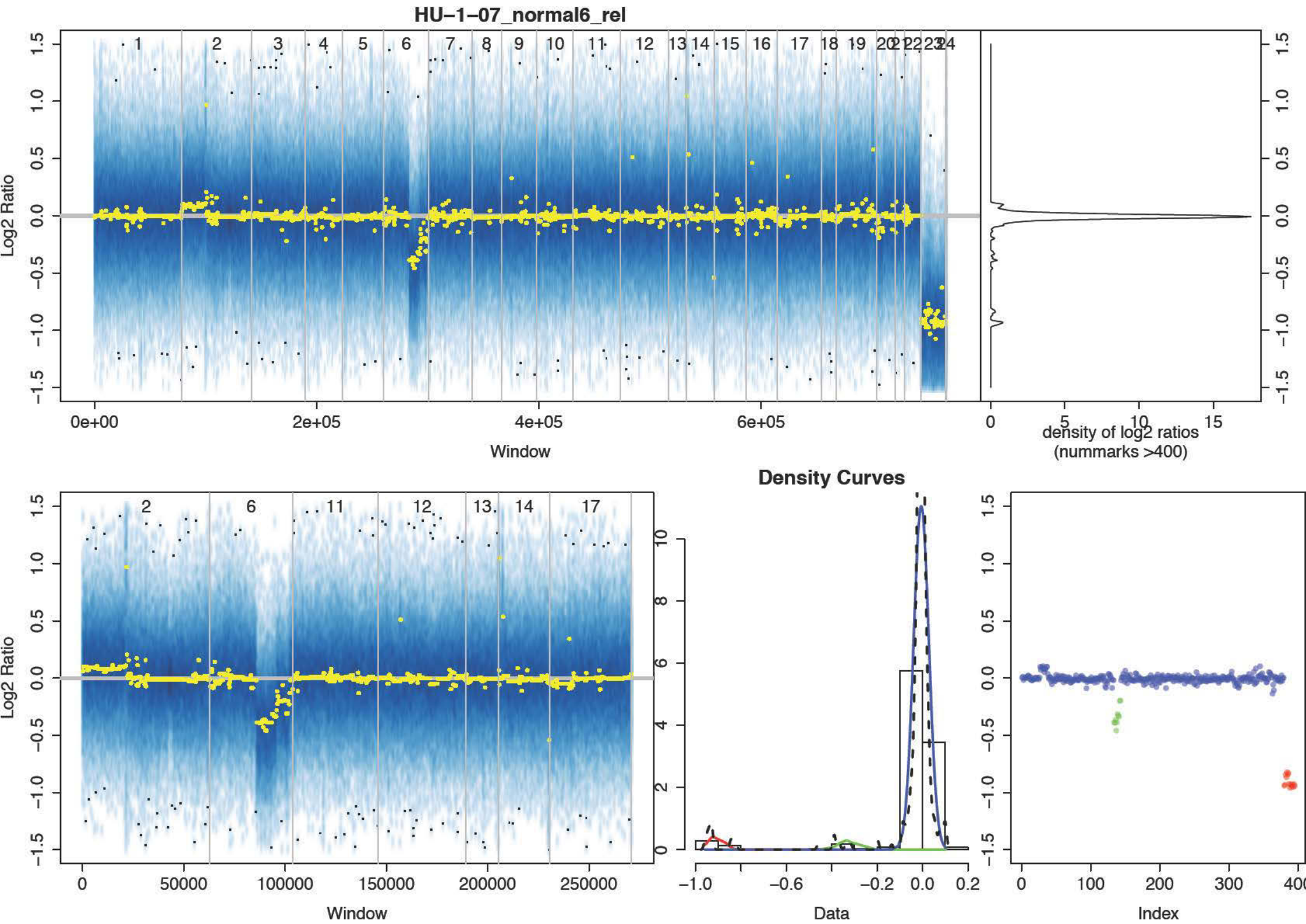
HU−1−07_normal6_rel
Log2 Ratio
Window
density of log2 ratios
(nummarks >400)
Density Curves
Data
Index

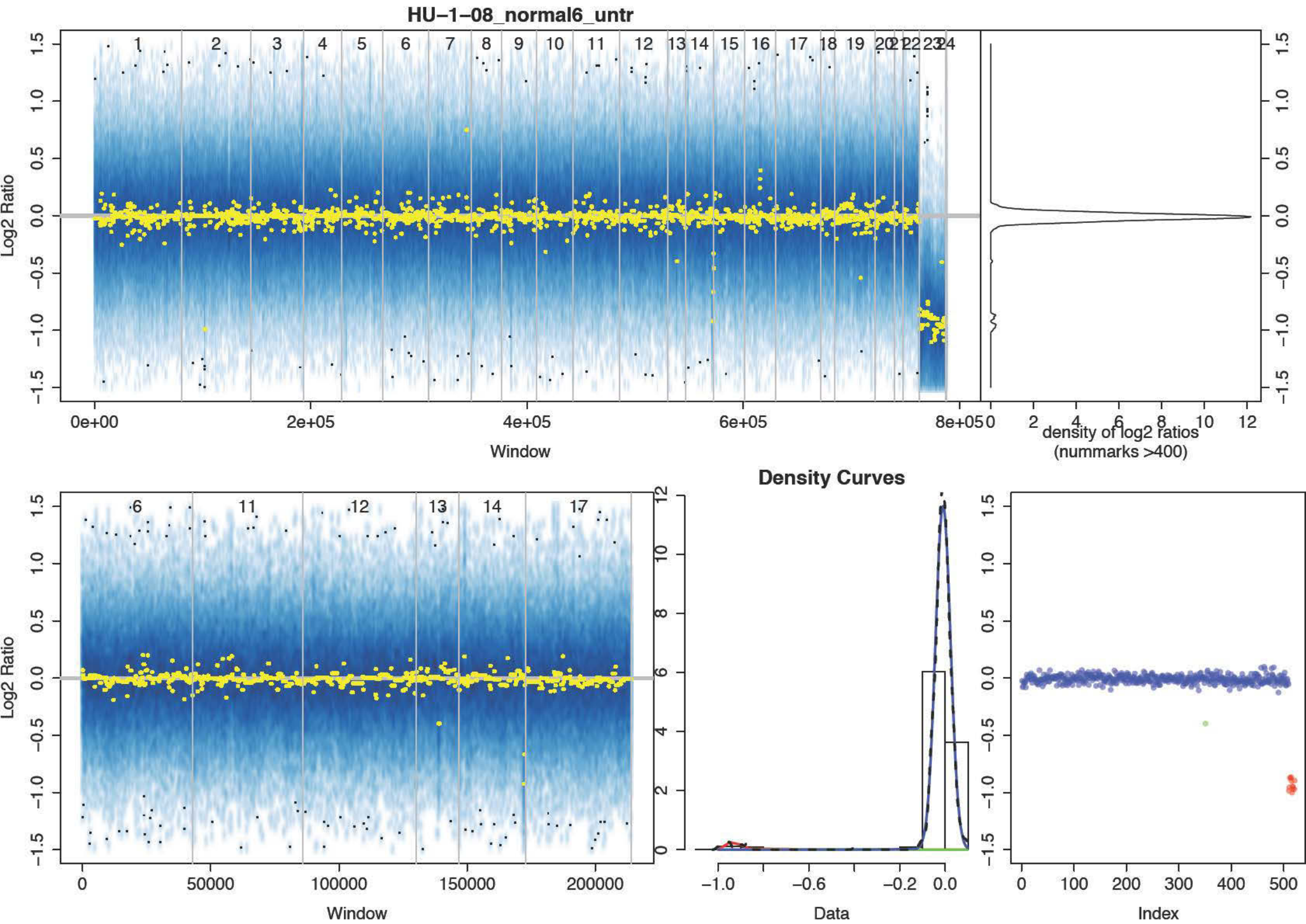
HU−1−08_normal6_untr
Log2 Ratio
Window
density of log2 ratios
(nummarks >400)
Density Curves
Data
Index

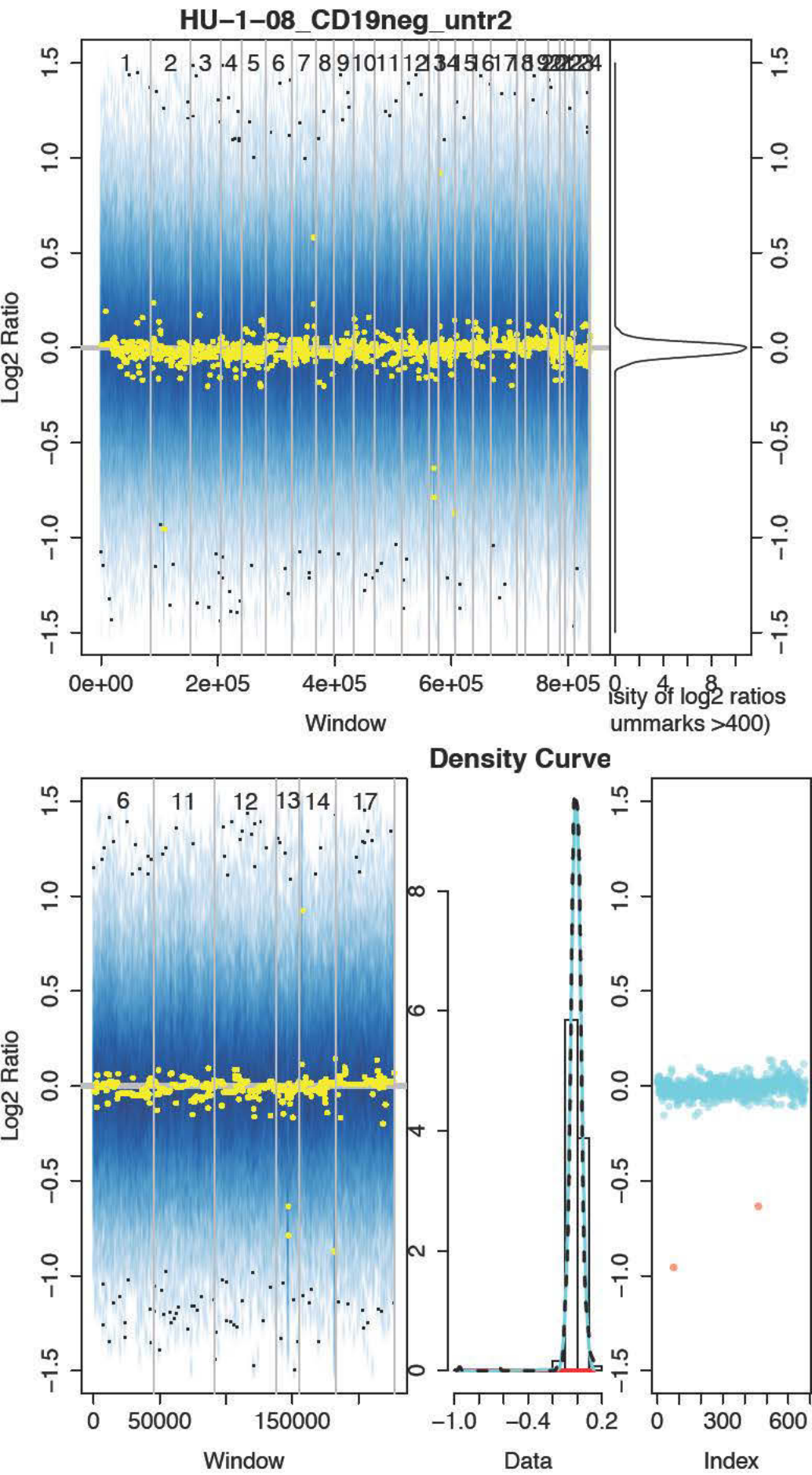
HU−1−08_CD19neg_untr2
Log2 Ratio
Window
0e+00
2e+05
4e+05
6e+05
8e+05
Density Curve
Data
Index
Window
0
50000
150000
−1.0
−0.4
0.2
0
300
600

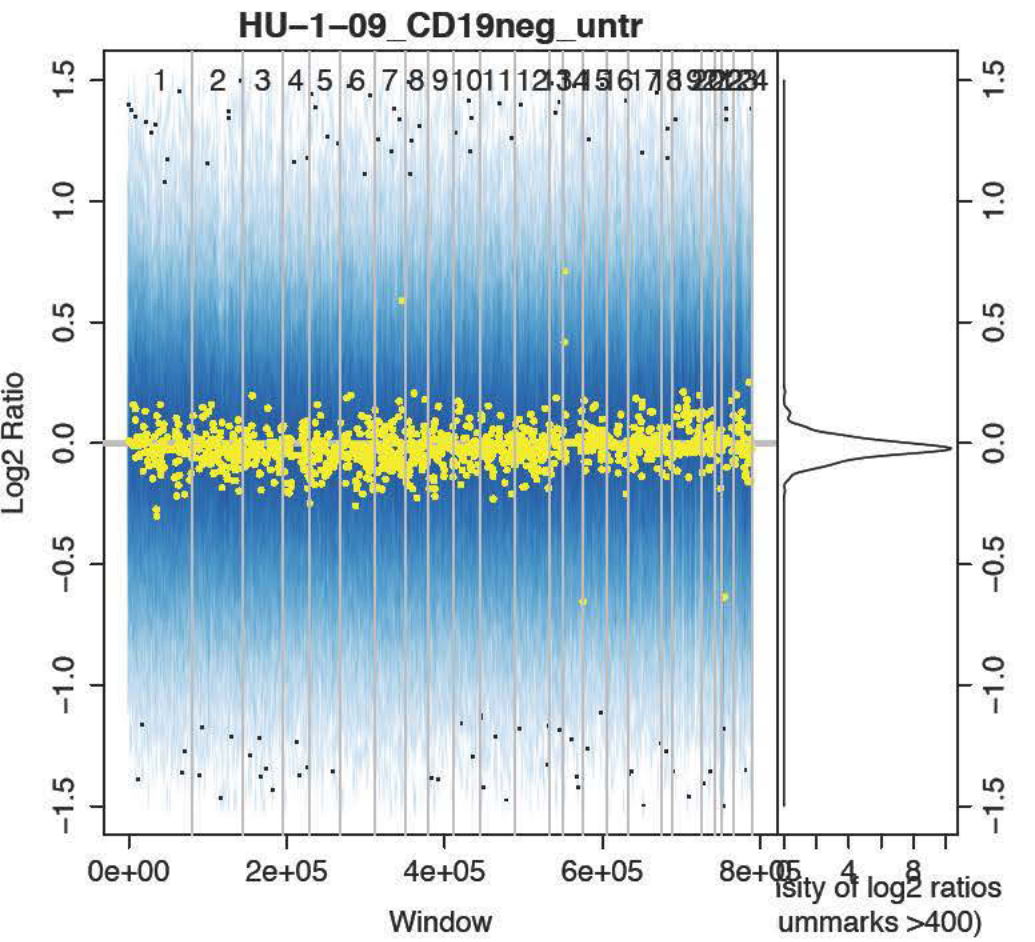
HU−1−09_CD19neg_untr
Log2 Ratio
Window
0e+00
2e+05
4e+05
6e+05
8e+05
sity of log2 ratios
ummarks >400)

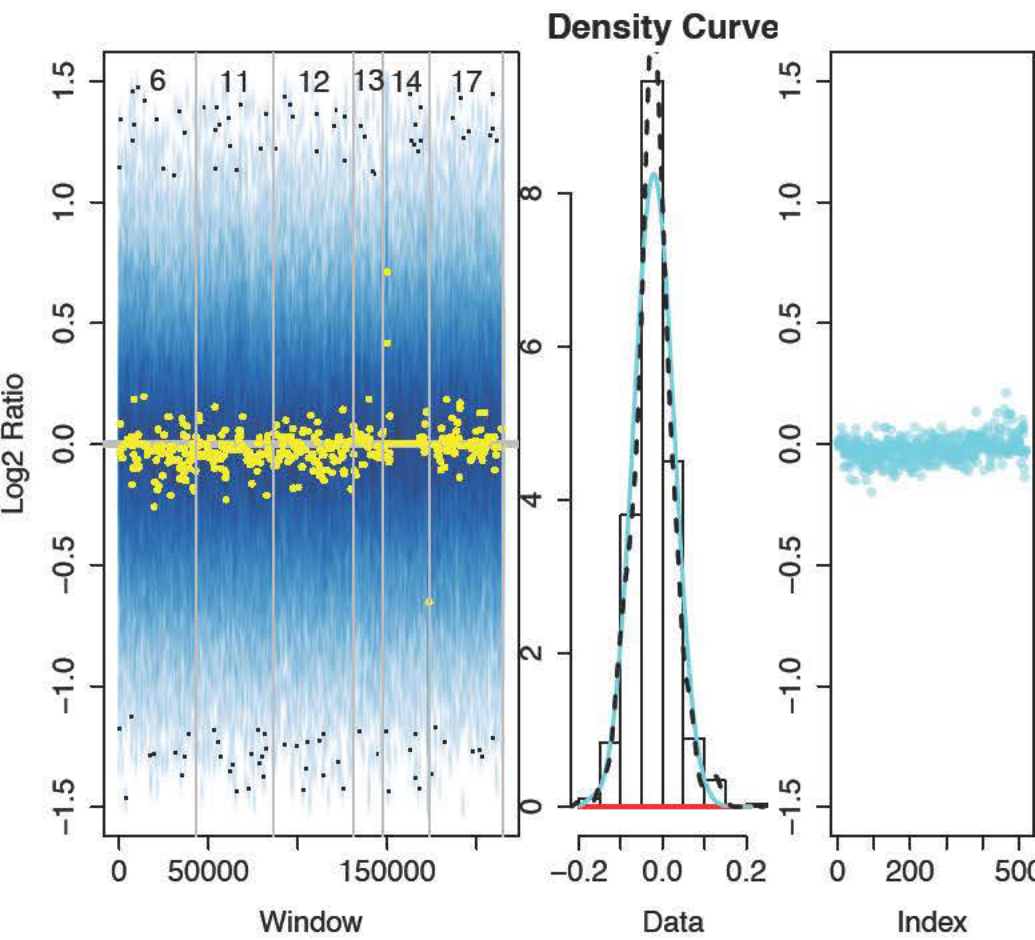
Density Curve
Log2 Ratio
Window
Data
Index

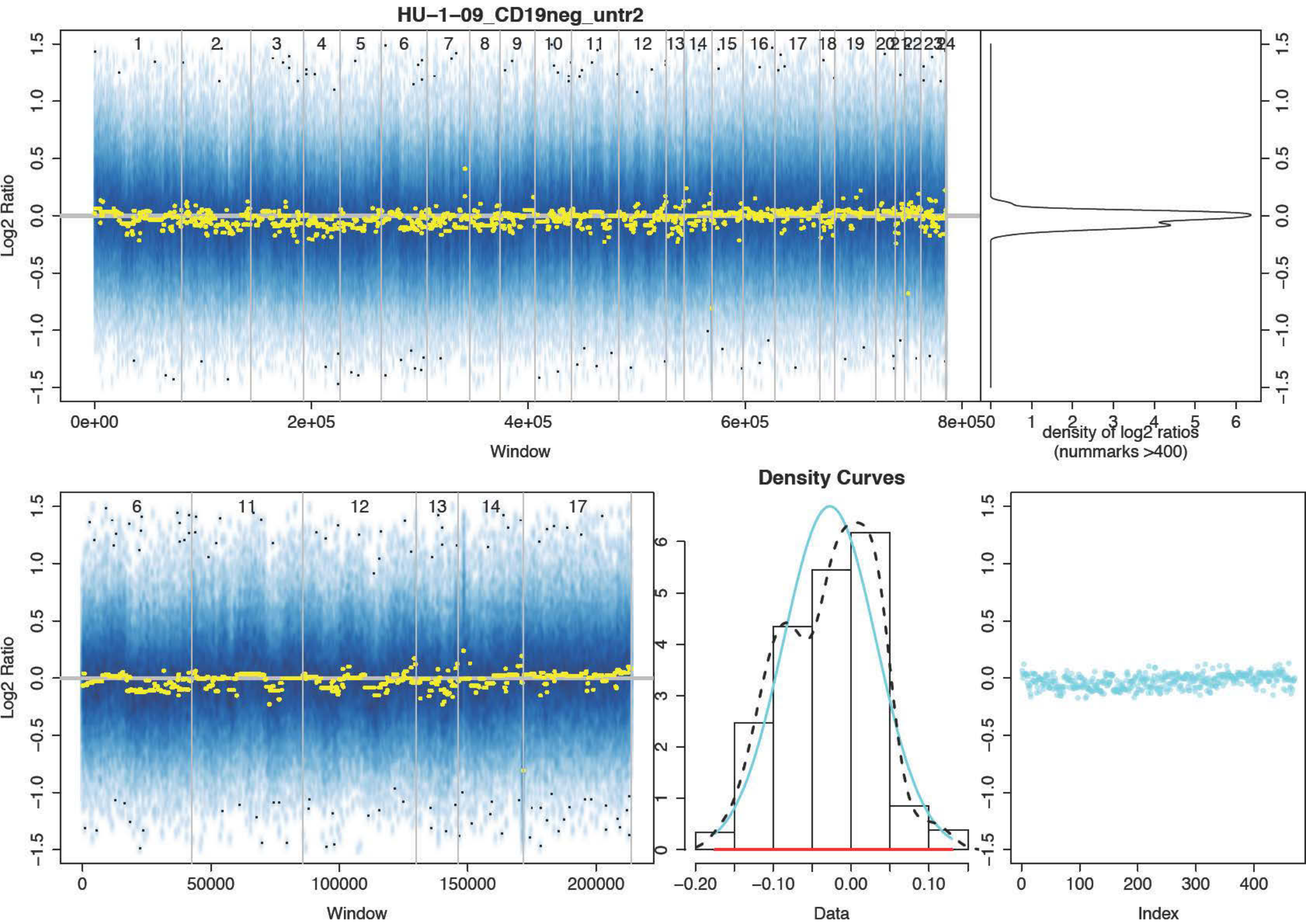
HU−1−09_CD19neg_untr2
Log2 Ratio
Window
density of log2 ratios
(nummarks >400)
Density Curves
Data
Index

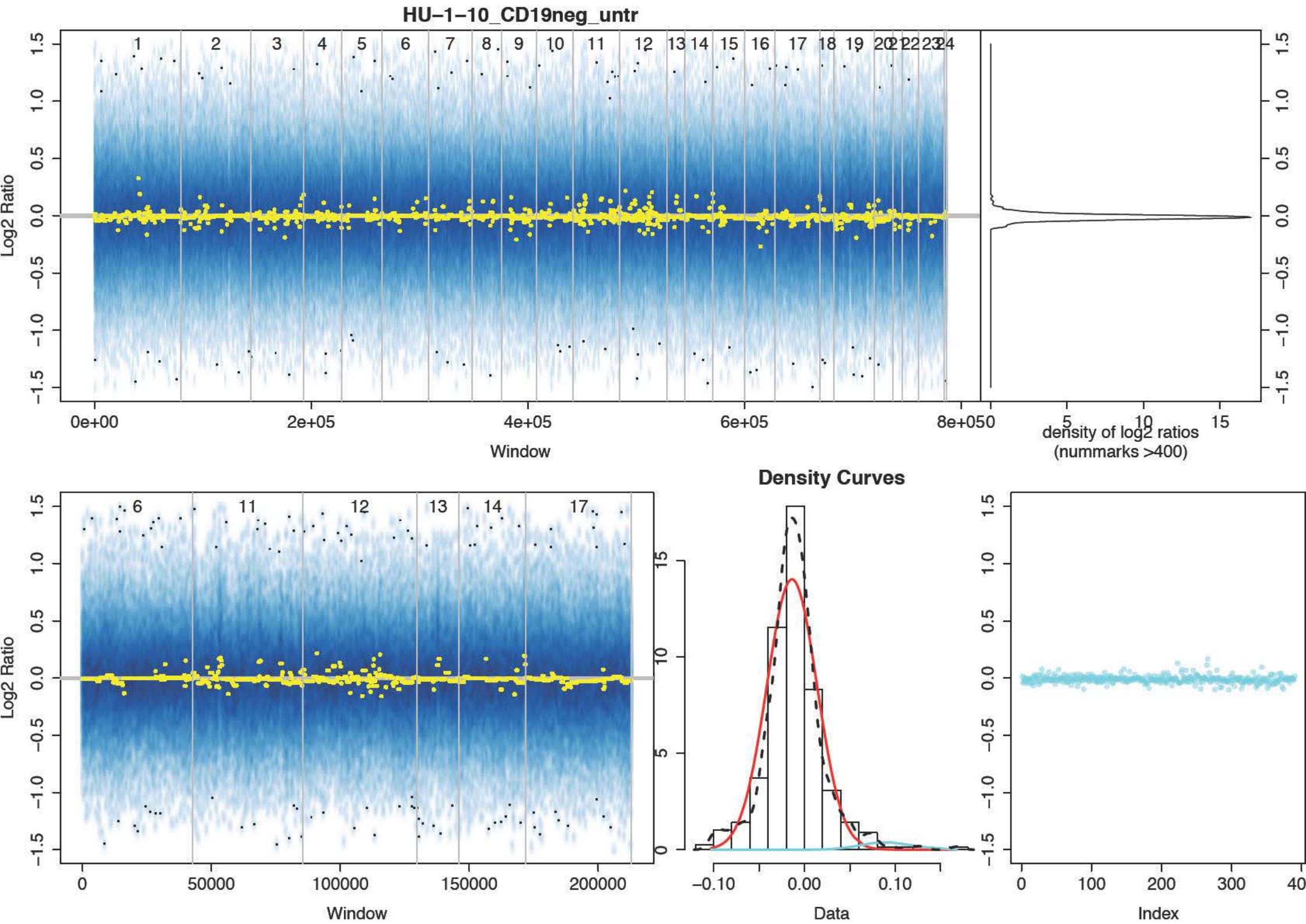
HU−1−10_CD19neg_untr
Log2 Ratio
Window
density of log2 ratios
(nummarks >400)
Density Curves
Data
Index

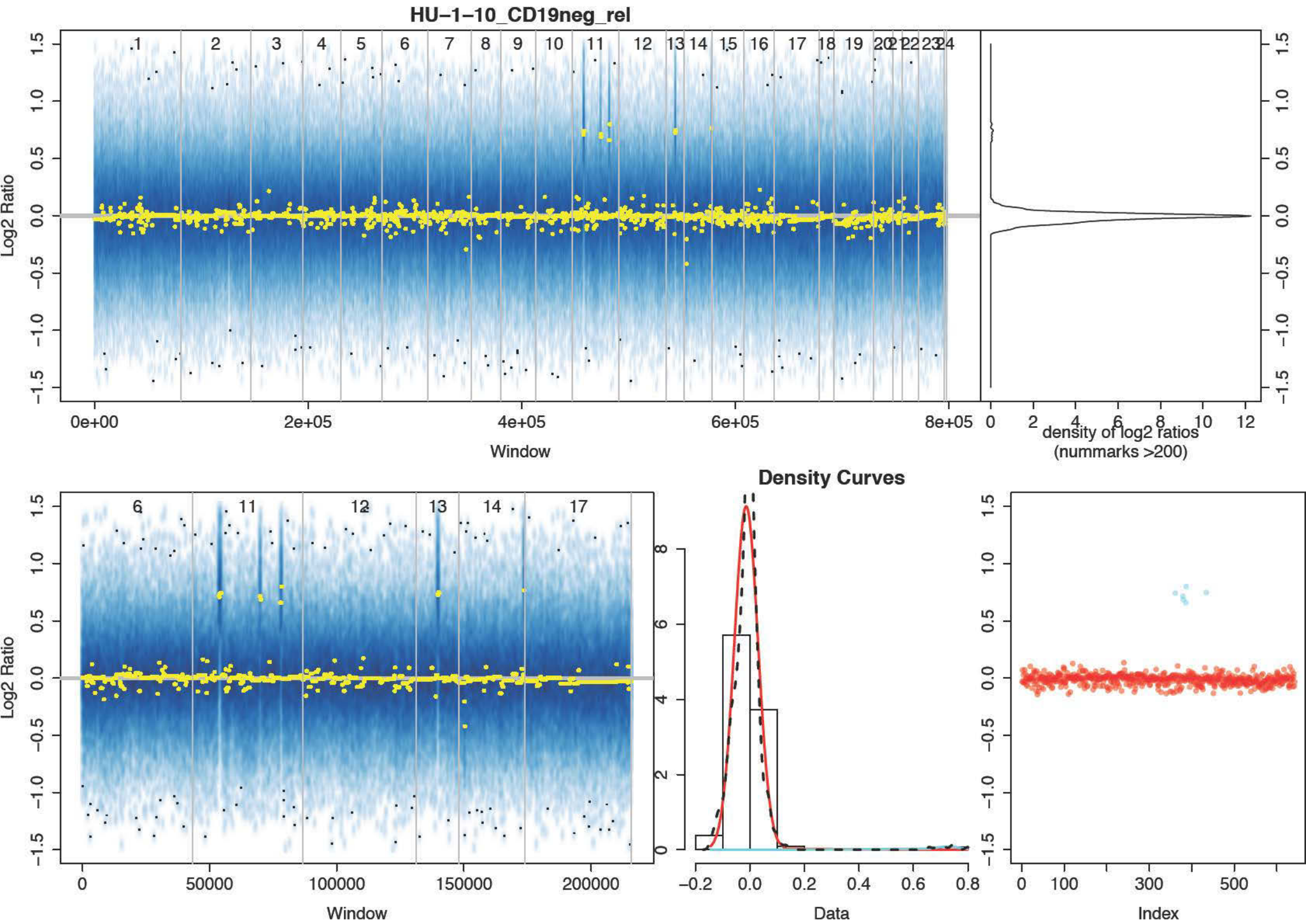
HU−1−10_CD19neg_rel
Log2 Ratio
Window
density of log2 ratios
(nummarks >200)
Density Curves
Data
Index

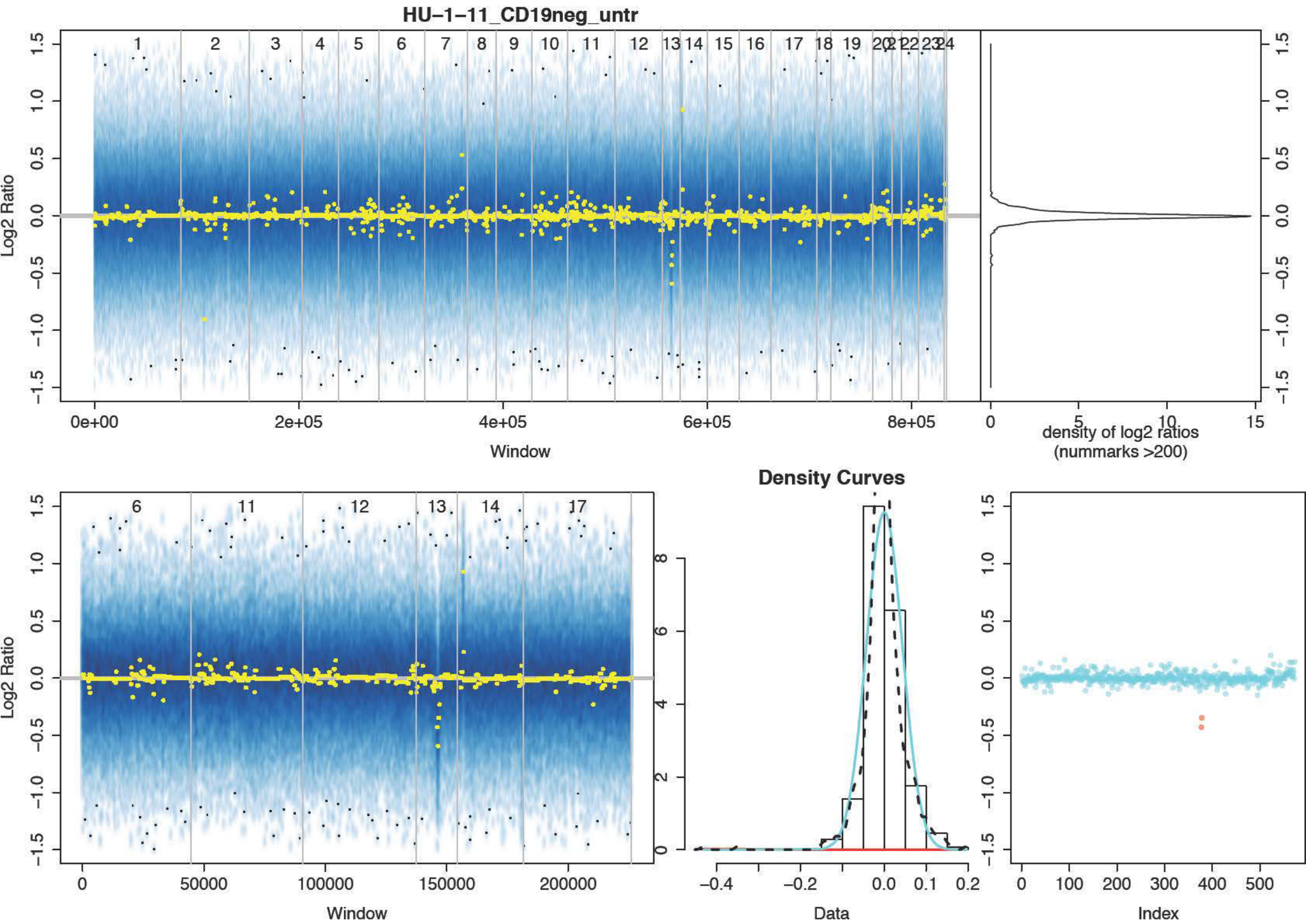
HU−1−11_CD19neg_untr
Log2 Ratio
Window
density of log2 ratios
(nummarks >200)
Density Curves
Data
Index

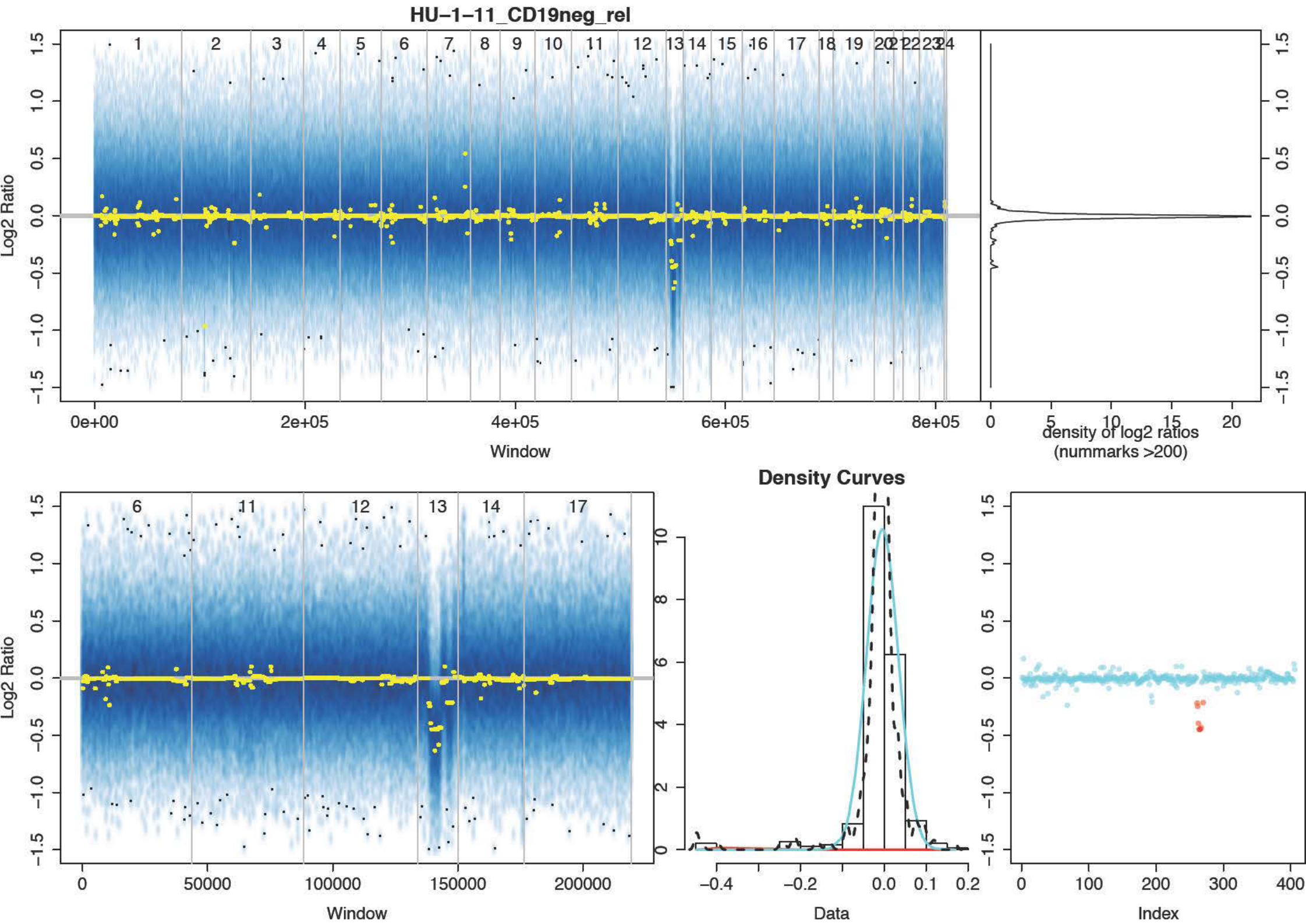
HU−1−11_CD19neg_rel
Log2 Ratio
Window
density of log2 ratios
(nummarks >200)
Density Curves
Data
Index

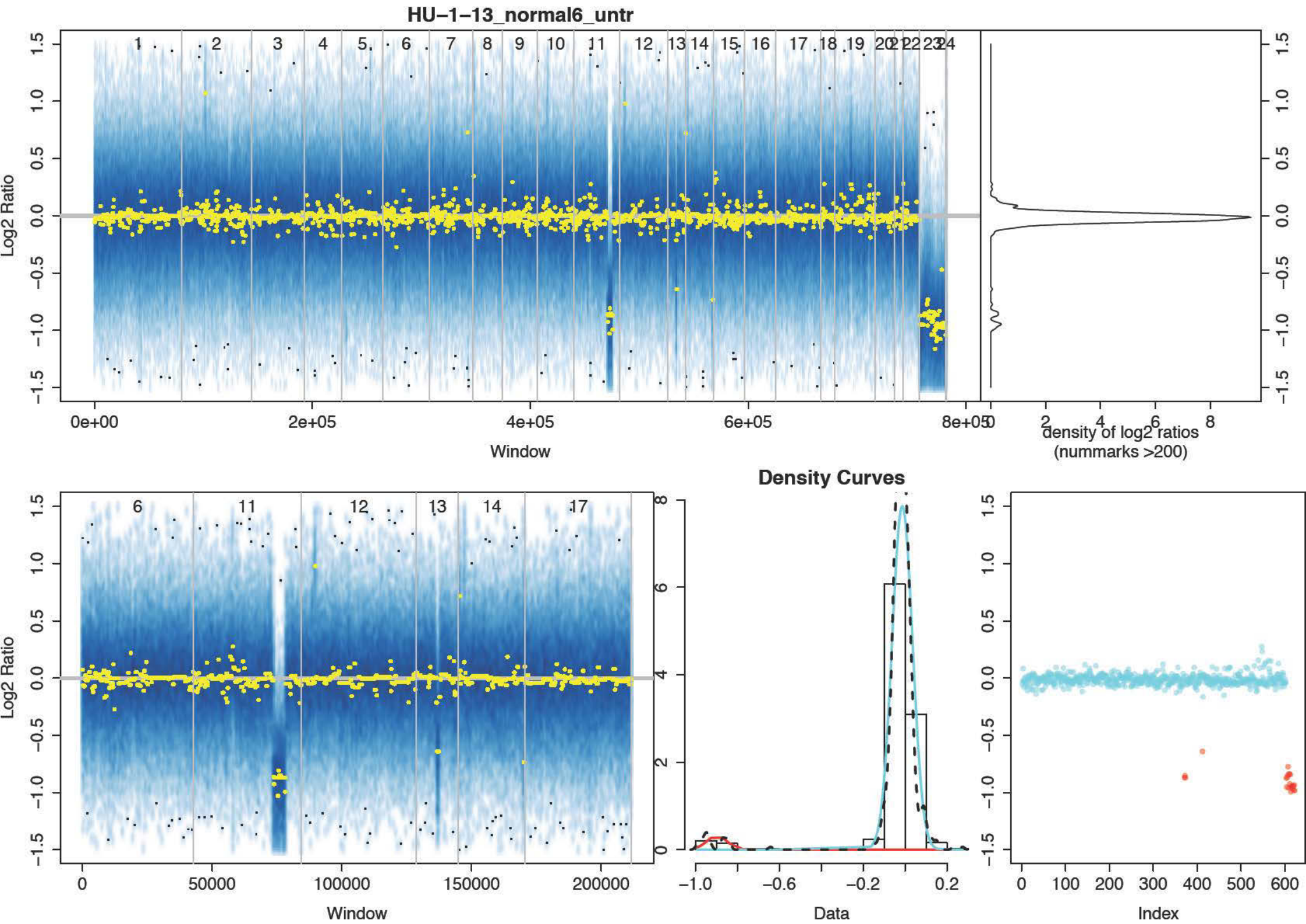
HU−1−13_normal6_untr
Log2 Ratio
Window
density of log2 ratios
(nummarks >200)
Density Curves
Data
Index

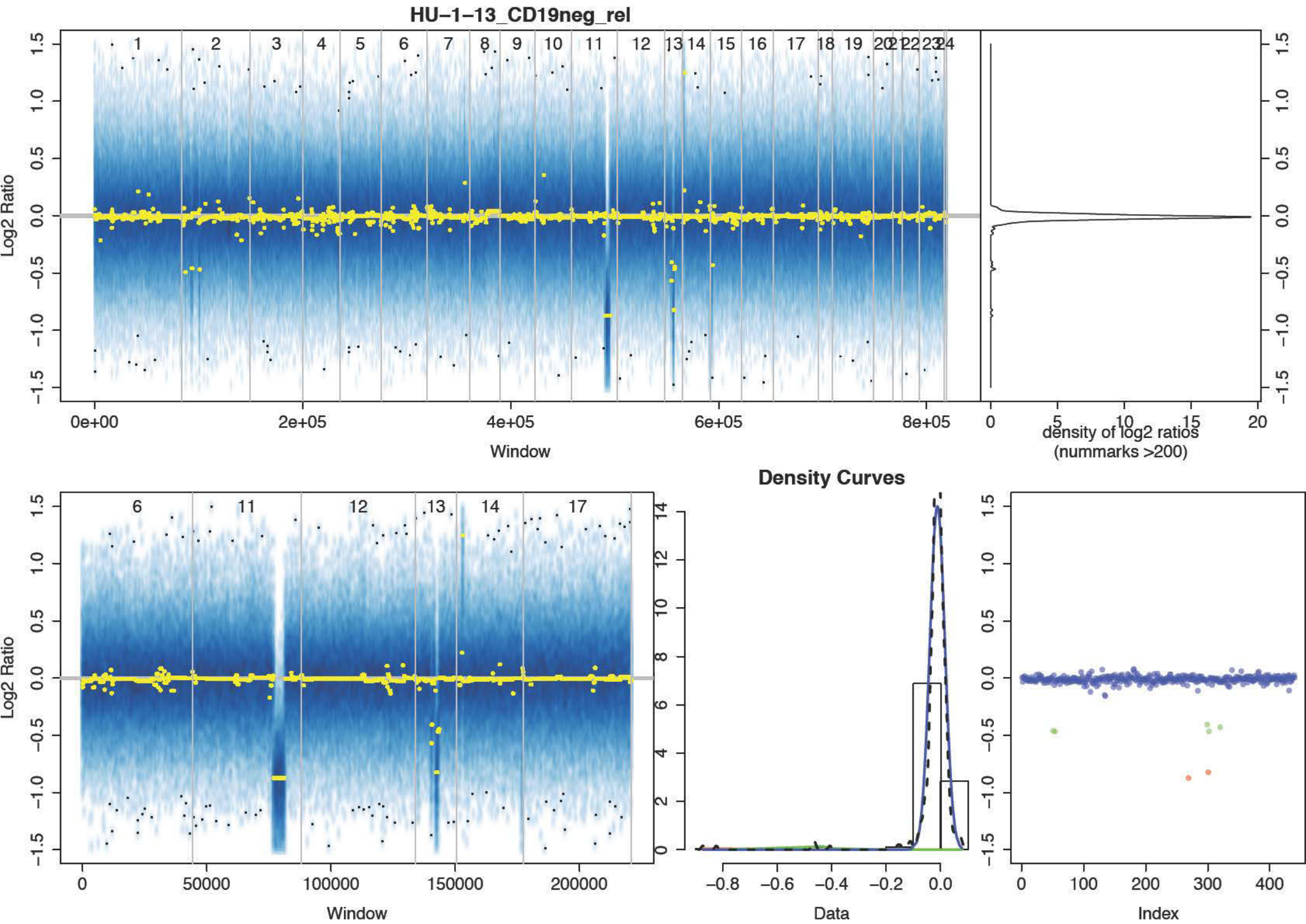
HU−1−13_CD19neg_rel
Log2 Ratio
Window
density of log2 ratios
(nummarks >200)
Density Curves
Data
Index

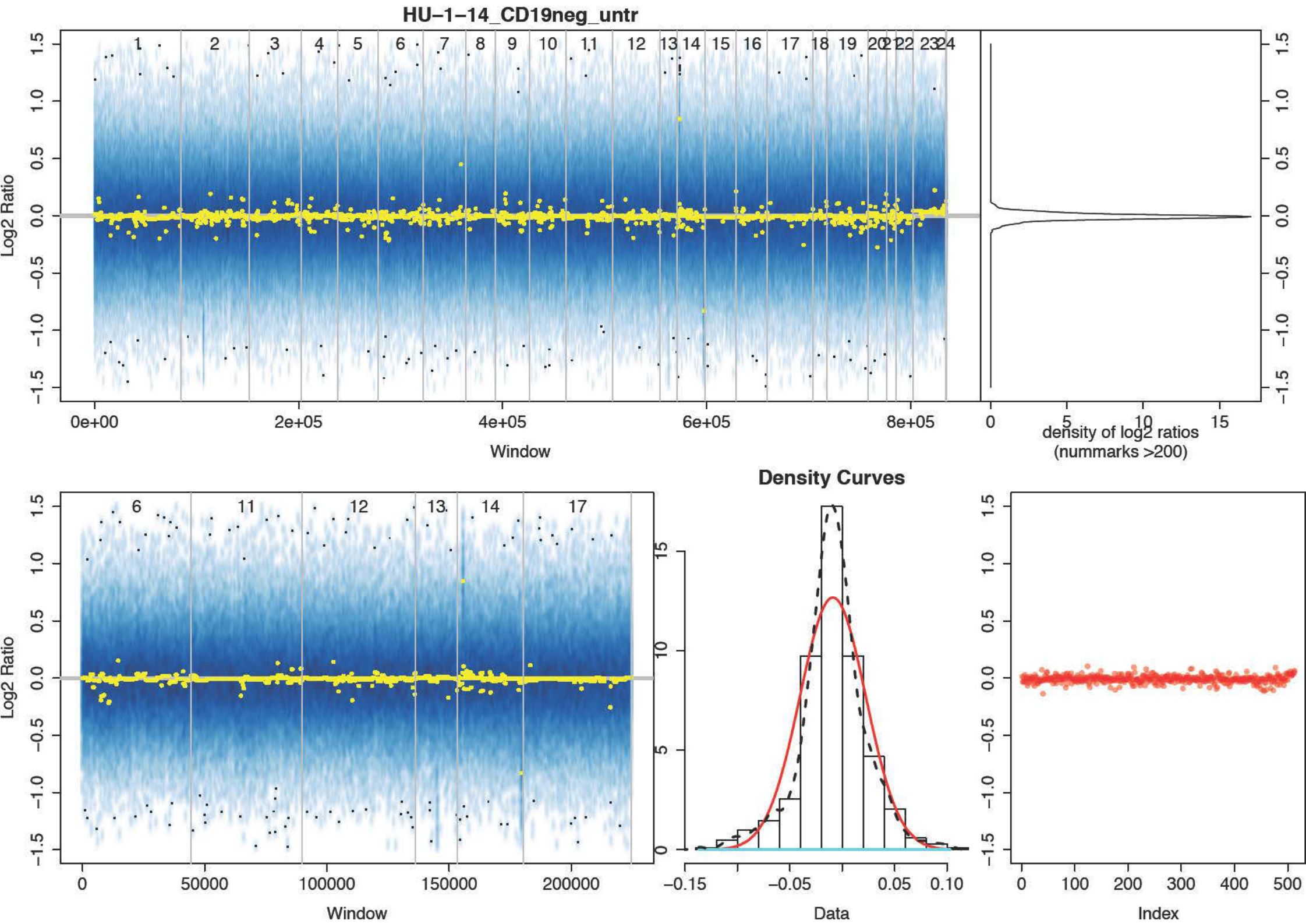
HU−1−14_CD19neg_untr
Log2 Ratio
Window
density of log2 ratios
(nummarks >200)
Density Curves
Data
Index

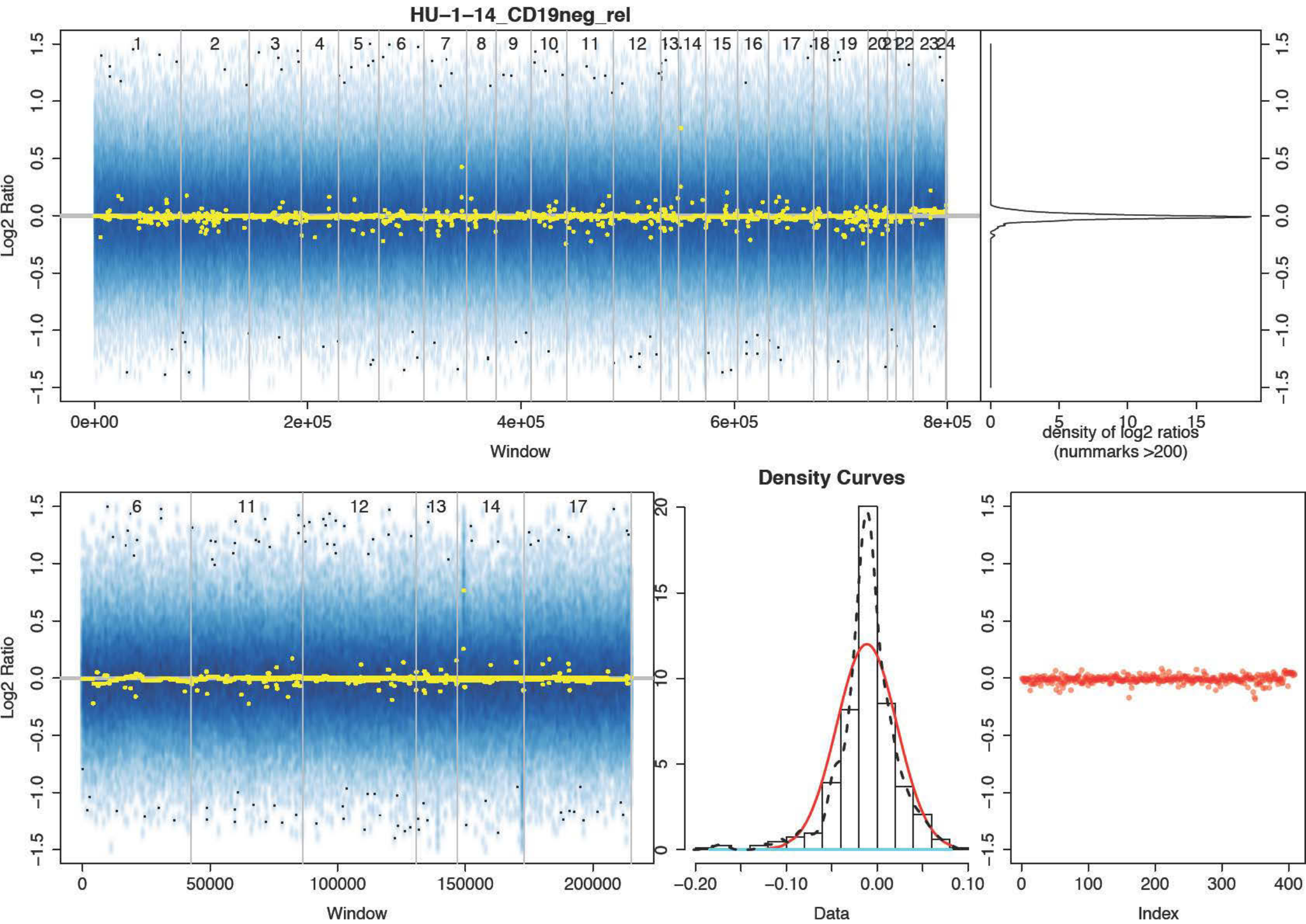
HU−1−14_CD19neg_rel
Log2 Ratio
Window
density of log2 ratios
(nummarks >200)
Density Curves
Data
Index

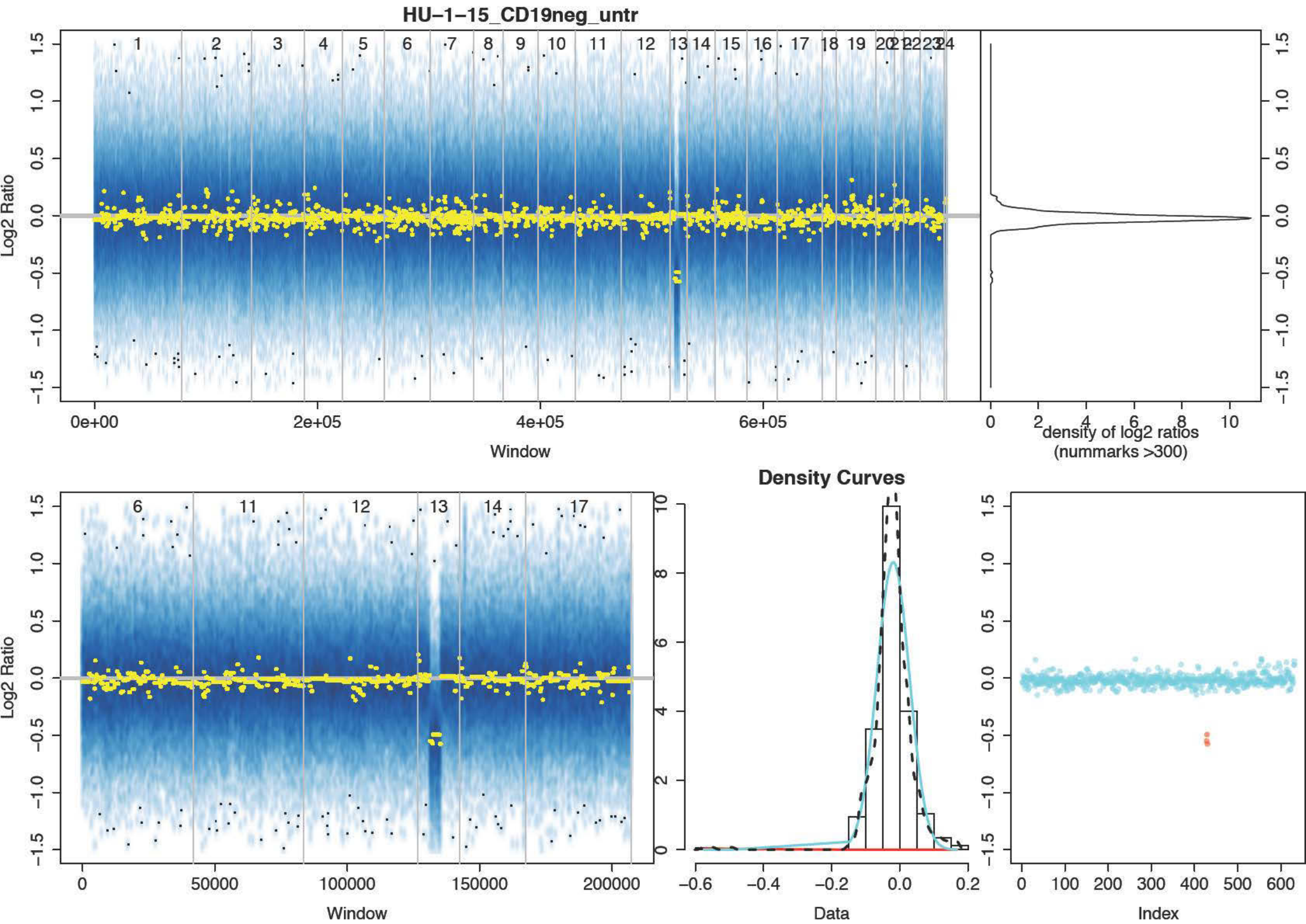
HU−1−15_CD19neg_untr
Log2 Ratio
Window
density of log2 ratios
(nummarks >300)
Density Curves
Data
Index

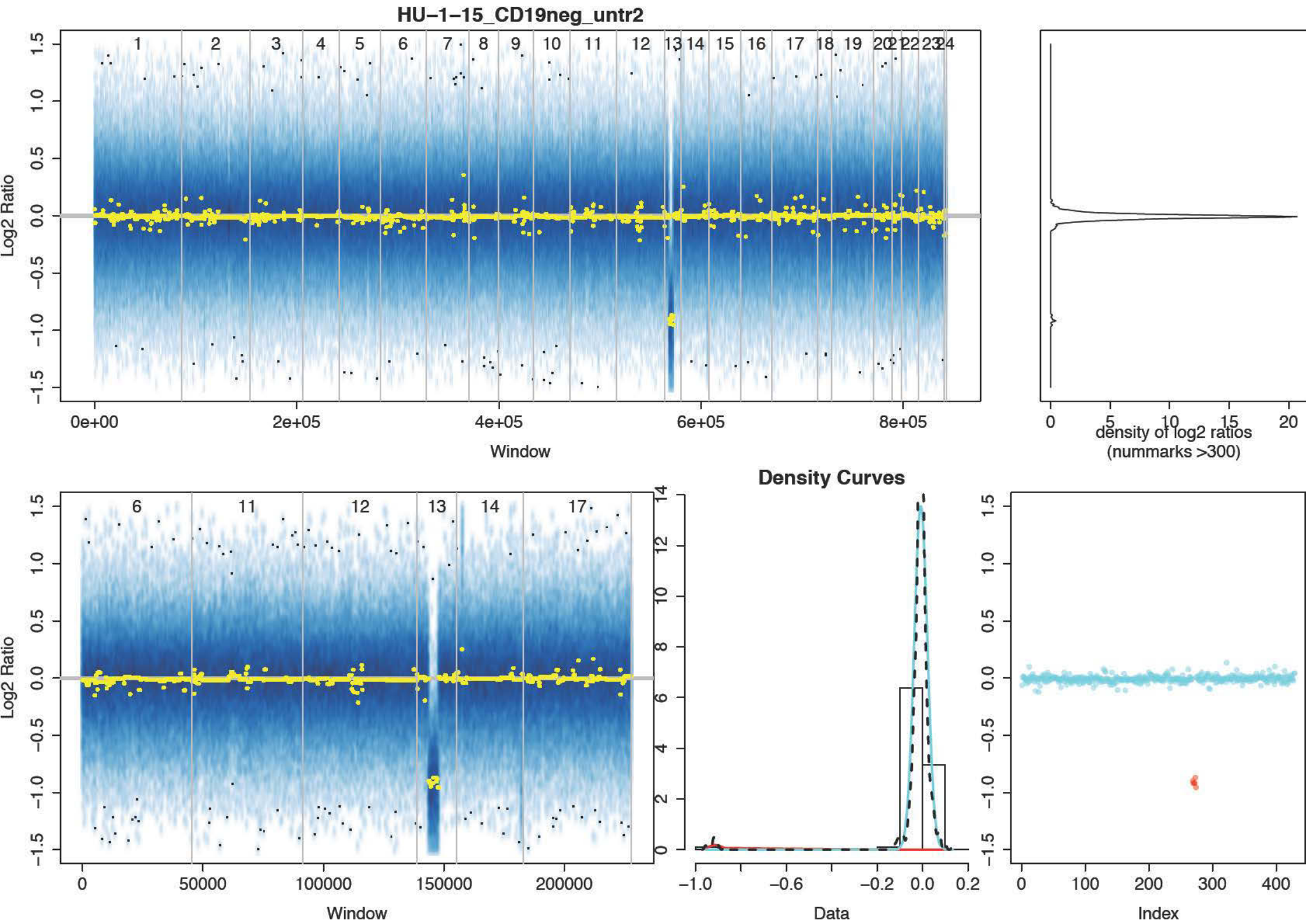
HU−1−15_CD19neg_untr2
Log2 Ratio
Window
density of log2 ratios
(nummarks >300)
Density Curves
Data
Index

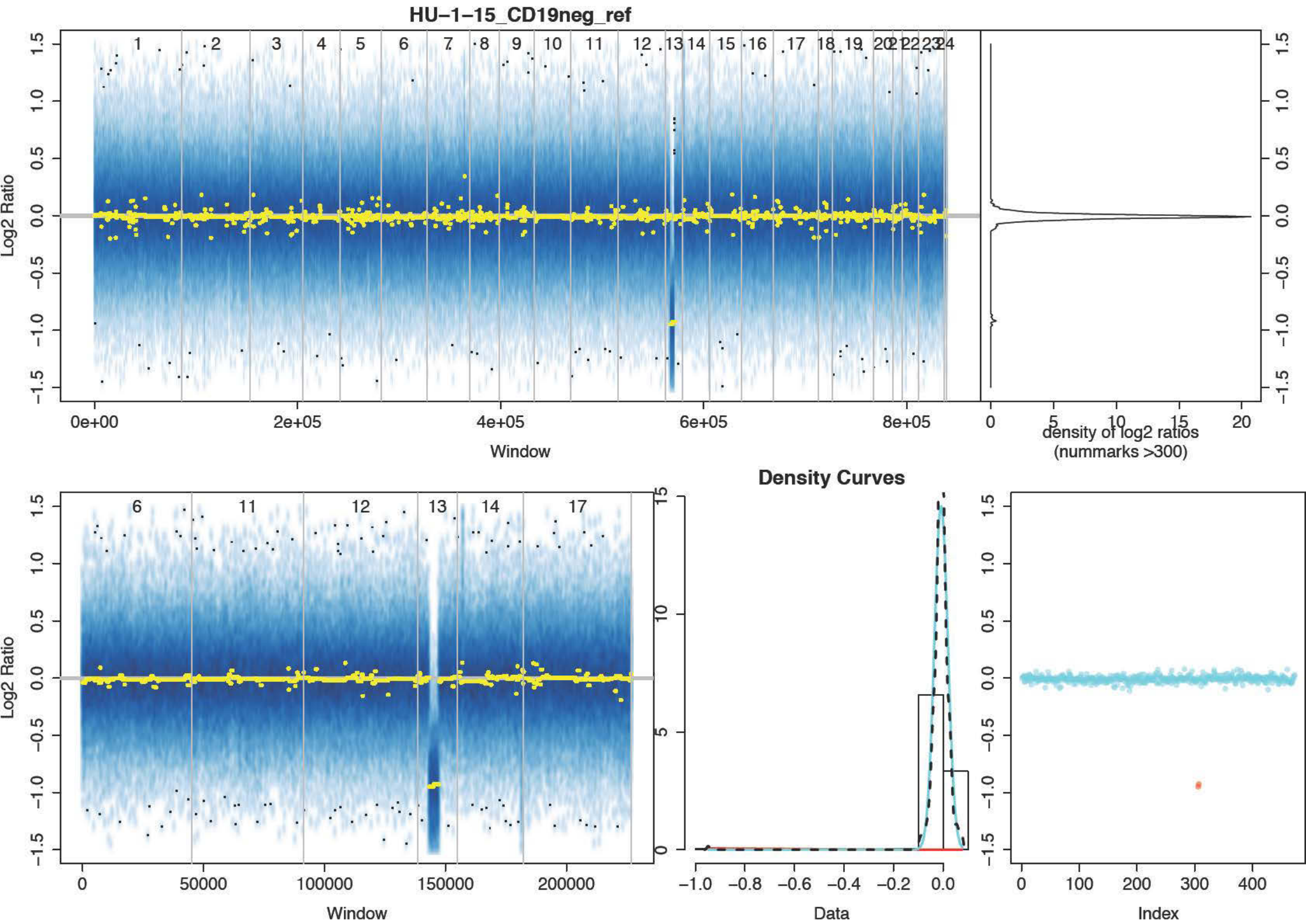
HU−1−15_CD19neg_ref
Log2 Ratio
Window
density of log2 ratios
(nummarks >300)
Density Curves
Data
Index

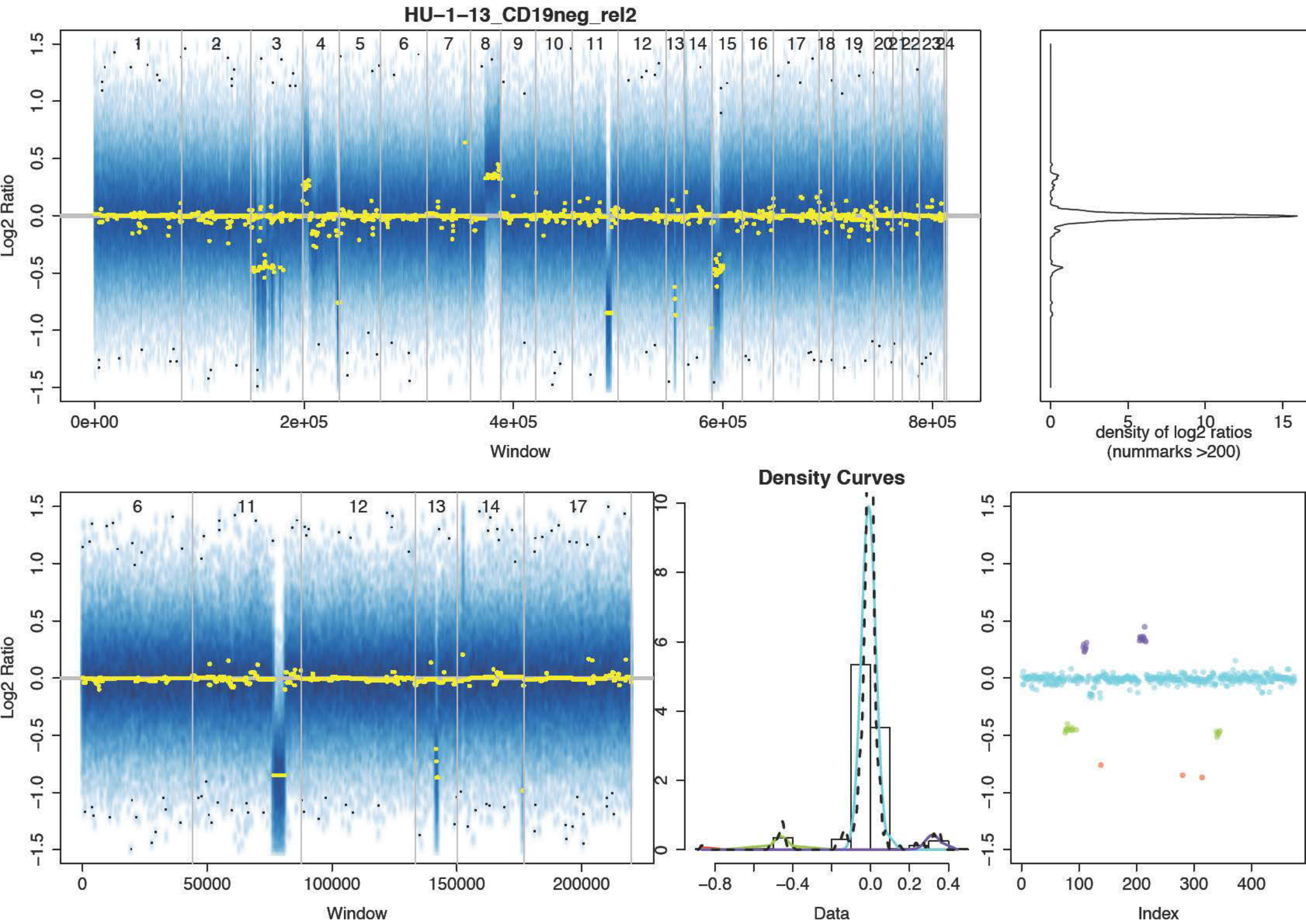
HU–1–13_CD19neg_rel2
Log2 Ratio
Window
density of log2 ratios
(nummarks >200)
Density Curves
Data
Index

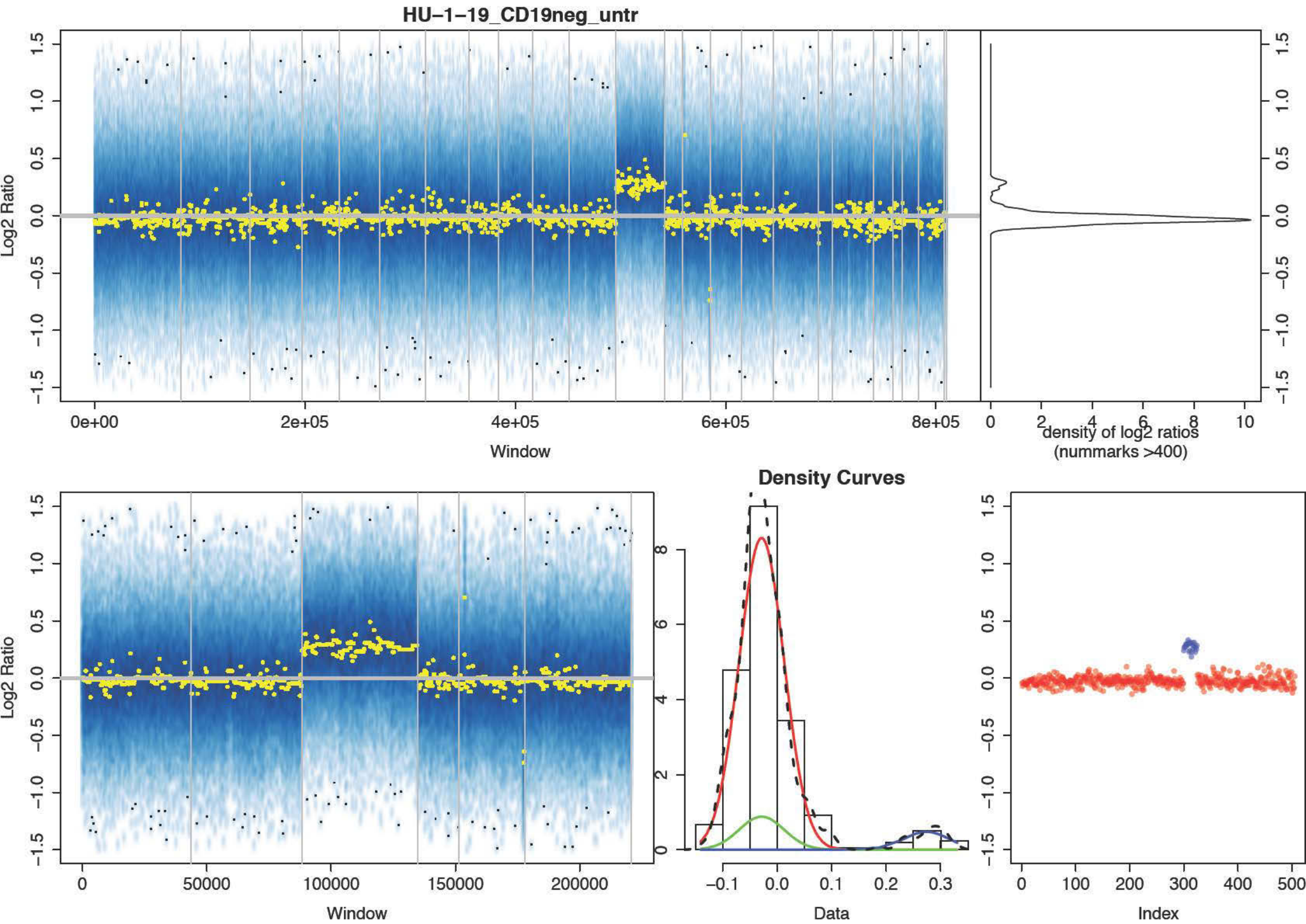
HU−1−19_CD19neg_untr
Log2 Ratio
Window
density of log2 ratios
(nummarks >400)
Density Curves
Data
Index

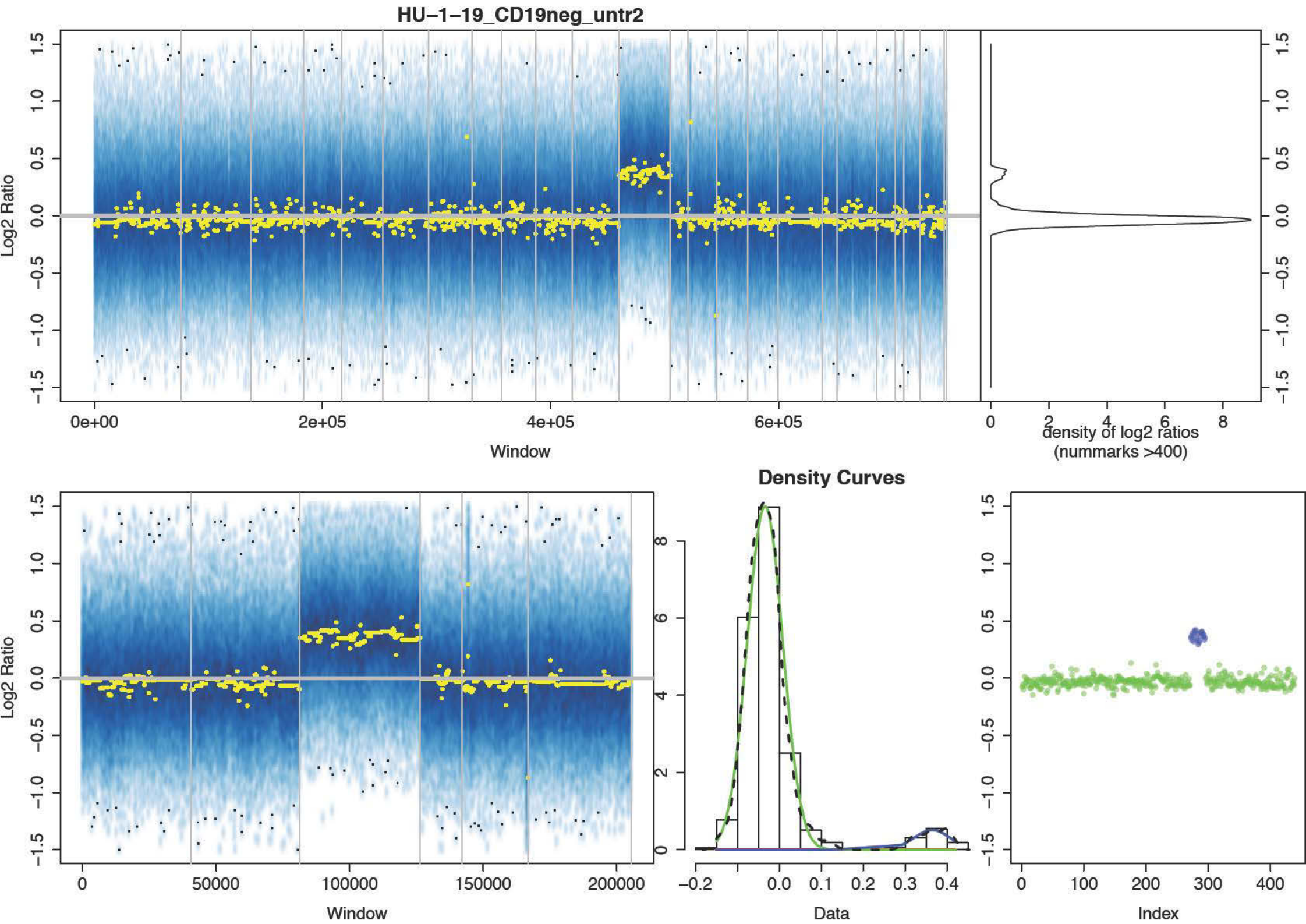
HU−1−19_CD19neg_untr2
Log2 Ratio
Window
density of log2 ratios
(nummarks >400)
Density Curves
Log2 Ratio
Window
Data
Index

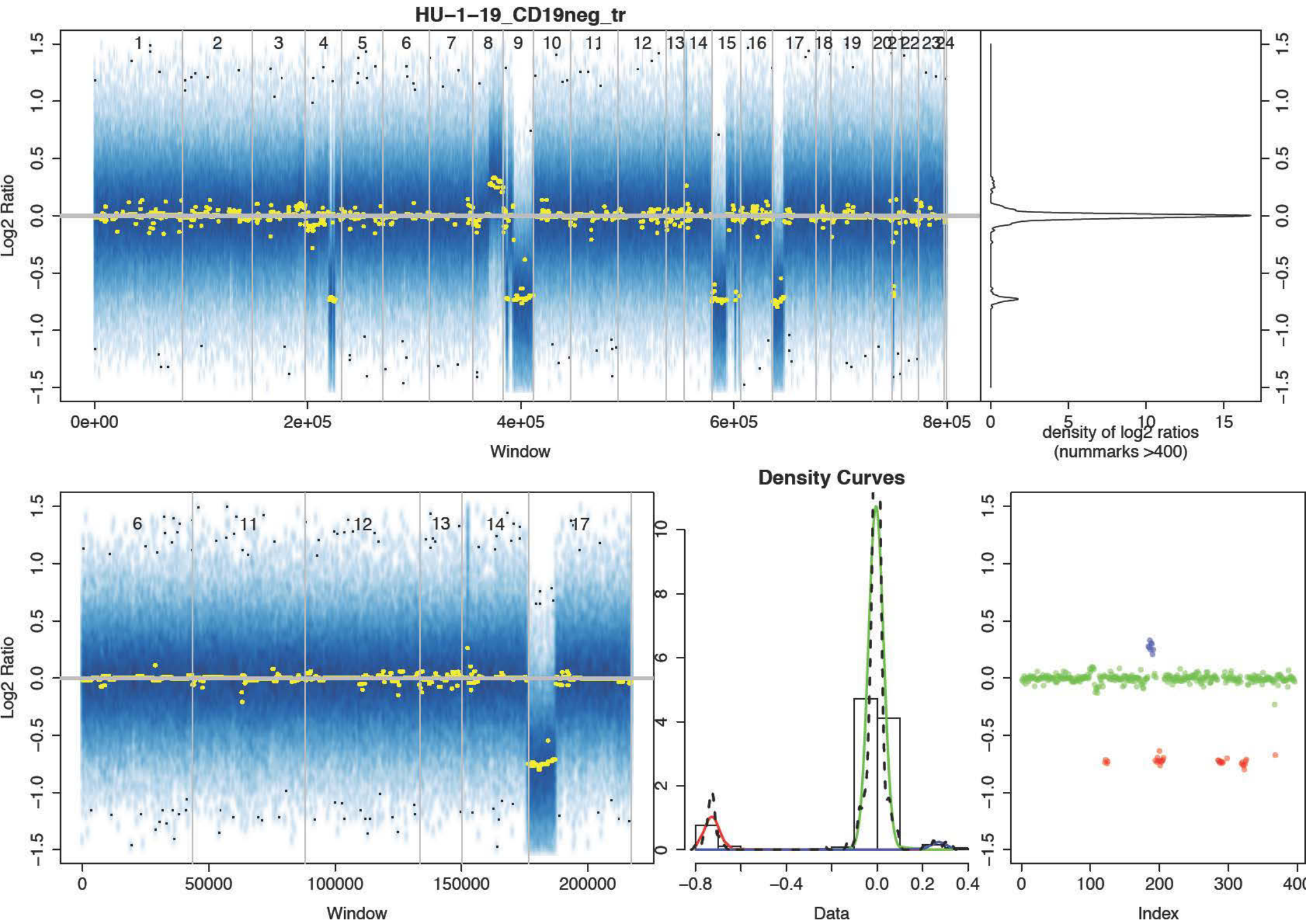
HU−1−19_CD19neg_tr
Log2 Ratio
Window
density of log2 ratios
(nummarks >400)
Density Curves
Data
Index

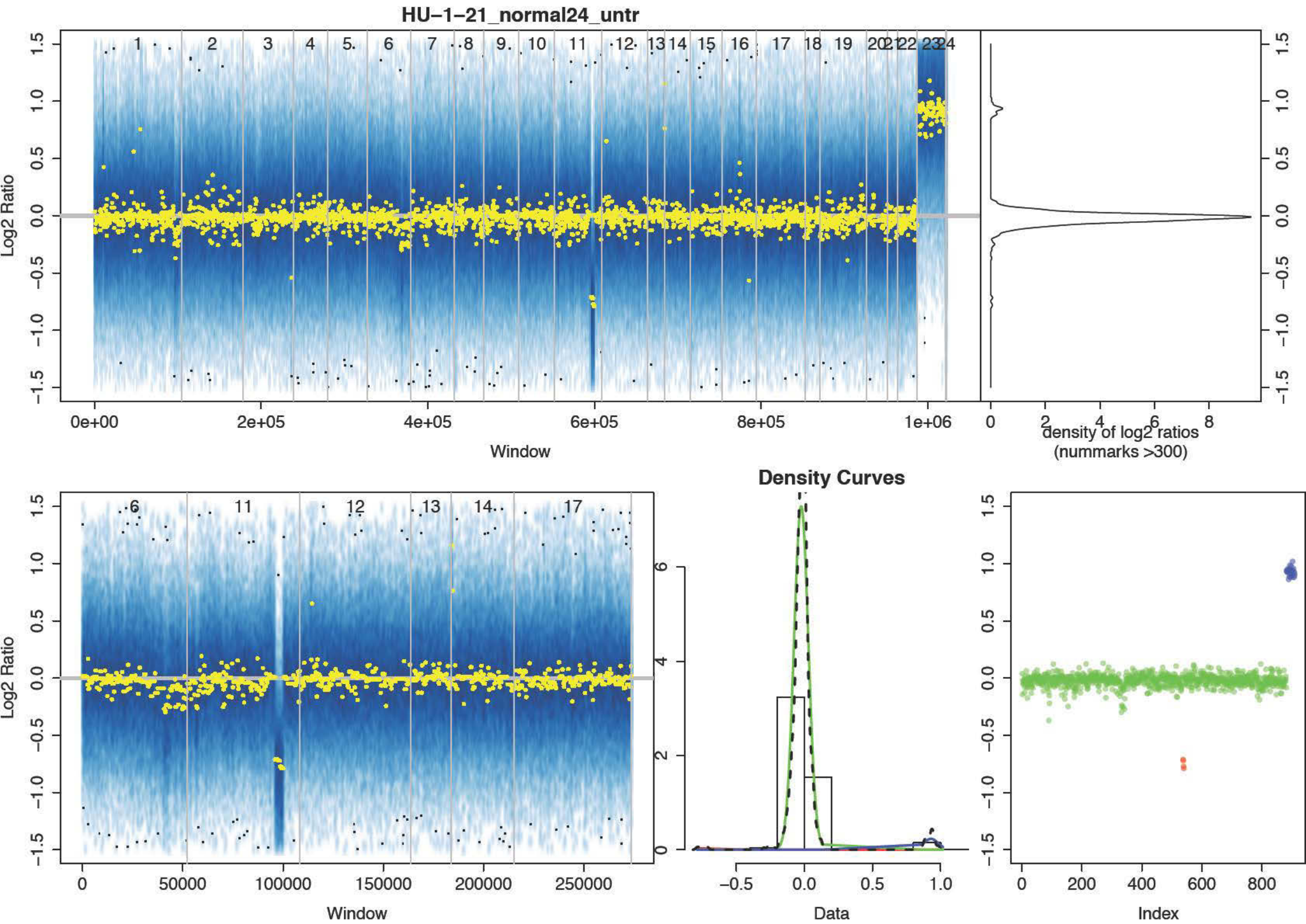
HU−1−21_normal24_untr
Log2 Ratio
Window
density of log2 ratios
(nummarks >300)
Density Curves
Data
Index

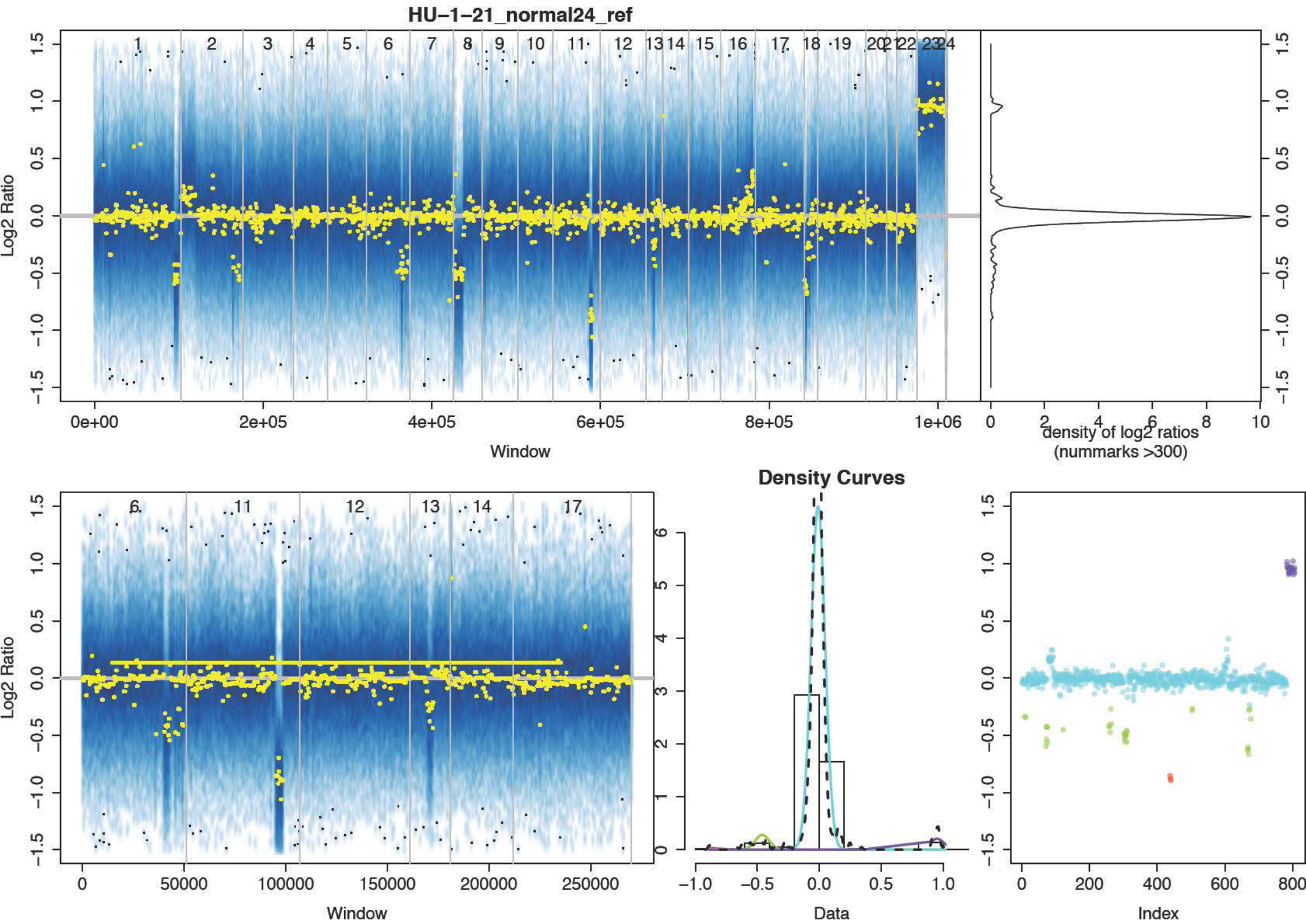
HU−1−21_normal24_ref
Log2 Ratio
Window
density of log2 ratios
(nummarks >300)
Density Curves
Data
Index

Suppl. figure 4: Changes in cancer cell fraction (CCF) with annotation of genes listed in the Catalogue of Somatic Mutations in Cancer (COSMIC). Significant changes in CCF are highlighted by red (reduced CCF) or green color (increased CCF). Genes represented in COSMIC are highlighted in purple.

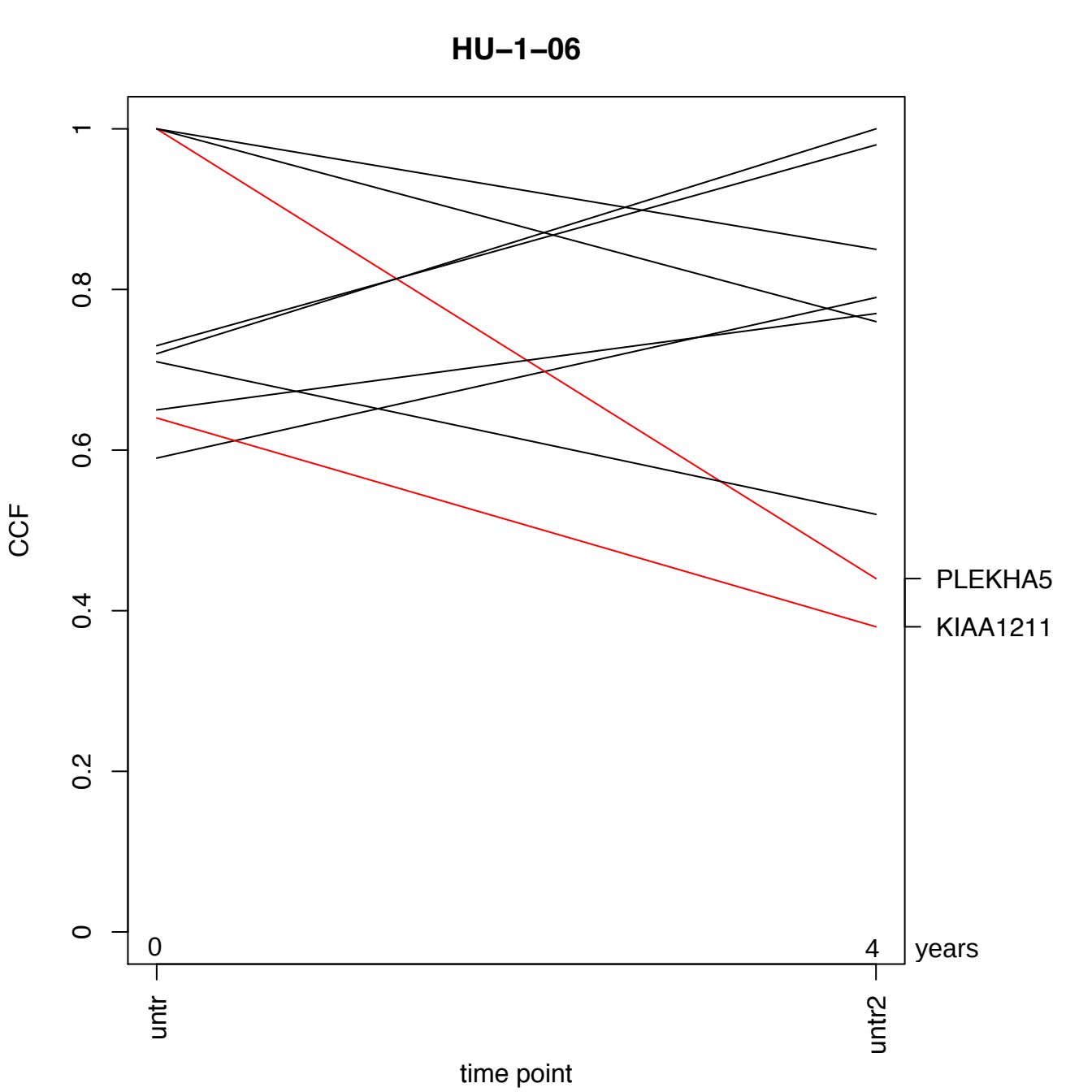
HU−1−06
CCF
1
0.8
0.6
0.4
0.2
0
PLEKHA5
KIAA1211
0
4
years
untr
untr2
time point

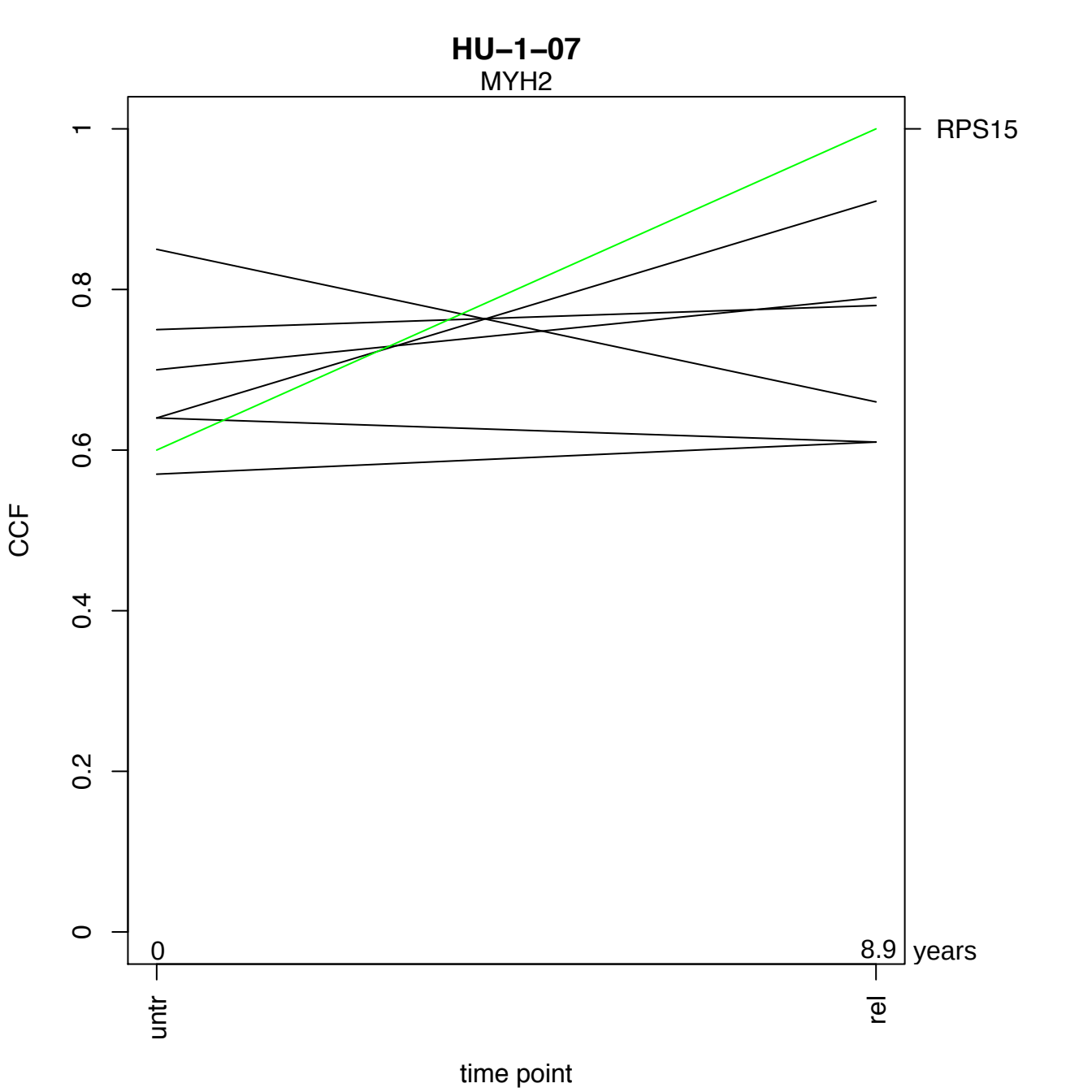
HU−1−07
MYH2
RPS15
CCF
1
0.8
0.6
0.4
0.2
0
0
8.9
years
untr
rel
time point

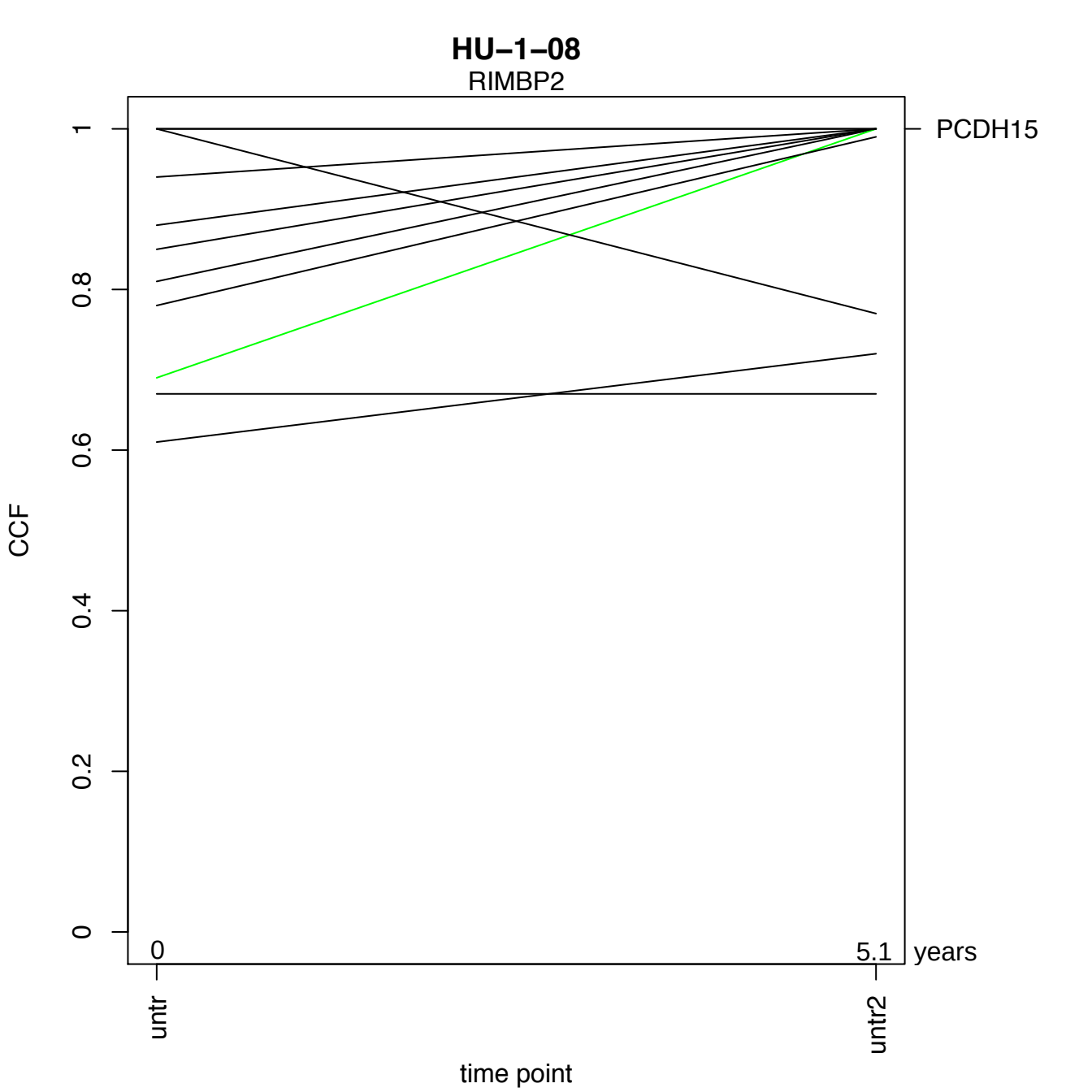
HU−1−08
RIMBP2
PCDH15
CCF
1
0.8
0.6
0.4
0.2
0
0
5.1
years
untr
untr2
time point

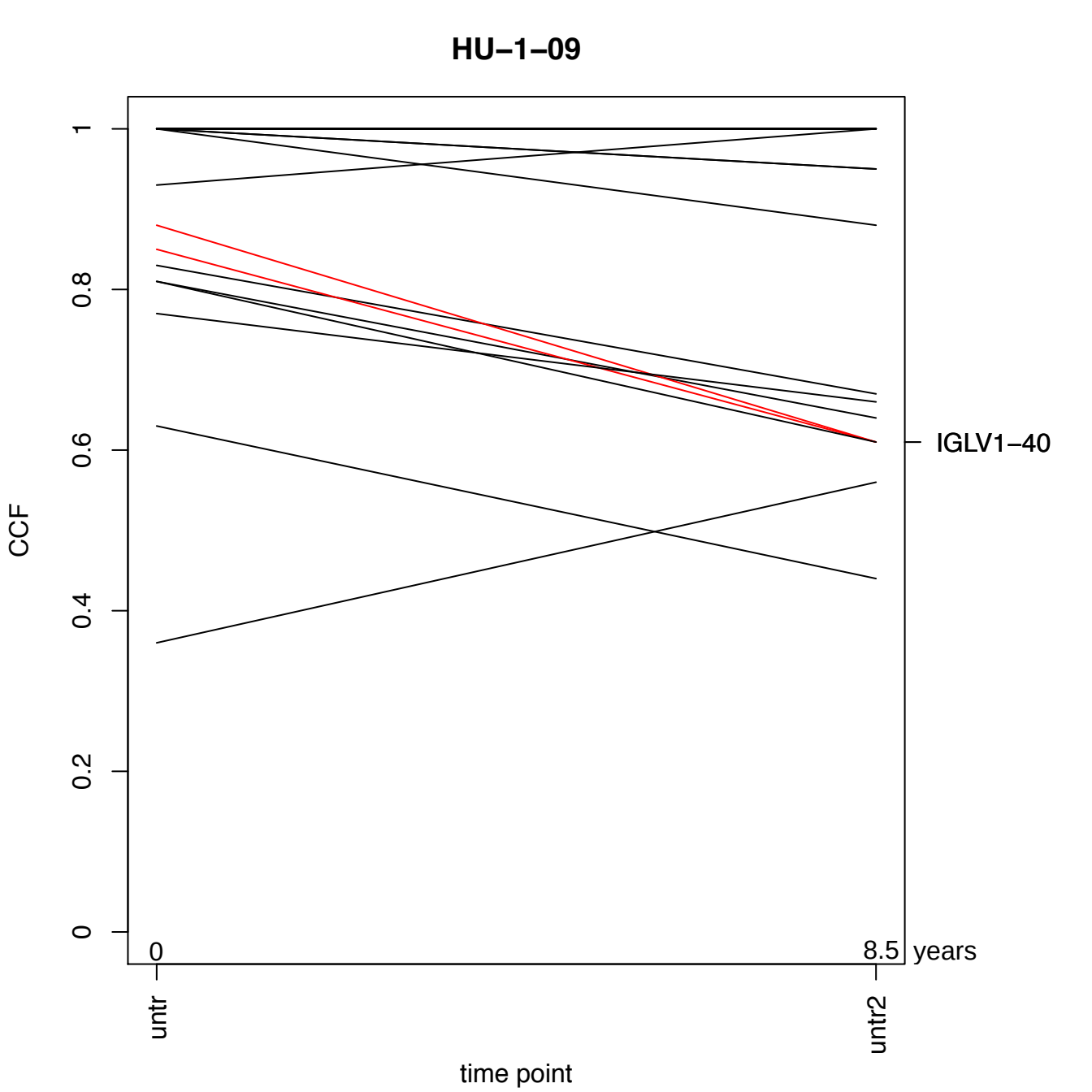
HU−1−09
CCF
1
0.8
0.6
0.4
0.2
0
IGLV1−40
0
8.5
years
untr
untr2
time point

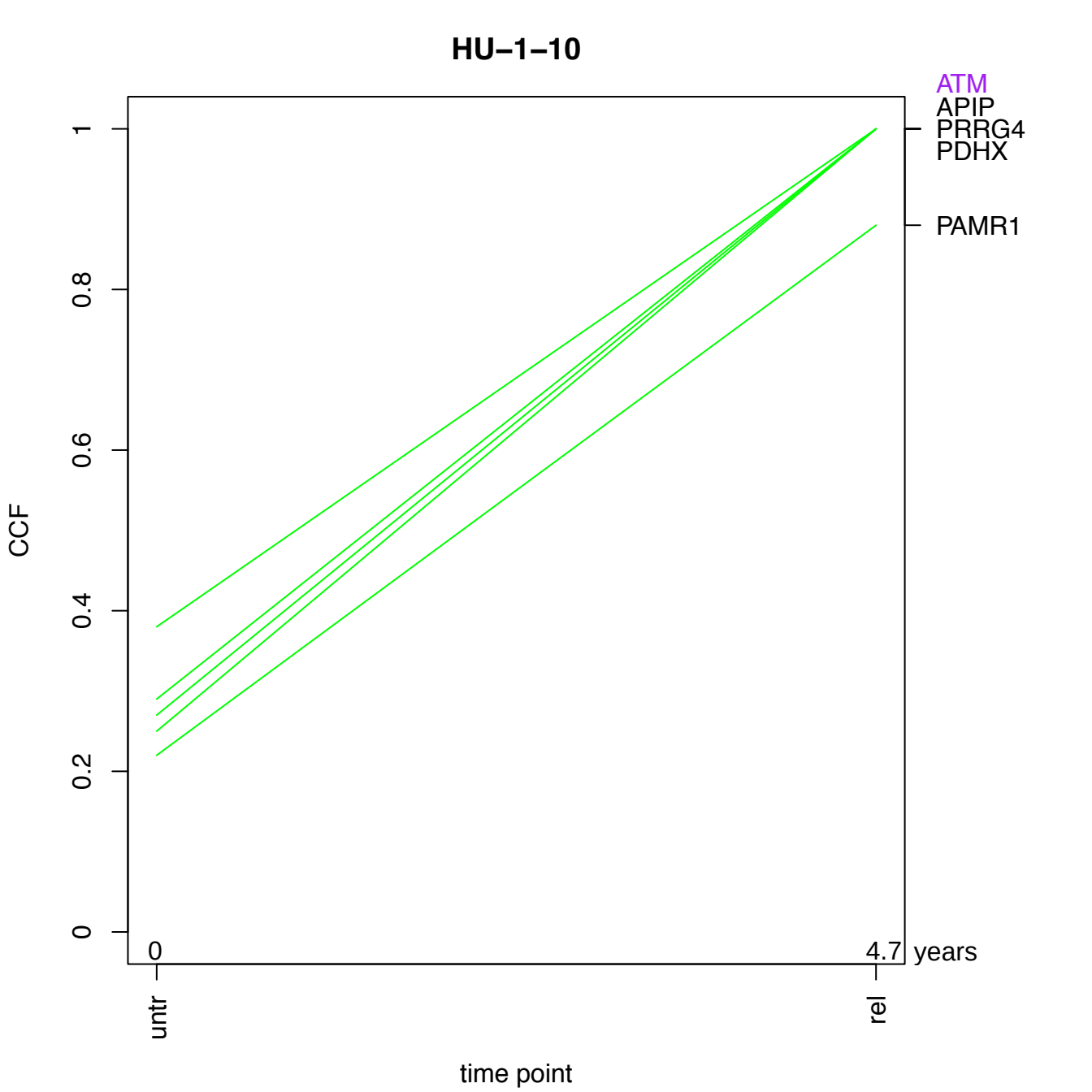
HU−1−10
ATM
APIP
PRRG4
PDHX
PAMR1
CCF
0
0.2
0.4
0.6
0.8
1
0
4.7
years
untr
rel
time point

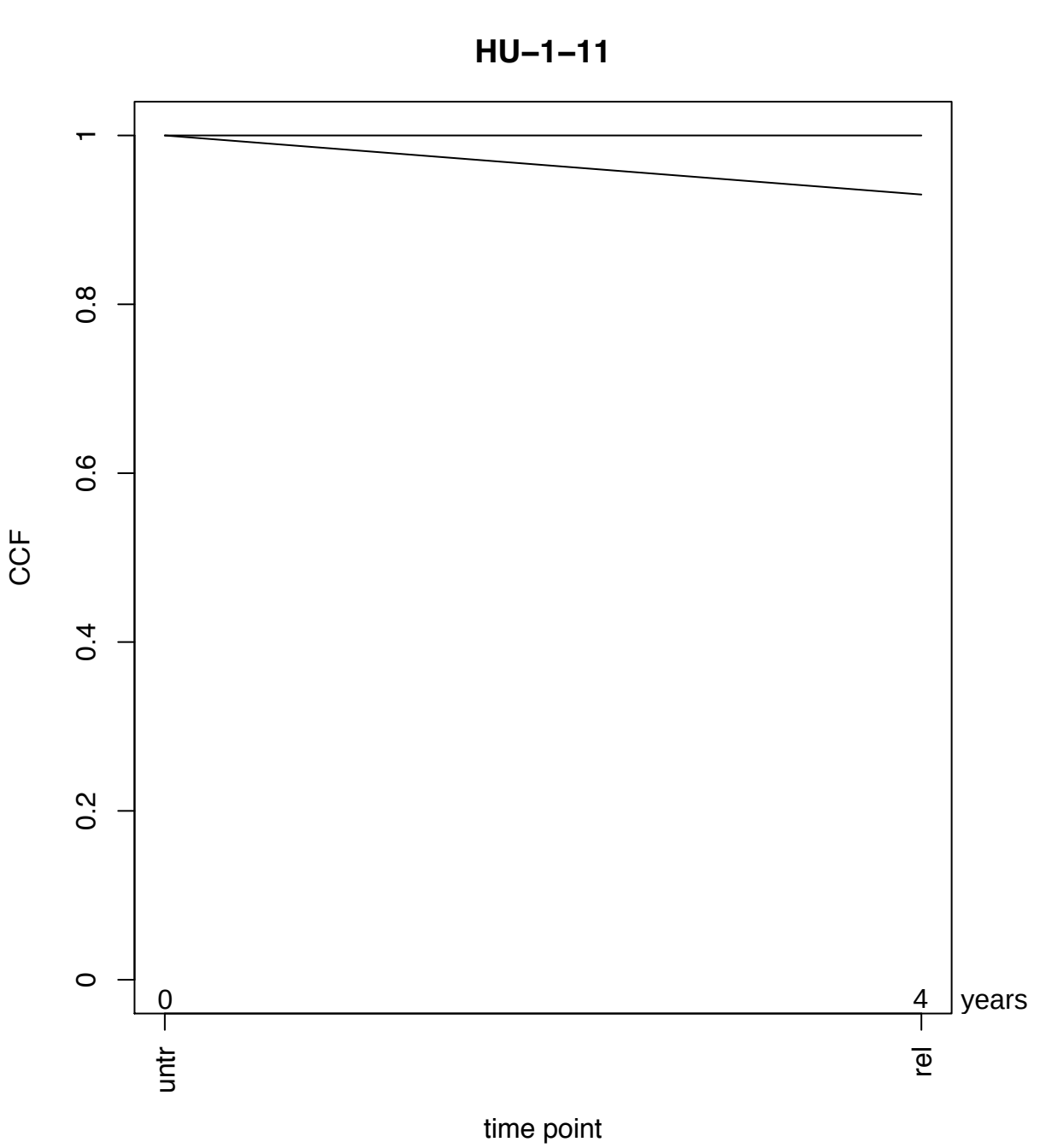
HU−1−11
CCF
0
0.2
0.4
0.6
0.8
1
0
4
years
untr
rel
time point

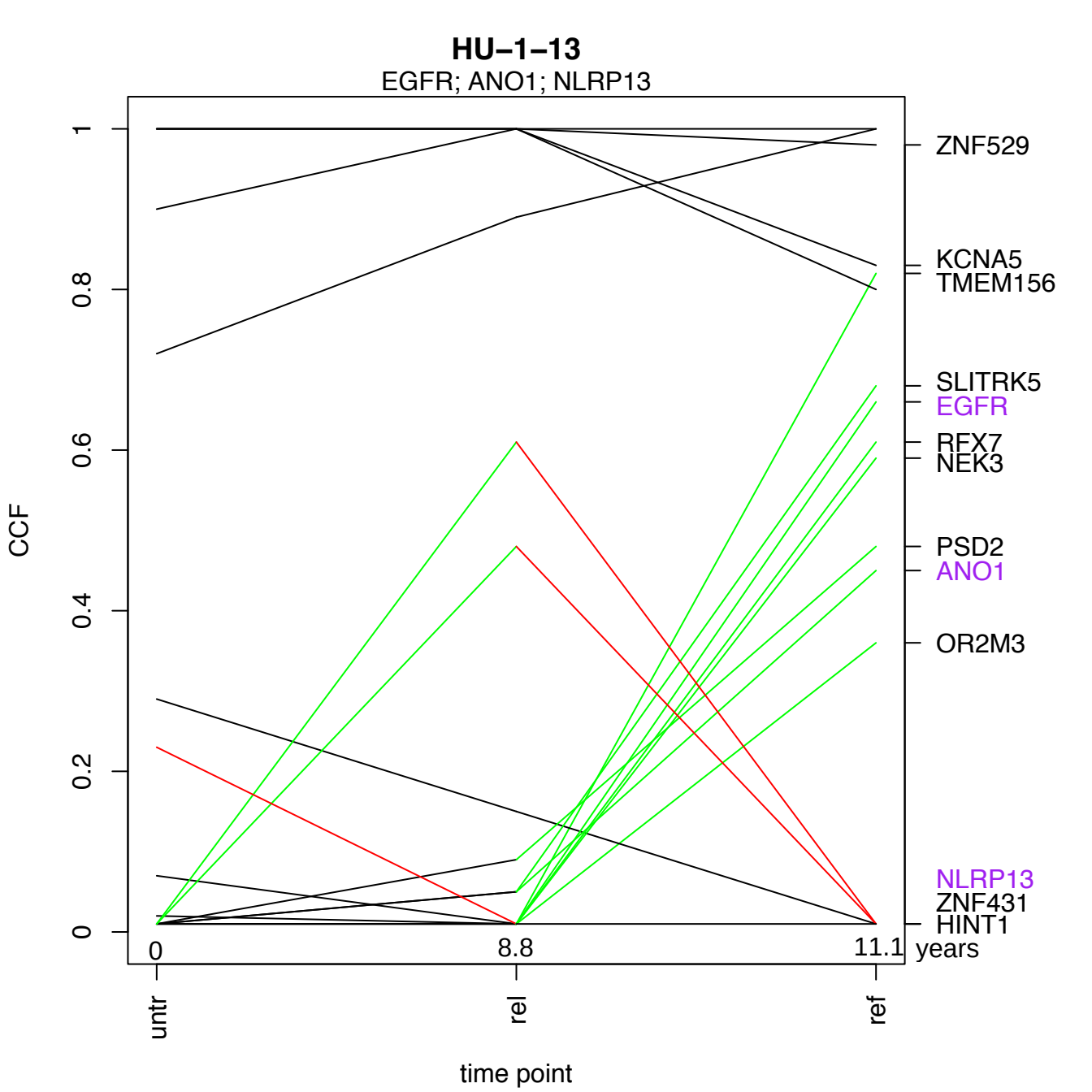
HU−1−13
EGFR; ANO1; NLRP13
CCF
1
0.8
0.6
0.4
0.2
0
0
8.8
11.1
years
untr
rel
ref
time point
ZNF529
KCNA5
TMEM156
SLITRK5
EGFR
RFX7
NEK3
PSD2
ANO1
OR2M3
NLRP13
ZNF431
HINT1

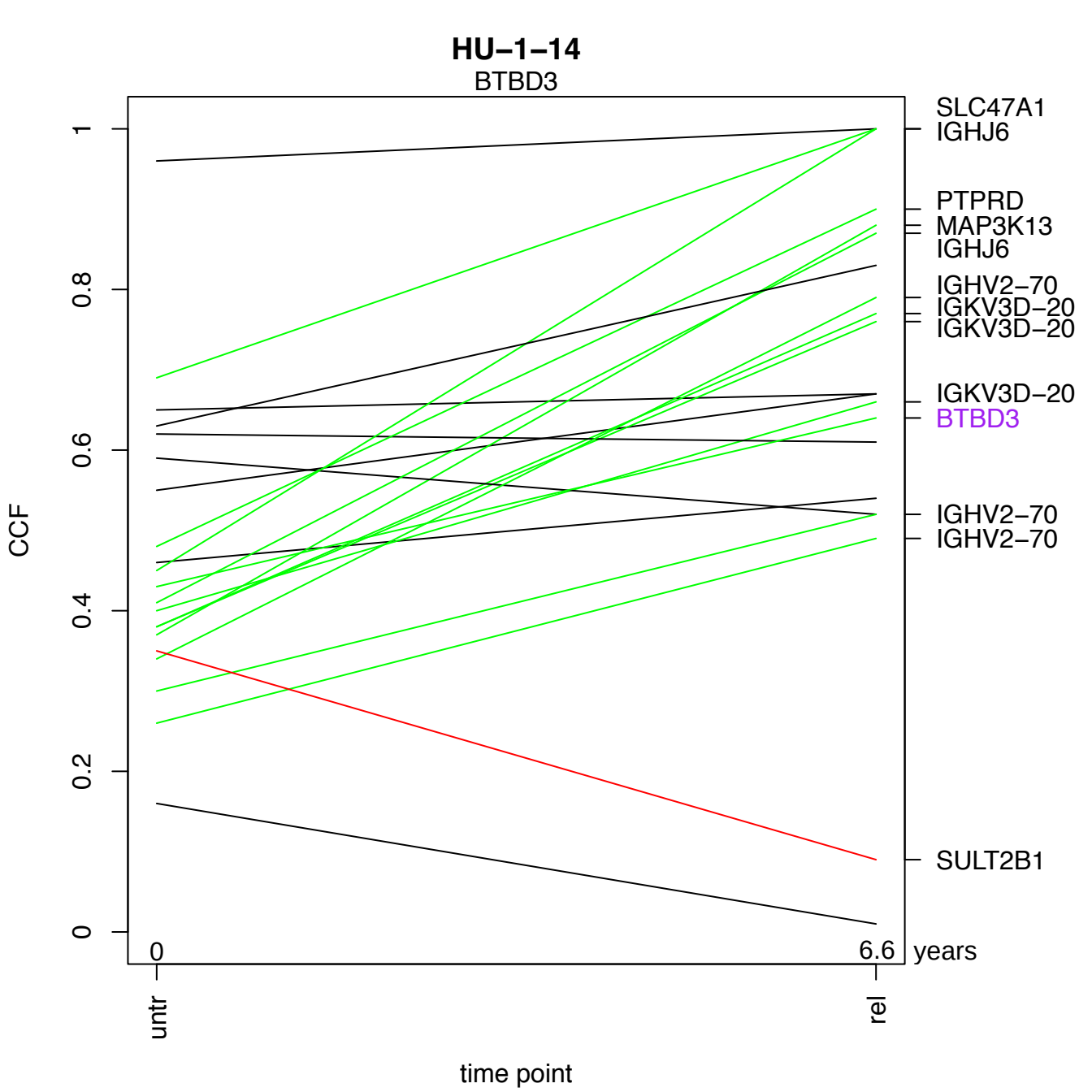
HU−1−14
BTBD3
CCF
0
0.2
0.4
0.6
0.8
1
SLC47A1
IGHJ6
PTPRD
MAP3K13
IGHJ6
IGHV2−70
IGKV3D−20
IGKV3D−20
IGKV3D−20
BTBD3
IGHV2−70
IGHV2−70
SULT2B1
0
6.6
years
untr
rel
time point

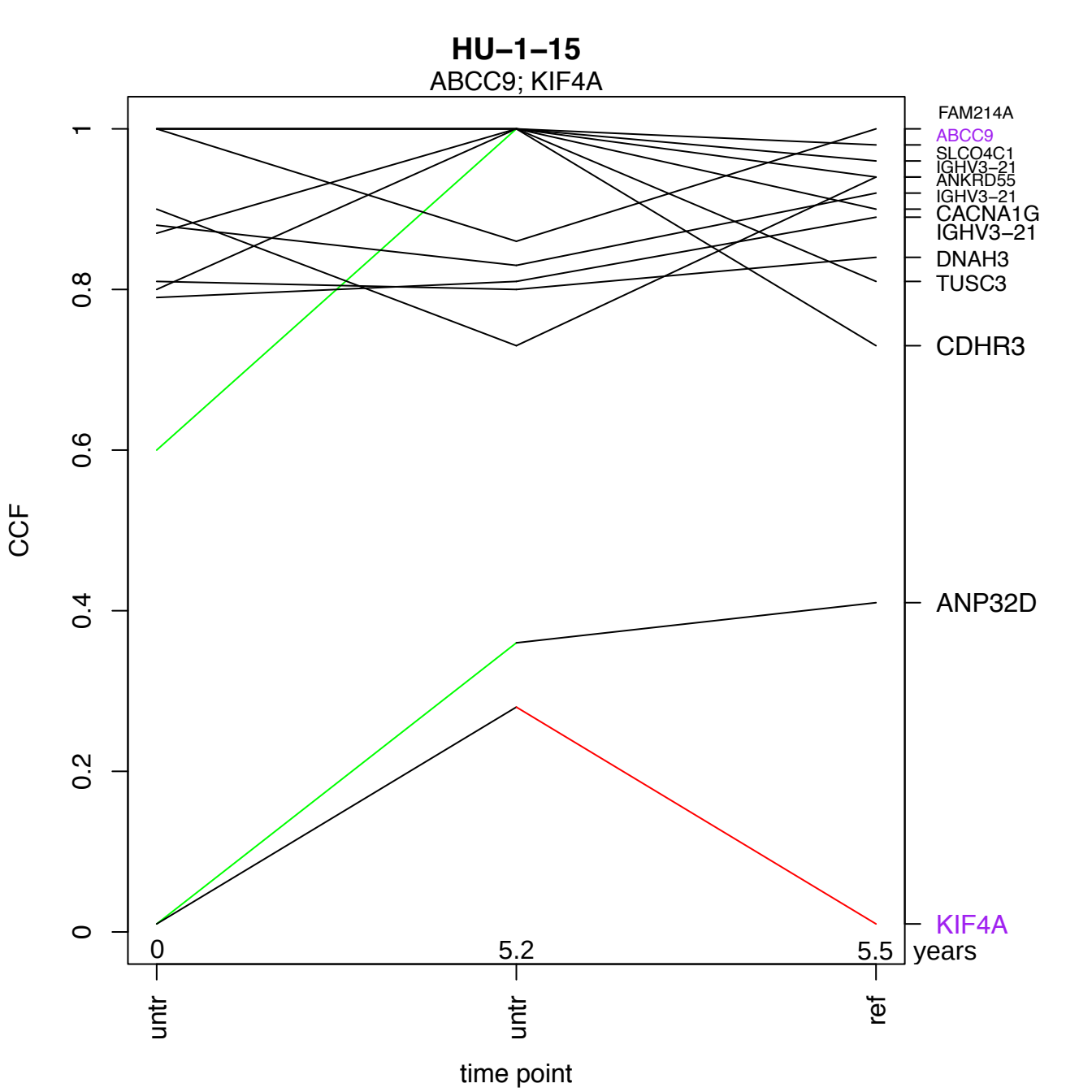
HU−1−15
ABCC9; KIF4A
CCF
1
0.8
0.6
0.4
0.2
0
FAM214A
ABCC9
SLCO4C1
IGHV3−21
ANKRD55
IGHV3−21
CACNA1G
IGHV3−21
DNAH3
TUSC3
CDHR3
ANP32D
KIF4A
0
5.2
5.5
years
untr
untr
ref
time point

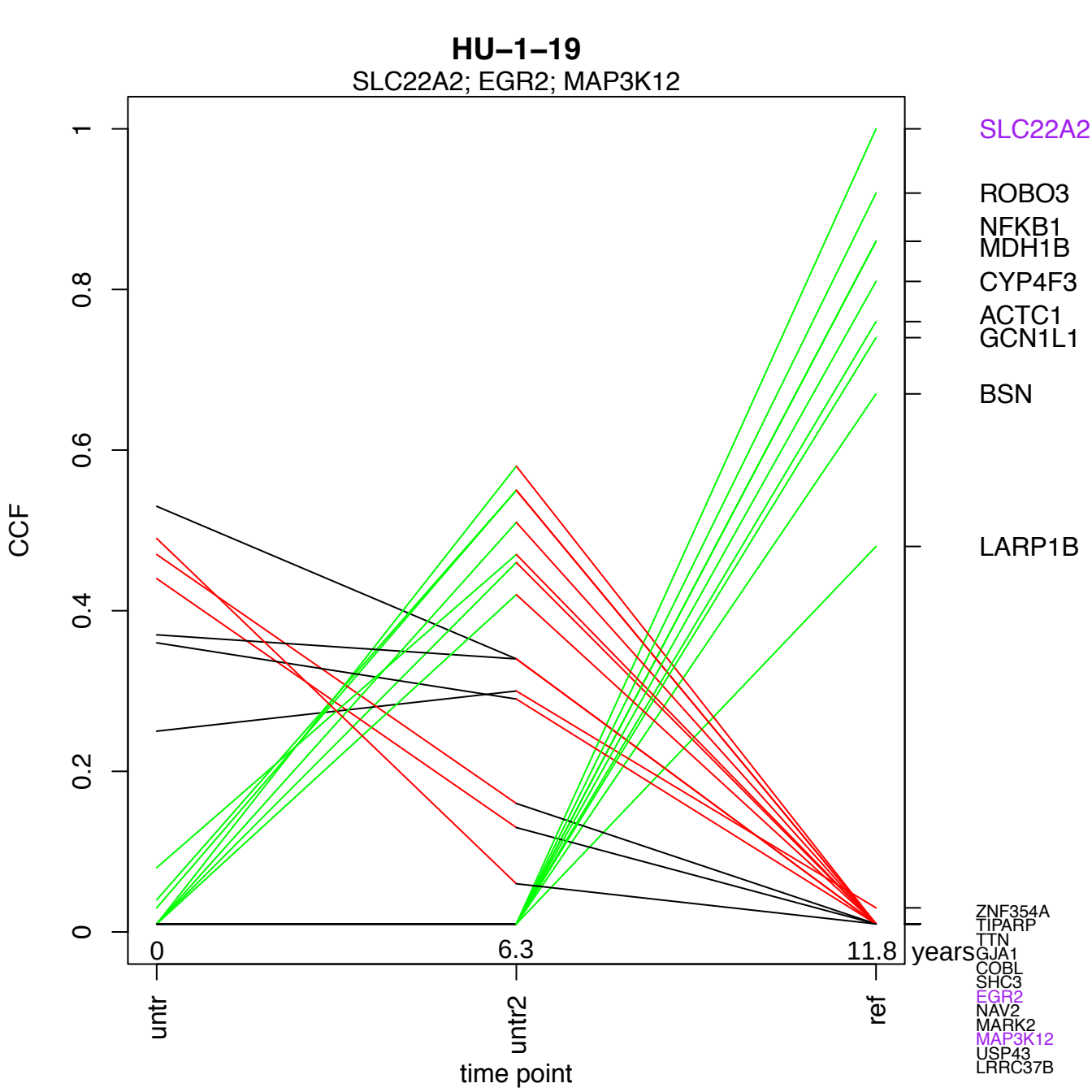
HU−1−19
SLC22A2; EGR2; MAP3K12
CCF
0
0.2
0.4
0.6
0.8
1
0
6.3
11.8
years
untr
untr2
ref
time point
SLC22A2
ROBO3
NFKB1
MDH1B
CYP4F3
ACTC1
GCN1L1
BSN
LARP1B
ZNF354A
TIPARP
TTN
GJA1
COBL
SHC3
EGR2
NAV2
MARK2
MAP3K12
USP43
LRRC37B

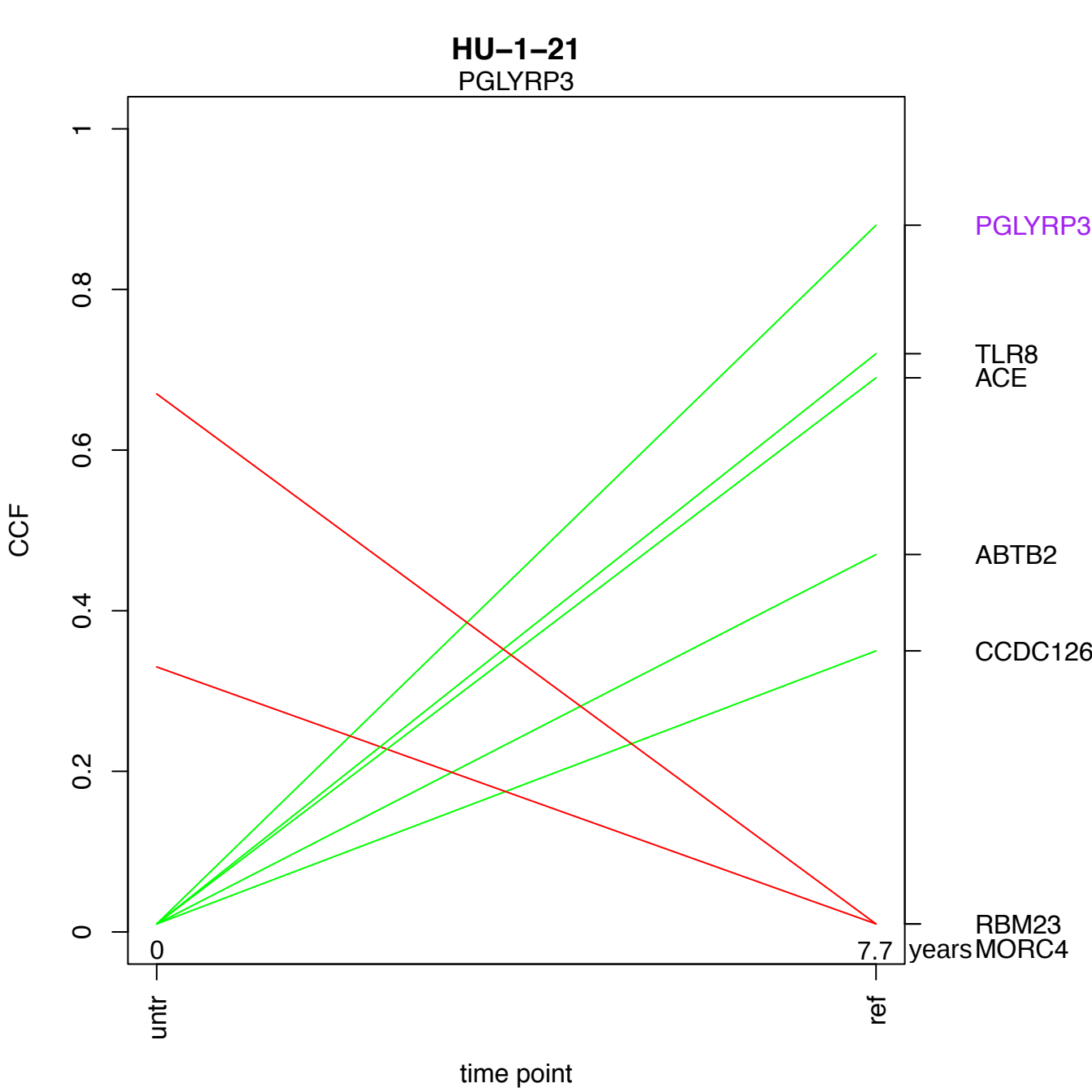
HU−1−21
PGLYRP3
CCF
0
0.2
0.4
0.6
0.8
1
0
7.7
years
untr
ref
time point
PGLYRP3
TLR8
ACE
ABTB2
CCDC126
RBM23
MORC4

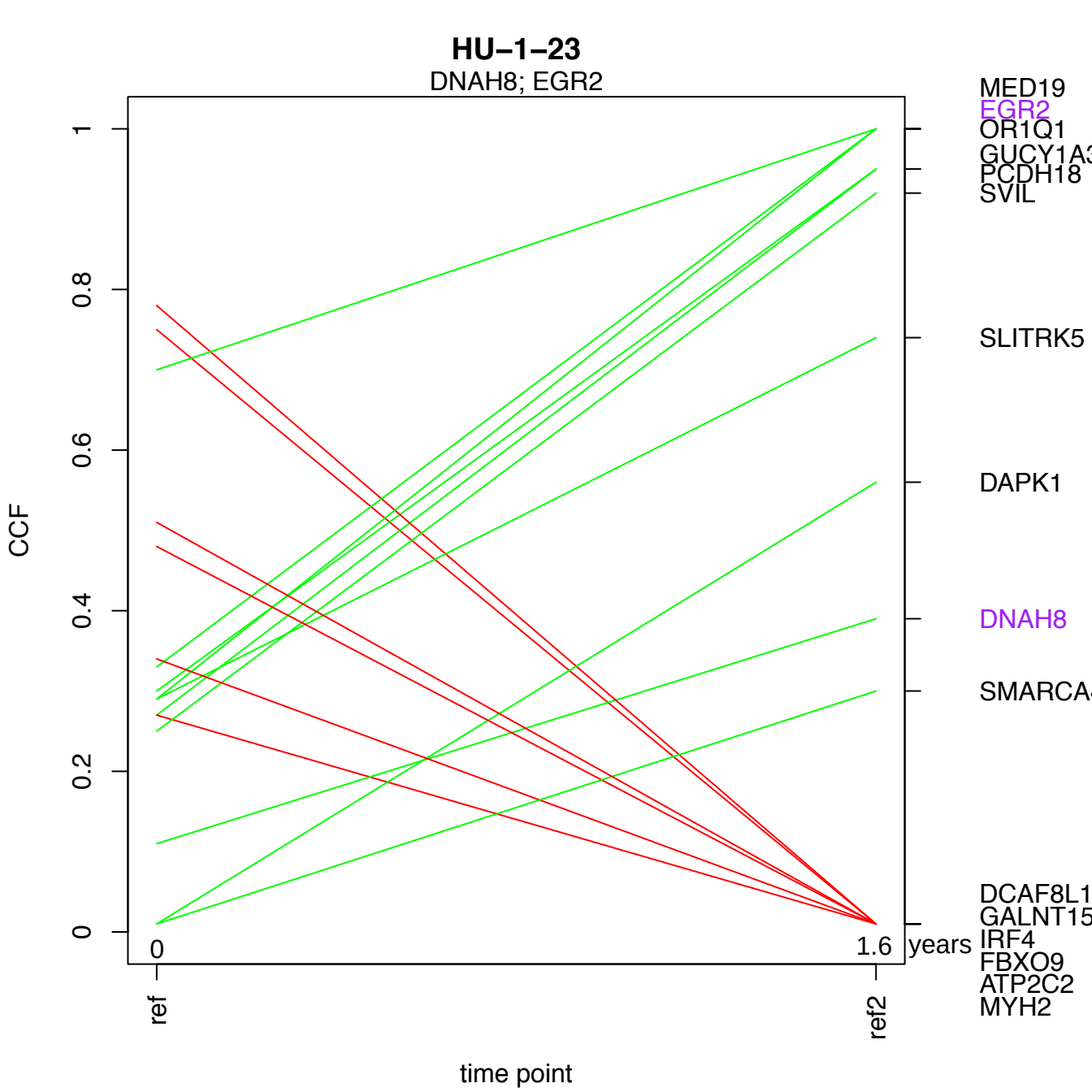
HU−1−23
DNAH8; EGR2
CCF
0
0.2
0.4
0.6
0.8
1
ref
ref2
time point
0
1.6
years
MED19
EGR2
OR1Q1
GUCY1A3
PCDH18
SVIL
SLITRK5
DAPK1
DNAH8
SMARCA
DCAF8L1
GALNT15
IRF4
FBXO9
ATP2C2
MYH2

Suppl. figure 5: Density contour plots of methylation values at two consecutive time points for long-term untreated, relapsed and refractory CLL cases. For each patient, the methylation values of the overall 40,000 most variable CpGs were used to calculate the square of the Pearson correlation coefficient (R^2) between time points.

Long-term untreated phases

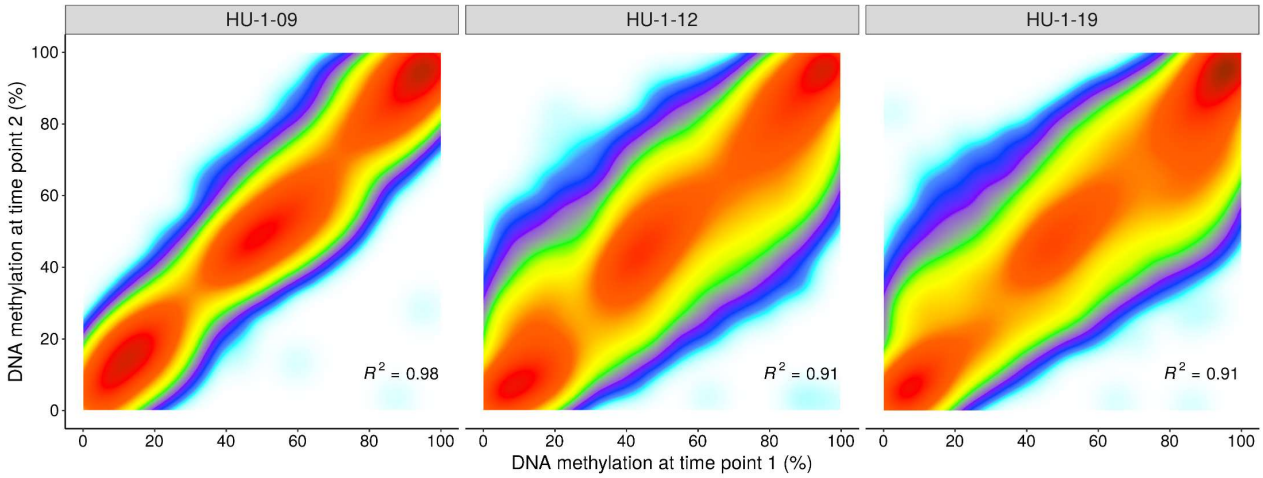

Relapsed phases

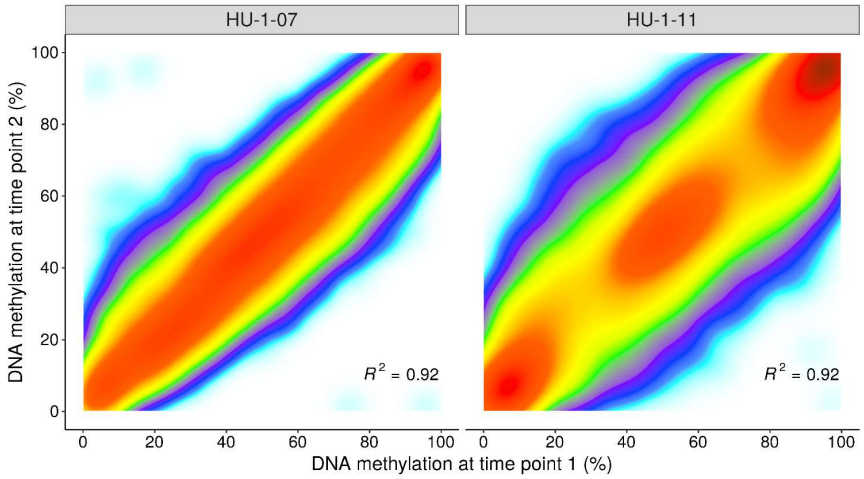

Refractory phases